Cobalt Porphyrin–Thiazyl Radical Coordination Polymers: Toward Metal-Organic Electronics

Supporting Information

Delia A. Haynes,*,† Laura J. van Laeren,† and Orde Q. Munro*,‡

†*Department of Chemistry and Polymer Science, Stellenbosch University, Private Bag X1, Stellenbosch 7600, South Africa. E-mail dhaynes@sun.ac.za.* ‡*School of Chemistry, University of the Witwatersrand, Private Bag 3, PO WITS 2050, Johannesburg, South Africa. E-mail: orde.munro@wits.ac.za.*

Contents

1. Chemical Structure Information 5
Scheme S1. Chemical Structures 5
2. Experimental Section 5
2.1. General Methods and Reagents 5
2.2. Synthesis of Compound **2** 5
2.3. Synthesis of Coordination Polymer **3** 6
2.4. Crystal Structure Determination of CP **3** 6
2.5. Mass Spectrometry 7
2.6. NMR Spectroscopy 7
2.7. EPR Spectroscopy 7
2.8. FTIR Spectroscopy 7
2.9. Beer-Lambert Law Experiments 8
2.10. DFT Simulations 8
3. Supporting Figures 10
Figure S1. Thermal ellipsoid illustrations (50% probability surfaces) of the two independent symmetry-unique structures of CP **3**: (a), molecule 1; (b), molecule 2. For the two independent coordination polymer chains, molecules governed by the symmetry operator [x, y, z] are depicted with thermal ellipsoids; symmetry-related congeners in the chain are depicted as wireframe models. Selected atom labels are shown; all H-atoms and solvent molecules (THF) have been omitted for clarity. 10
Figure S2. (a) View down the a-axis of the asymmetric unit of CP **3**. Molecules are colored by symmetry operator and are rendered as stick models. (b) Crystal packing view for the lattice of CP **3** with THF solvent molecules included. The upper and lower images in the box show the lattice contents as stick and space-fill (van der Waals) models, respectively. (c) The same views as in Part (b), but with solvent molecules omitted to highlight the nature of the solvent channels that run co-linear with the a-axis in the lattice 11
Figure S3. Plot of the S–S bond distance for 117 crystallographically-characterized derivatives of **2** contained within the Cambridge Structural Database (CSD: v. 5.38 + 3 updates). The normal distribution curve fitting the histogram data is indicated (red line) along with the fit statistics. The mean (and standard deviation) of the distribution is 2.089(10) Å. 12

Figure S4. Plot of the Co–$N_{porphyrin}$ bond distance for 105 crystallographically-characterized Co(II) porphyrin derivatives (with 0, 1, or 2 axial ligands of any type) contained within the CSD. The normal distribution curve fitting the data is indicated (red line) along with the fit statistics. The mean (and standard deviation) of the distribution is 1.967(26) Å. 12

Figure S5. (a) Experimental FTIR spectrum of a representative sample of radical **2** (sublimed solid). 13

Figure S6. Solid state FTIR spectra of coordination polymer **3**, sublimed radical **2**, and Co(TPP)Cl as a reference. This figure is reproduced from the main paper to permit further discussion of the low frequency band assignments. 14

Figure S7. (a) Graph of the DFT-calculated C–H stretching frequencies (symmetric and antisymmetric modes) for the pyridyl CH groups of py-DTDA (compound **2**) as a function of the molecular charge; the α-CH groups are adjacent to the pyridine N atom. (b) Graph of the DFT-calculated C–H bond distance as a function of the molecular charge for py-DTDA in different redox states. Comparing the data from the two plots shows: (i) that longer C–H distances correlate with lower bond stretching frequencies and (ii) that the α- and β-CH groups have intrinsically different bond lengths and hence stretching frequencies due to their slightly different bond orders (or force constants in classical mechanics). 16

Figure S8. Solid-state UV-visible-NIR absorption spectrum of CP **3**. (a) Details of data smoothing and background subtraction. (b) Deconvoluted (Voigt functions) experimental solid state electronic spectrum of coordination polymer 3. The band assignments are discussed in the paper. 17

Figure S9. Full range TD-DFT calculated spectrum of solid state tetrameric $\{\mathbf{3}\}_4$. A full list of the 140 transitions and their MO components making up the spectrum is given in Table S6. The spectral envelope is plotted as molar absorptivity (left axis, ε, M^{-1} cm^{-1}) with an intrinsic band width of 1400 cm^{-1} (full width at half maximum) for each transition. Transition energies are represented as vertical green lines with heights governed by the oscillator strength (right axis) for the transition. 18

Figure S10. Graph of the DFT-calculated frontier molecular orbital (FMO) energy gap and first excited state energies for 1D CP **3** (X-ray coordinates) vs. chain length. The FMO energy gap at infinite chain length will be equivalent to the band gap of the material. 19

Figure S11. EPR titration spectra (X-band) for py-DTDA$^{\bullet}$ (**2**, top) and Ph-DTDA$^{\bullet}$ (bottom) in DCM with increasing Co^{II}(TPP) (**1**) concentration, at ambient temperature, forming Co^{II}(TPP)(*S*-py-DTDA) and Co^{II}(TPP)(*S*-Ph-DTDA), respectively. The original (starting) dithiadiazolyl radical spectrum is shown in red. The final addition of Co^{II}(TPP) is shown in blue with intermediate additions shown in grey. 20

Figure S12. (a) Depiction of the most likely FMO interaction between two 5-coordinate monomeric Co(TPP)(S-py-DTDA) complexes that leads to chain growth by Co–N bond formation and oligomerization to 1D CP **3**. (b) Illustration of a tetramer chain unit for CP **3** in which formerly unpaired spins become spin paired in Co–S bonds of coupled radicals. The Co–N bonds (blue) are normal dative covalent bonds in the 1D metal-organic chain structure. The chain growth direction is from left to right. 21

Figure S13. (a) Comparison of the spectra of CP **3** recorded in DMSO and DCM at a concentration of 30 μM (ambient temperature). (b) Deconvoluted (Voigt functions) UV spectrum of 30-μM CP **3** in dichloromethane. (c) Deconvoluted (Voigt functions) UV spectrum of 30-μM CP **3** in DMSO). DMSO clearly monomerizes the coordination polymer to a greater degree than DCM through the formation of 6-coordinate Co^{III}(TPP)(N-py-DTDA)(*O*-DMSO), species **3b**·(*O*-DMSO), as evidenced by ^{1}H NMR spectroscopy (Figure S18). Abbreviations: 6CM, 6-coordinate monomer; M, monomer; O, oligomer; P, polymer. 23

Figure S14. TD-DFT calculated electronic spectra (60 excited singlet states) for 5-coordinate Co(TPP)(*S*-py-DTDA), species **3a**, in 1,2-dichloroethane. Left: full spectral range. Right: visible region. The spectral envelope is plotted as molar absorptivity (left axis, ε, M^{-1} cm^{-1}) with an intrinsic band width of 1400 cm^{-1} (full width at half maximum) for each transition. Transition energies are represented as vertical green lines with heights governed by the oscillator strength (right axis) for the transition. 24

Figure S15a. TD-DFT calculated electronic spectra (60 excited singlet states) for low-spin (S = 0) 5-coordinate Co(TPP)(*N*-py-DTDA), species **3b**, in 1,2-dichloroethane. Left: full spectral range. Right: visible region. The spectral envelope is plotted as molar absorptivity (left axis, ε, M^{-1} cm^{-1}) with an intrinsic band width of 1400 cm^{-1}

(full width at half maximum) for each transition. Transition energies are represented as vertical green lines with heights governed by the oscillator strength (right axis) for the transition. 24

Figure S15b. Illustration of one possible disproportionation pathway (photochemical) for species **3b**. The lowest-energy transition is a LMCT transition from the HOMO to the LUMO of **3b**. Transfer of the electron into the σ* MO of the Co–N bond is expected to enhance bond dissociation by decreasing the Co–N bond order from 1 to 0.5. The first excited state occurs at 7867 nm in the thermal IR region of the spectrum. Dissociation of the axial ligand after electron transfer generates neutral radical **2** and the Co(II) porphyrin **1**. These species are seen in the UV-visible-NIR spectrum of the system at high dilution (Figure 11a of the main paper). 25

Figure S16. TD-DFT calculated electronic spectra (60 excited states) for high-spin (S = 1) triplet state 5-coordinate Co^{II}(TPP)(*N*-py-DTDA$^{\bullet}$), S = 1 species **3b′**, in 1,2-dichloroethane. Left: full spectral range. Right: visible region. The spectral envelope is plotted as molar absorptivity (left axis, ε, M^{-1} cm^{-1}) with an intrinsic band width of 1400 cm^{-1} (full width at half maximum) for each transition. Transition energies are represented as vertical green lines with heights governed by the oscillator strength (right axis) for the transition. 27

Figure S17. ^{1}H NMR spectrum (300 MHz) of **3a**·(*O*-DMSO), or more formally Co(TPP)(S-py-DTDA)(*O*-DMSO), generated by the reaction of a 1:1.1 mole ratio of Co^{II}(TPP), **1**, and py-DTDA$^{\bullet}$, **2**, in DMSO-d_6. The DFT-calculated structure and GIAO-calculated chemical shift values are given for comparison. The absence of signals in the experimental spectrum between 4.5–6.5 ppm confirms that that axial py-DTDA ligand is not N-bound in this structure. 28

Figure S18. NMR spectra (298 K) of CP **3** dissolved in DMSO-d_6. (a) ^{59}Co NMR spectrum (142.36 MHz). The peak position and linewidth were determined from a least-squares fit of the spectral data to a hybrid Lorentzian-Gaussian function (49% Gaussian). (b) Expansions of the pyridyl proton signals in the ^{1}H NMR spectrum (299.74 MHz). DFT-calculated proton chemical shifts are indicated on the structure (ppm). (c) Full-range ^{1}H NMR spectrum. The coordination polymer **3** dissociates to an equilibrium mixture mostly comprising **3b**·(*O*-DMSO). Evidence for some oligomeric $\{\mathbf{3}\}_n$ is possibly reflected by the additional signals (marked *) that parallel those of **3b**·(*O*-DMSO) in the ^{1}H NMR spectrum. The spectral data confirm that the Co–S bond of CP **3** dissociates when the polymer dissolves. 30

Figure S19. Experimental ESI+ Mass spectrum of CP **3** dissolved in acetonitrile (left) with fragment assignments and calculated monoisotopic masses. The calculated mass spectral signal patterns (IsoPro 3.1) expected from fragments W through Z are shown at the lower right side of the figure on a normalized abundance scale. 31

Figure S20. MS-MS spectrum of CP **3** dissolved in acetonitrile confirming that the species at m/z = 853 contains both **1** (m/z = 671) and **2** (m/z = 182). 32

Figure S21. Mass spectrum of CP **3** dissolved in acetonitrile from m/z 50–350 showing relevant assignments. 33

Figure S22. MS-MS spectrum of radical **2**. The signal at m/z = 91 is possibly present but its weak intensity reflects a very low abundance for the fragment C_6H_5N (Figure S21). This is expected since the metalloporphyrin may in fact assist the fragmentation of species **Y** to **Z** (Figure S19), which is the origin of this slightly more abundant low mass fragment in Figure S21. 33

4. Supporting Tables 34

Table S1. Experimental details for the X-ray structure determination of CP **3**. 34

Table S2. Selected geometric parameters (Å, °) for CP **3**. 35

Table S3. Crystallographic data compiled from the Cambridge Structural Database (CSD) for Co(II/III) porphyrins axially-ligated by ≥ 1 pyridine ligand. 41

Table S4. Experimental and calculated infrared spectra for radical **2** (solid state, sublimed compound).[a] 42

Table S5. DFT-calculated metal orbital populations (NBO 3.0) and energies for **3b** and the five-coordinate pyridine analogue, Co(TPP)(py). 43

Table S6. TD-DFT calculated singlet excited states and transition components for coordination polymer **3**. 44

Table S7. Selected TD-DFT calculated Vis-NIR electronic transitions and assignments for tetrameric **3**.[a] 50

Table S8. TD-DFT calculated singlet excited states and transition components for **3a**, Co^{II}(TPP)(*S*-py-DTDA), in 1,2-dichloroethane 51
Table S9. TD-DFT calculated singlet excited states and transition components for **3b**, Co^{III}(TPP)(*N*-py-$DTDA^{-}$), in 1,2-dichloroethane 56
Table S10. Selected TD-DFT calculated Vis-NIR electronic transitions and assignments for **3b**.[a] 60
5. Cartesian Coordinates: DFT Structures 62
5.1. py-DTDA in Five Redox States 62
5.1.1. Neutral Radical **2** 62
5.1.2. Cationic py-DTDA, $\mathbf{2}^{+}$ 62
5.1.3. Anionic py-DTDA, $\mathbf{2}^{-}$ 63
5.1.4. Di-cationic py-DTDA, $\mathbf{2}^{2+}$ 63
5.1.5. Di-anionic py-DTDA, $\mathbf{2}^{2-}$ 64
5.1.6. π-π dimer, $\{py\text{-}DTDA\}_2$ 64
5.2. Five-Coordinate Co(TPP)(L) Complexes 64
5.2.1. Co(TPP)(*S*-py-DTDA), compound **3a** 64
5.2.2. Co(TPP)(*N*-py-DTDA), compound **3b** 67
5.3. Six-Coordinate Co(TPP)(L) Complexes 70
5.3.1. Co(TPP)(*S*-py-DTDA)(DMSO) 70
5.3.2. Co(TPP)(*N*-py-DTDA)(DMSO) 71
5.4. Dimeric $\{Co(TPP)(L)\}_2$ Complexes 72
5.4.1. CP Dimer, $\{Co(TPP)(S\text{-py-}DTDA)\}_2$ 72
6. References and Notes 74

1. Chemical Structure Information

The supporting information in this document pertains to the structures depicted below (Scheme 1).

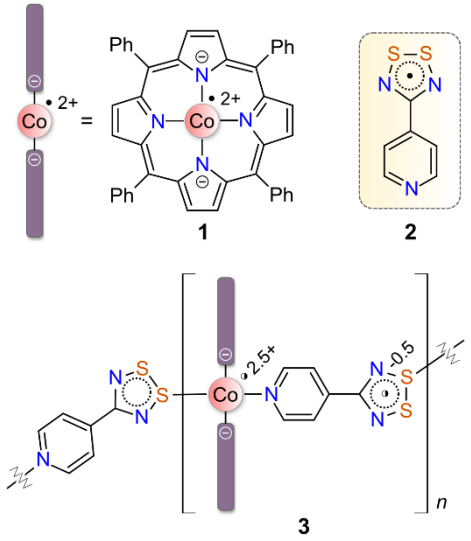

Scheme S1. Chemical Structures

2. Experimental Section

2.1. General Methods and Reagents

All chemicals including deuterated NMR solvents were purchased from Sigma-Aldrich and, unless otherwise indicated, were used as received. Solvents for spectroscopy (DMSO, 1,2-dichloroethane) were high-purity anhydrous Sure/Seal™ solvents from Sigma-Aldrich. Solvents for synthesis were freshly distilled over sodium metal cuttings (THF) and calcium hydride (dichloromethane) before use. The metalloporphyrin 5,10,15,20-tetraphenylporphyrinatocobalt(II) (compound **1**, Co(TPP)) was prepared from readily available starting materials using established synthetic routes.[1]

Data analysis and graphing were performed with OriginPro 9.1.0 (64-bit).[2] Spectral peak deconvolutions and background fitting were performed with Fityk 0.9.8.[3]

2.2. Synthesis of Compound 2

The literature methods[4] were followed for the synthesis of 4-(4'-pyridyl)-1,2,3,5-dithiadiazolyl radical (compound **2**, or py-DTDA). The exact method used is given here for completeness and because the isolated yield of the product after sublimation is quite variable.

Dry diethyl ether (30 mL) was placed in a nitrogen-filled Schlenk flask and cooled to –78 °C. Hexamethyldisilylazane (2.0 mL, 9.6 mmol) and n-butyl lithium (7.2 mL, 1.6M, 11.52 mmol) were added. The cooling bath was removed and the solution was stirred for 45 minutes until warmed to room temperature and the solution was clear. 4-Pyridinecarbonitrile (1.002 g, 9.62 mmol) was added to the solution, which was left to stir overnight. The ochre-colored solution was subsequently cooled to 0 °C. Sulfur dichloride (1.2 mL, 19.2 mmol) was added slowly with vigorous stirring. After complete addition, the solution was allowed to warm to room temperature and stirred for a further 1 hour. Stirring was then stopped and the yellow-

orange precipitate allowed to settle. Excess solvent was removed by cannula filtration. The remaining precipitate was washed with dry diethyl ether (3 x 10 mL), then dried under vacuum. The dry dithiadiazolylium chloride salt (1.502 g, 6.92 mmol) was transferred to a clean, dry Schlenk flask under nitrogen. Triphenylantimony (1.222 g, 3.46 mmol) was added to the flask and the contents were gently mixed. The mixture was heated to 70 °C for approximately 3 hours, when a complete colour change from yellow-orange to purple was observed. The flask was fitted with a water-cooled cold finger, placed under vacuum and sealed. Heating was increased to 140 °C and the product, py-DTDA, was isolated by sublimation onto the water-cooled cold finger as dark blocks (0.252 g, 1.385 mmol, 14% yield). (+)-ESI-MS: m/z 182.9915. EPR (9.878 GHz, CH_2Cl_2): 3515 G (pentet, a_n = 5.0 G), g = 2.008.

2.3. Synthesis of Coordination Polymer 3

Radical **2** (0.020 g, 0.110 mmol) was transferred under an inert atmosphere to a clean, dry Schlenk tube. Tetrahydrofuran (5.0 mL, stored over molecular sieves) was added to the tube, followed by Co(TPP) (0.072 g, 0.107 mmol). The resulting blood-red solution was heated gently, and then layered with hexane (approximately 5 mL, stored over molecular sieves). Shiny purple-blue crystals appeared on the sides of the tube. After approximately two days, the resulting solid was filtered, washed with hexane and air-dried to give coordination polymer **3** as a purple-black powder (0.022 g, 0.022 mmol, 20.6% yield assuming full occupancy of THF). TOF MS (ES+): *m/z* 853.1500 (calc $C_{50}H_{32}N_7S_2Co$, 853.1515), M^+.[5] IR (powder cm^{-1}): 3052 m, 3023 m, 2995 m, 2922 m (ν{α-CH}, py-DTDA), 2851 m (ν{β-CH}, py-DTDA), 1691 w, 1597 w, 1435 w, 1350 w, 1313 w, 155 w, 1139 m br (ν{C–C, C–N} py-DTDA), 1070 m, 1052 m (δ{CC^{β}–H}, py-DTDA), 1007 s, 793 s, 751 s (ν_a{N–S}, py-DTDA), 700 s, 581 w (δ_{ip}{C–N_{py}–C}, py-DTDA), 565 w (δ_{ip}{N–C–N}, py-DTDA). Abbreviations: w, weak; m, medium; s, strong; br, broad. UV-vis (CH_2Cl_2) [λ_{max}, nm (ε, M^{-1} cm^{-1})]: 417 (1.62×10^5), 520 (1.03×10^4), 650 (2.31×10^3). Solution phase NMR data for the polymer are unavailable due to its monomerization in DMSO, DCM, and DCE. NMR data for the monomeric species derived from dissociation of the polymer (de-polymerization) in DCE are given in the paper; data for the monomer obtained in DMSO are given in Figure S18.

Note that this synthetic procedure also occasionally yields an additional green precipitate, which has not yet been fully characterized. Initial EPR investigations indicate that the green material also contains DTDA radical. Based on the TD-DFT calculated spectrum of oligomeric {**3**}$_4$ (Figure S9), which has a prominent absorption band at 700 nm, it is possible that the green solid formed in the reaction is a lower molecular weight oligomer, {**3**}$_n$, with an N-bound py-DTDA$^{\bullet}$ radical capping group on the starting Co(TPP) molecule in the chain. This would leave the DTDA ring (and thus unpaired spin) effectively isolated at the chain end and thus account for the observed EPR signal (see Figure S12b, which schematically depicts a tetramer chain with a capping radical ligand).

2.4. Crystal Structure Determination of CP 3

Intensity data were collected on a Bruker Apex DUO CCD diffractometer with a multilayer monochromator. Mo-Kα radiation (λ= 0.71073 Å) was used, and the temperature of the crystal was controlled using an Oxford Cryosystems cryostat. The crystal was mounted on a MiTeGen mount in Paratone® oil. Data reduction, absorption corrections and unit cell determination were carried out using the diffractometer software (APEXII, Bruker).[6] Structures were solved and refined using the SHELX-97[7] package implemented through X-Seed.[8] Hydrogen atoms were placed in calculated positions using the standard riding model of SHELX-97. Figures were generated using Mercury.[9]

The occupancies of the four THF molecules in the asymmetric unit were allowed to refine, resulting in an average occupancy of 85.5%. There are thus 1.71 molecules of THF for every Co(TPP)(*S*-py-DTDA) pair.

2.5. Mass Spectrometry

Mass spectrometry was carried out on a Waters Synapt G2 instrument with direct injection of 1 μL of **3** dissolved in acetonitrile into a stream of 100% acetonitrile (Waters UPLC) at a flow rate of 0.2 mL min^{-1} (+ESI, capillary voltage 3 kV, cone voltage 40 kV). MSMS was performed with a collision energy of 50 V. Spectral simulations were carried out with IsoPro 3.1. This software is freely available for download on the web (https://sites.google.com/site/isoproms/home).

2.6. NMR Spectroscopy

Most, but not all, ^{1}H and ^{59}Co nuclear magnetic resonance spectra were obtained using a Varian Unity Inova 300 MHz spectrometer or a Varian Unity Inova 600 MHz spectrometer. Chemical shifts (δ) are reported in ppm. Spectra were obtained at 25 °C. For spectra of **3**, 13.5 mg of the crystalline coordination polymer was dissolved in 0.6 mL DMSO-d_6. ^{1}H and ^{59}Co NMR spectra were recorded on the same sample using the 600 MHz instrument (142 MHz for ^{59}Co). Note that DMSO-d_6 effectively and rapidly monomerizes **3** upon dissolution and neither the ^{1}H nor the ^{59}Co NMR spectrum of the coordination polymer could be recorded. The nature of the diamagnetic monomeric species could, however, be determined from the spectra of **3** dissolved in DMSO-d_6. Experiments involving the addition of Co(TPP), compound **1**, to radical **2** were as follows. An aliquot (0.30 mL) of a 2.51-mM solution of **1** dissolved in DMSO-d_6 was reacted with a DMSO-d_6 solution of **2** (0.70 mL, 1.19 mM) to give final concentrations (1.0 mL total volume) of 0.75 mM **1** and 0.83 mM **2** (mole ratio 1:1.1). The NMR tube was capped and sealed before immediately acquiring the spectral data (300 MHz spectrometer).

Additional NMR experiments in 1,2-dichloroethane-d_4 (DCE-d_4; stored over CaH_2 for 24 h) were performed with a 500 MHz Bruker Avance III spectrometer equipped with an Oxford magnet (11.744 T). A stock solution of 0.518 mg of CP **3** dissolved in 1.00 mL DCE-d_4 was prepared (this took about 40 min to dissolve with occasional swirling) before making two dilute solutions at concentrations of 18 μM (18 μL stock added to 580 μL DCE-d_4) and 96 μM (96 μL stock added to 500 μL DCE-d_4). These concentrations correspond to monomeric and mainly oligomeric species derived from dissolution of coordination polymer **3**. Spectral acquisition over 50 h afforded acceptable spectra at these very dilute concentrations.

2.7. EPR Spectroscopy

EPR studies were carried out with spectroscopic-grade solvents using a Bruker EMX-plus X-band ESR spectrometer with a high-sensitivity X-band resonator. The reaction between **1** and **2** was carried out in a flat cell in dimethylsulfoxide (DMSO) at room temperature. The reaction between 4-phenyl-1,2,3,5-dithiadiazolyl (Ph-DTDA) and **1** was carried out in a 4 mm quartz EPR tube in dichloromethane (DCM) filtered through dry, activated alumina. In these experiments, successive aliquots of a concentrated solution of **1** dissolved in the relevant solvent were added directly to the either the py-DTDA or Ph-DTDA radical in solution until the signal from the free radical had been quenched.

2.8. FTIR Spectroscopy

FTIR spectra were recorded on polycrystalline material at ambient temperature directly with a Bruker Alpha FTIR spectrometer fitted with a diamond crystal Platinum ATR sampling accessory. Solid state spectra were also recorded with a Nexus Thermo-Nicolet Avatar 330 FT-IR instrument equipped with a Smart Performer Zn/Se ATR attachment.

2.9. Beer-Lambert Law Experiments

Electronic spectra for the Beer-Lambert law dilution experiments were recorded on an Analytik Jena Specord 210 Plus double-beam spectrometer with matched quartz cuvettes (1 mm path length) using spectroscopic grade solvents and a data sampling rate of 10 points/nm. Neat solvent was used as a reference in all spectral scans, which were recorded at ambient temperature (ca. 25–27 °C). For experiments in DMSO, a 10-mL stock solution of **3** was prepared from 4.8 mg of the crystalline coordination polymer prior to serial dilution for spectroscopic measurements. A further, more concentrated 5.0-mL stock solution was prepared by dissolving 3.4 mg of the crystalline coordination polymer in DMSO. This solution was used directly to collect the absorbance data for the highest concentration on the plot. For experiments in DCM, a stock solution containing 2.1 mg of crystalline **3** dissolved in 5.0 mL of DCM was serially diluted for spectroscopy. A further, more concentrated solution was prepared by dissolving 2.6 mg of crystalline **3** in 5.0 mL of DCM and used to collect the absorbance data for the highest concentration on the plot. In all cases, the molecular weight of **3** used to calculate concentration was 998 g mol^{-1}. This is the molar mass of the asymmetric unit of **3** assuming full occupancy of THF, i.e. 2.0 moles of THF per mole of Co(TPP)(py-DTDA), and equates directly to the concentration of the polymer repeat unit (five-coordinate monomer). It is possible that some THF could be lost from crystalline **3** during weighing and storage, so actual concentrations may in fact be slightly higher.

For stock solutions in DCM and DMSO, difficulty was experienced in completely dissolving the crystalline coordination polymer. Sonication was used to aid dissolution. Even once the sample had completely dissolved, slow precipitation of solid **3** upon standing from the most concentrated solutions was observed. Because spectral data were recorded promptly on fresh solutions, the effect on the spectroscopic data appears to have been negligible (close adherence to Beer's Law).

For Beer-Lambert law experiments in 1,2-dichloroethane (DCE) at 298 K, 0.540 mg of polycrystalline CP **3** was dissolved in 1.20 mL dry DCE (sufficiently good solubility) to give a brown-green stock solution (451 μM). Aliquots of the stock solution were successively added to 2.00 mL of dry DCE in a 1.0 cm pathlength quartz cuvette (the reference cell contained 2.00 mL of dry DCE). After each aliquot addition, the spectrum was recorded at a scan rate of 480 nm min^{-1} (1.0 cm slit width, 200–1100 nm) with a Perkin-Elmer Lambda 25 double beam spectrometer, until the absorbance approached the limit for the optical pathlength. A 200-μL aliquot of the reaction mixture was transferred to a 0.1 cm pathlength quartz cuvette, the reference cell switch to a 0.1 cm pathlength cell filled with DCE, and the repetitive addition of aliquots of the stock solution continued until the limit for the optical pathlength was reached.

2.10. DFT Simulations

General methods (simple molecules). All calculations on monomeric species were performed with Gaussian 09W-64 Rev. C.01[10] at the HSEH1PBE[11]/6-31G(d,p)[12] level of theory. GausView 5.0.9 was used to set up and analyze job files, while GaussSum 3.0[13] was used to process output from TD-DFT jobs for tabulation and analysis. Starting structures were derived by editing the X-ray coordinates of **3** or building **2** in GausView. Structures were symmetrized to the highest available symmetry point groups and the symmetry then fixed during simulations when warranted. Full geometry optimizations followed by frequency calculations were effected for species both *in vacuo* and in the appropriate solvent continuum (dimethyl sulfoxide, dichloromethane, or 1,2-dichloroethane) using Gaussian's default polarization continuum model (PCM).[14] All structures were true minima on the potential energy surface (no negative frequency eigenvalues). Magnetic shielding tensors were computed using the default gauge-independent atomic orbital (GIAO)[15] method in Gaussian 09W-64. Relative Gibbs energy differences given in the paper for linkage isomers (e.g. **3a** vs **3b**) were obtained from thermochemical calculations at 298.15 K. (The sum of the electronic and thermal free energies from the frequency job outputs was used as G for a given stationary point structure. This was followed by calculation of the appropriate energy difference, ΔG, between structures of the same molecular formula in the same solvent continuum).

Complex molecules. Calculations on π-π dimers of **2** were performed at the B3LYP[16]/6-31G(d,p) level of theory (full geometry optimizations followed by vibrational frequency calculations). Calculations on metalloporphyrin oligomers, $\{\mathbf{3}\}_n$, were performed at the B3LYP/SDD[17] level of theory. The DFT calculations on oligomers of **3** were carried out at the B3LYP/SDD level of theory for two reasons: (i) NIST frequency scale factors are available for this functional and effective core potential (ECP) basis set; these are equivalent to those for the 6-31G(d,p) basis set, thereby allowing more accurate comparisons to be made between vibrational frequency simulations on low molecular weight and macromolecular systems. (ii) Use of a widely-used and accurate ECP basis set such as SDD is essential for time-efficient geometry optimizations and other calculations on larger-scale models of the system (i.e., dimers and higher oligomers). To facilitate assignment of the infrared spectrum of solid **3**, frequency calculations were performed on a fully geometry-optimized dimer, $\{\mathbf{3}\}_2$, as well as **2** in monomeric, ionic (+1/-1), and π-π dimerized states *in vacuo*.

Single-point TD-DFT simulations (B3LYP/SDD) on the X-ray structure of CP **3** with a chain length ranging from $n = 1$ to $n = 14$ were employed to delineate and assign the solid state electronic spectrum of the material as a function of chain length. The input structures for these calculations were prepared using Mercury CSD 3.9 (Build RC1)[9] by generating the coordination polymer chain of the desired length with fractional coordinates and symmetry operators for independent **molecule 1** in the asymmetric unit. All solvent molecules were removed for the simulations, which were carried out *in vacuo* with Gaussian 09W-64. The density of states (DOS) spectra for selected oligomers were calculated by extracting the required MO energies (states) from the Gaussian output (log) files with GaussSum 3.0 and carrying out a spectral convolution over all states with Gaussian bands of unit height and a band width of 0.30 eV (full width at half maximum, FWHM).

Monomerization routes for oligomeric 3. Concerning the species illustrated below (taken from Figure 10 of the paper), we were unable to calculate an antiferromagnetically-coupled singlet state ($S = 0$) for **3b′**, irrespective of the functional employed in the simulation (restricted- or unrestricted-spin singlet). Similarly, a stable triplet state was located for neither **3a** nor **3a′**, while the starting singlet state for **3a′** converged to the same structure as **3a**.

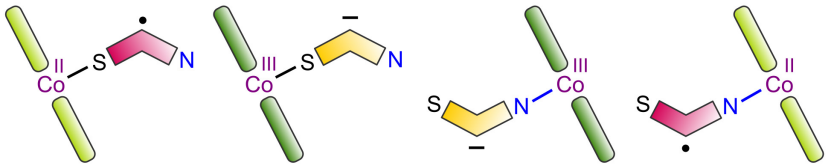

3. Supporting Figures

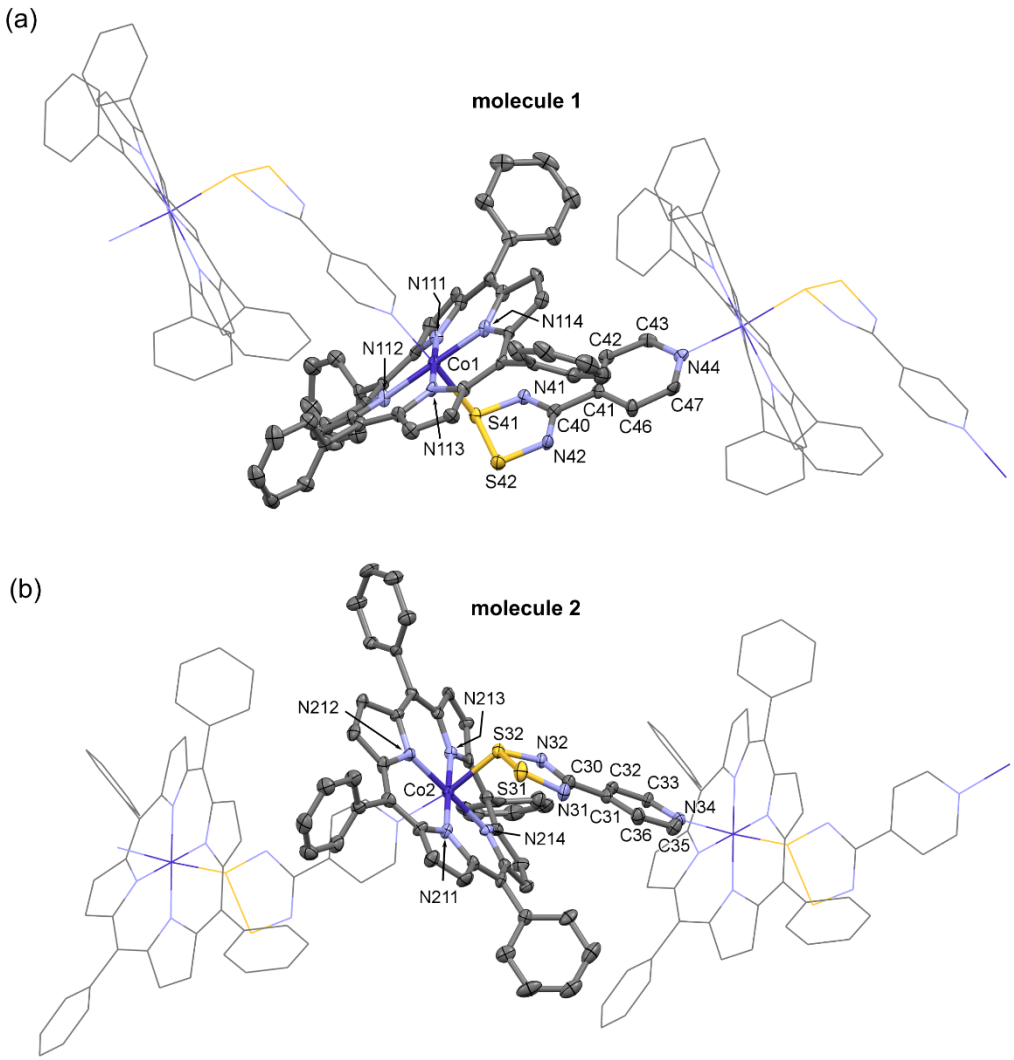

Figure S1. Thermal ellipsoid illustrations (50% probability surfaces) of the two independent symmetry-unique structures of CP **3**: (a), molecule **1**; (b), molecule **2**. For the two independent coordination polymer chains, molecules governed by the symmetry operator [x, y, z] are depicted with thermal ellipsoids; symmetry-related congeners in the chain are depicted as wireframe models. Selected atom labels are shown; all H-atoms and solvent molecules (THF) have been omitted for clarity.

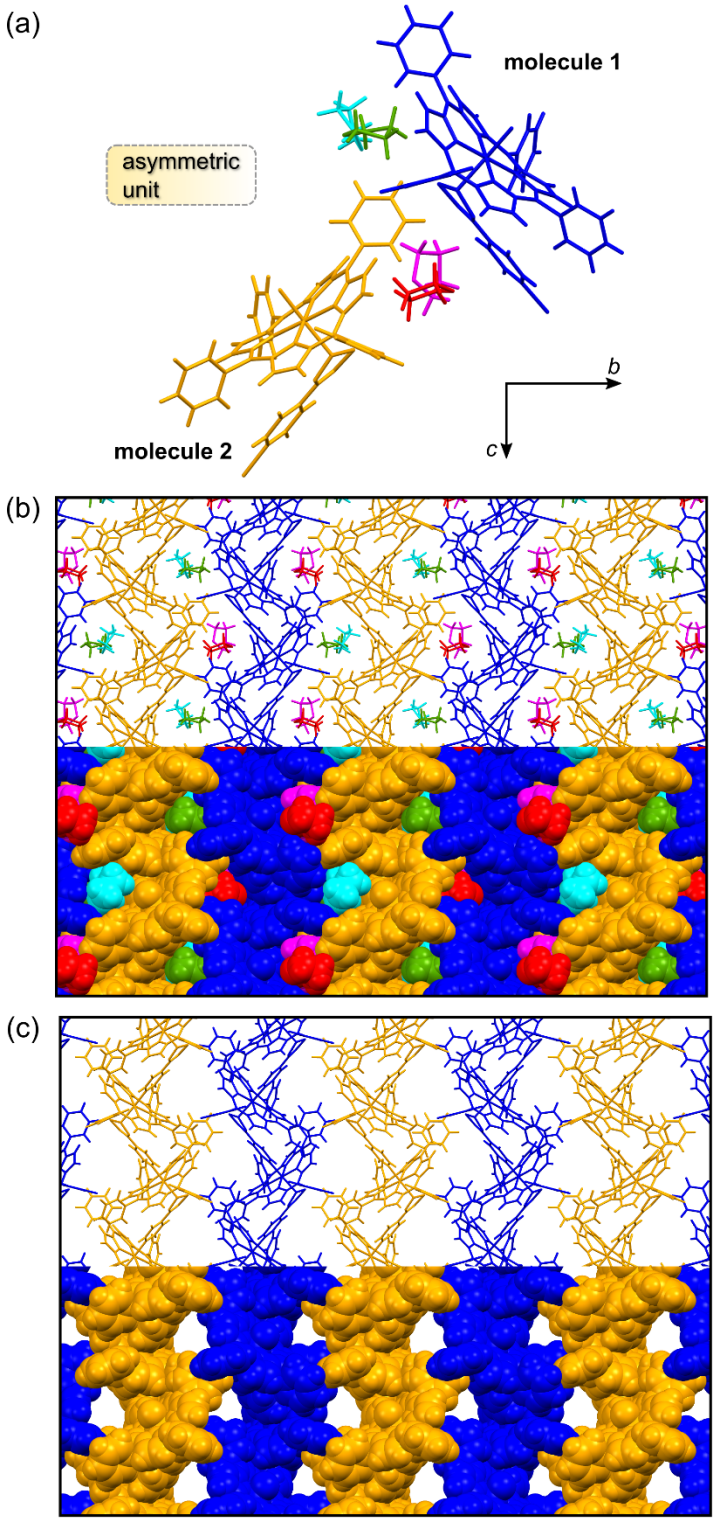

Figure S2. (a) View down the a-axis of the asymmetric unit of CP **3**. Molecules are colored by symmetry operator and are rendered as stick models. (b) Crystal packing view for the lattice of CP **3** with THF solvent molecules included. The upper and lower images in the box show the lattice contents as stick and space-fill (van der Waals) models, respectively. (c) The same views as in Part (b), but with solvent molecules omitted to highlight the nature of the solvent channels that run co-linear with the a-axis in the lattice.

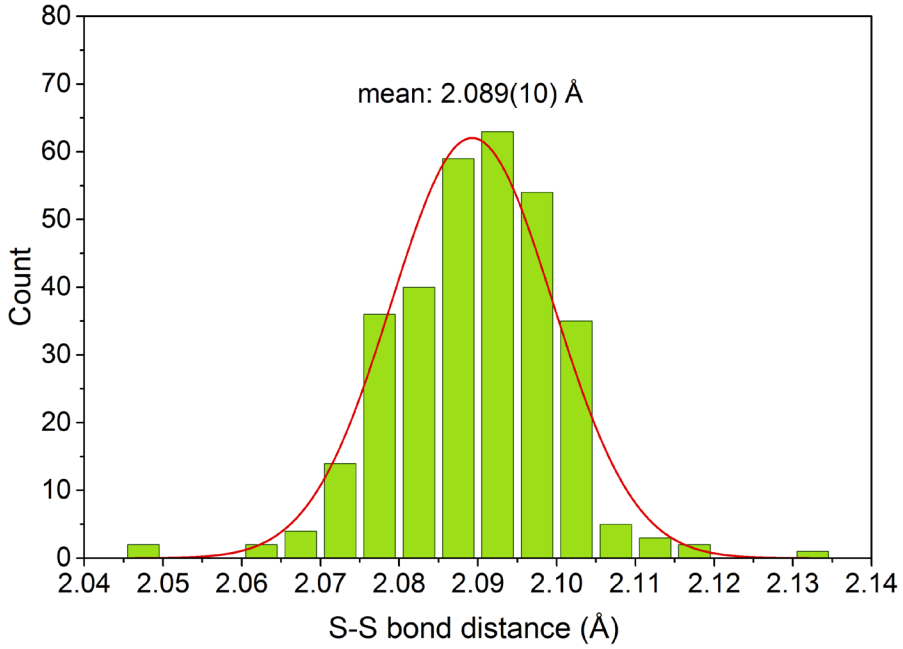

Figure S3. Plot of the S–S bond distance for 117 crystallographically-characterized derivatives of **2** contained within the Cambridge Structural Database (CSD: v. 5.38 + 3 updates).[18] The normal distribution curve fitting the histogram data is indicated (red line) along with the fit statistics. The mean (and standard deviation) of the distribution is 2.089(10) Å.[19]

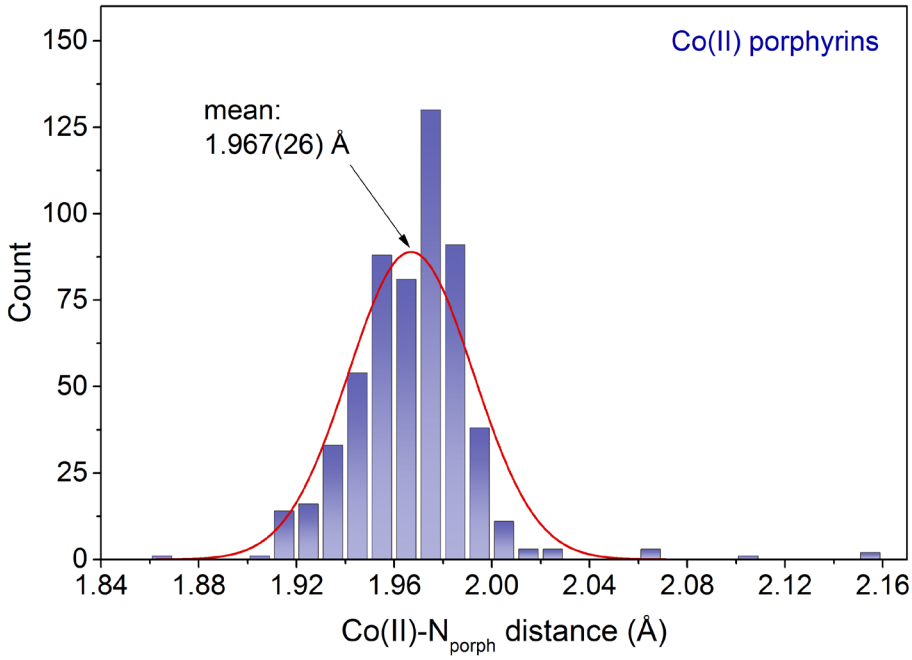

Figure S4. Plot of the Co–$N_{porphyrin}$ bond distance for 105 crystallographically-characterized Co(II) porphyrin derivatives (with 0, 1, or 2 axial ligands of any type) contained within the CSD. The normal distribution curve fitting the data is indicated (red line) along with the fit statistics. The mean (and standard deviation) of the distribution is 1.967(26) Å.

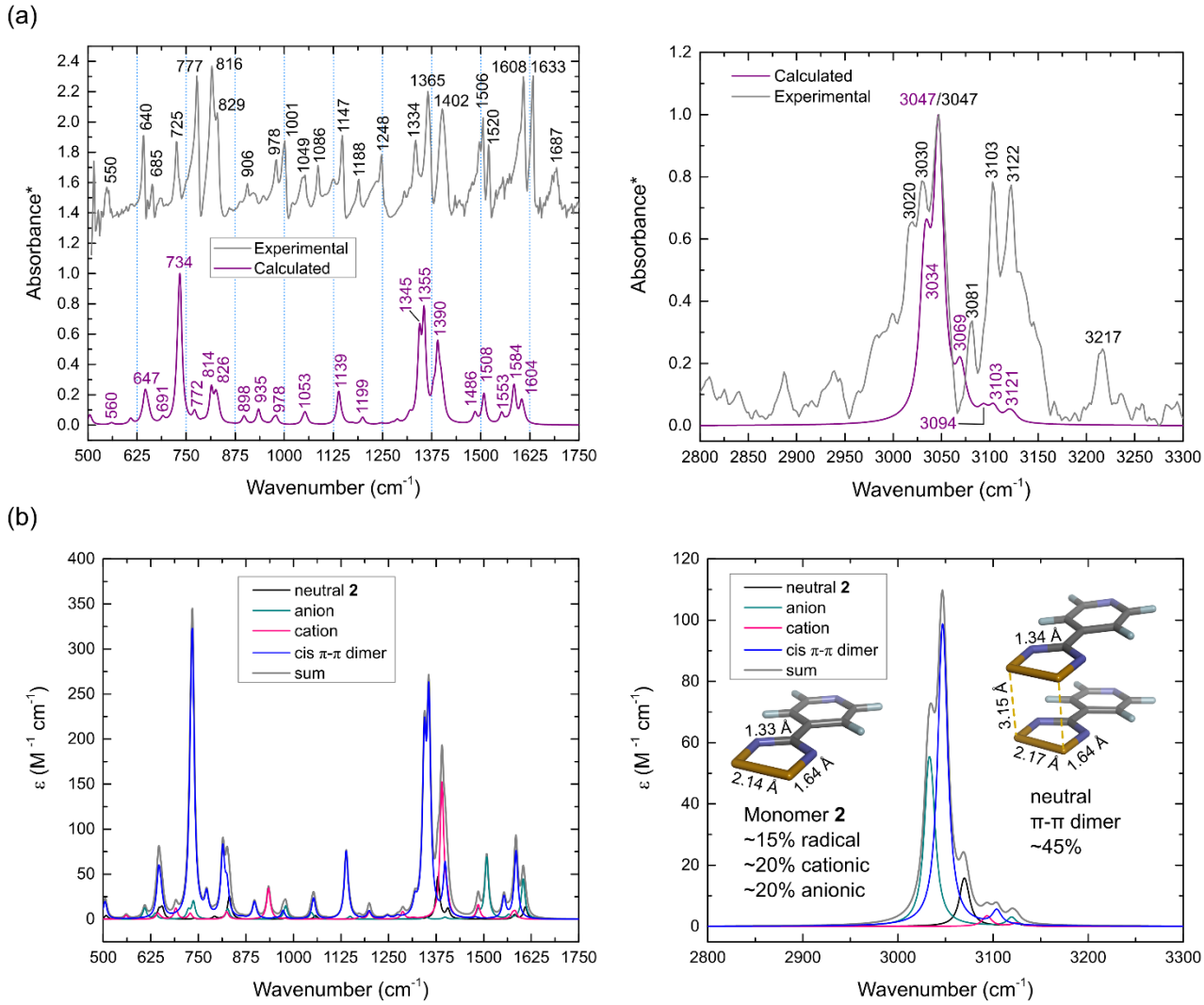

Figure S5. (a) Experimental FTIR spectrum of a representative sample of radical **2** (sublimed solid). The calculated spectrum for 2 embodies the weighted sum of 4 component spectra (6 cm^{-1} peak widths at half height) calculated at the B3LYP/6-31G(d,p) level of theory (gas phase). The calculated frequencies have been scaled by the NIST-published factor of 0.961 for the given method and basis set. Absorbance values are normalized; the absolute scales of the left and right spectra are not the same. (b) Calculated FTIR spectra for several species of **2**. The four spectral components making up the simulated spectral envelope are: neutral monomeric **2** (15%), anionic **2** (20%), cationic **2** (20%), and neutral π–π dimer in cis configuration (45%). In principle, cationic and anionic forms of **2** contributing to the overall spectral envelope of the powder may occur from complete transfer of an electron from one molecule of **2** to another. A recent solid-state charge-density study[20] on the perfluorinated analogue of **2** suggests that partial charge transfer between radicals in the condensed phase is actually feasible. Vibrational mode assignments based on matching the calculated spectral envelope to the experimental envelope are tabulated in Table S4.

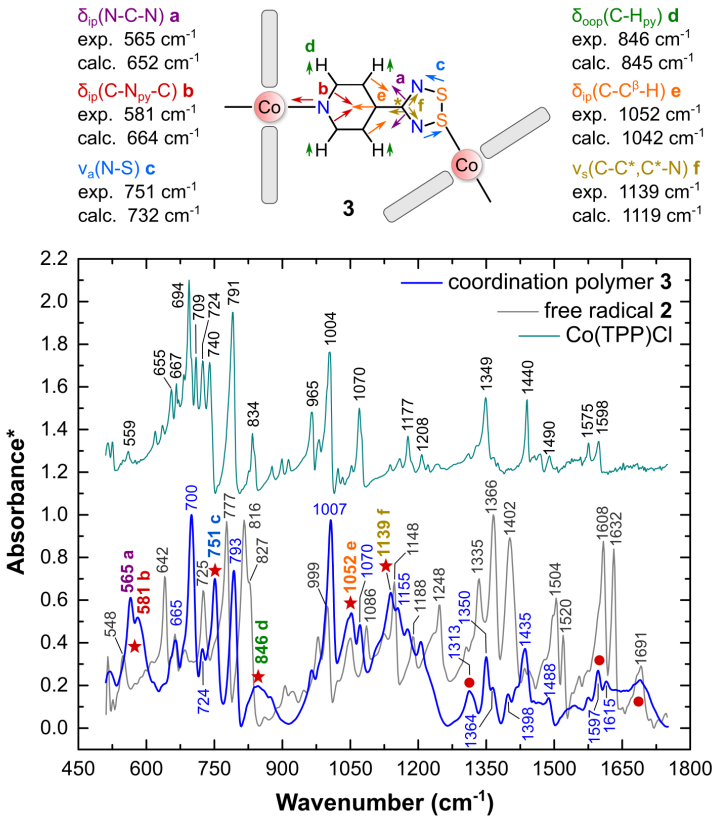

Figure S6. Solid state FTIR spectra of coordination polymer **3**, sublimed radical **2**, and Co(TPP)Cl as a reference. This figure is reproduced from the main paper to permit further discussion of the low frequency band assignments.

Comments on Figure S6. The in-plane bending vibration δ_{ip}(N–C–N) for the DTDA ring (band **a**) shifts to a lower frequency relative to the parent solid radical (725 cm^{-1} in **2**; 565 cm^{-1} in CP **3**). The experimental shift of 160 cm^{-1} is greater than that calculated for two isolated repeat units, $\{\mathbf{3}\}_2$, of the CP ($\overline{\nu}$, 652 cm^{-1}; $\Delta\overline{\nu}$, 73 cm^{-1}) and the antisymmetric and symmetric modes are separated by only a few wavenumbers, accounting (in part) for the broadened band at 565 cm^{-1} in the experimental spectrum of CP **3**. The symmetric in-plane bending vibration for the pyridyl nitrogen, $\delta_{ip/s}$(C–N$_{py}$–C), displays a similar shift of 61 cm^{-1} to lower frequency from 642 cm^{-1} in **2** to 581 cm^{-1} in CP **3** (band **b**). For both ring bending modes to shift to lower energy upon sandwiching **2** between Co(TPP) moieties, a substantial change in the electronic structure of the py-DTDA ligand would be required. Although the absolute calculated frequency (664 cm^{-1}) for this mode in $\{\mathbf{3}\}_2$ is a relatively poor match for the experimental frequency, the calculated frequency difference (12 cm^{-1}) for the two diagnostic bands (**a** and **b**) is consistent with that measured experimentally (16 cm^{-1}). Vibrational mode **c** is discussed in the main text of the paper; its large negative frequency shift reflects charge transfer from the metal ion to the bridging py-DTDA ligand. Complete transfer of the electron in the 3dz^2 orbital of Co^{II}(TPP) to the py-DTDA ligand would give a polymer repeat unit best formulated as Co^{III}(TPP)(*S*-py-DTDA$^-$), which would be diamagnetic (consistent with clean preparations of CP **3** which are EPR-silent). More generally, fractional electron transfer of *n* units of charge with no change in spin quantum number would, in principle, give a diamagnetic polymer repeat unit Co$^{(2+n)+}$(TPP)(*S*-py-DTDA^{n-}). Hence, *n* may assume any integer or non-integer value. For the present system with Co as the metal and its typical stable oxidation states of +2 and +3, *n* is likely to have integer limits of 0 and 1; non-integer values between 0 and 1 then reflect fractional electron transfer.

Bending vibrational modes **d** (846 cm^{-1}), **e** (1052 cm^{-1}), and stretch-bend mode **f** (1139 cm^{-1}) involve the pyridine ring of **3**. Mode **d** is the out-of-plane deformation of the ring hydrogen atoms, $\delta_{oop}(C–H_{py})$, while mode **e** involves in-plane angular deformations of the pyridyl C–H groups closest to the DTDA ring, $\delta_{ip}(C–C–H)$. Mode **f** is the in-plane stretch-bend vibration of the pyridine carbon atom linked to the DTDA ring which involves coupled C–C and $C–N_{DTDA}$ stretching deformations and may be written as the combination: $\nu(C–C_{DTDA}, C_{DTDA}–N_{DTDA})$, $\delta_{ip}(C–C^{4}_{py}–C)$. In the unbound radical, **2**, bands **d**–**f** occur at 827, 1049, and 1148 cm^{-1}, respectively. Coordination of **2** to Co(TPP) to form 1D chain structure **3** shifts and broadens the vibrational frequencies of these diagnostic modes. Band **d** in the CP shifts the most to higher frequency (~20 cm^{-1}); overlap with the $\delta_{oop}(C\text{-}H_{pyrrole})$ band of Co(TPP) (~834 cm^{-1}) accounts for the particularly broad nature of the band observed for the polymer in this spectral range. Of the three bands, only the stretch-bend combination mode **f** shifts to lower frequency ($\Delta\overline{\nu}$, 11 cm^{-1}) in polymeric **3**, perhaps because partial reduction of the DTDA ring via MLCT increases the N–C–N bond angle (Figure 2, main paper) and thus the intrinsic strain in the heterocyclic ring. The steric and electronic effects underpinning the magnitude of the positive frequency shift for vibrational mode **f** are likely counterbalanced by the shorter $C_{DTDA}–N_{DTDA}$ bonds for fully or partially anionic states of py-DTDA (Figure 2, main paper).

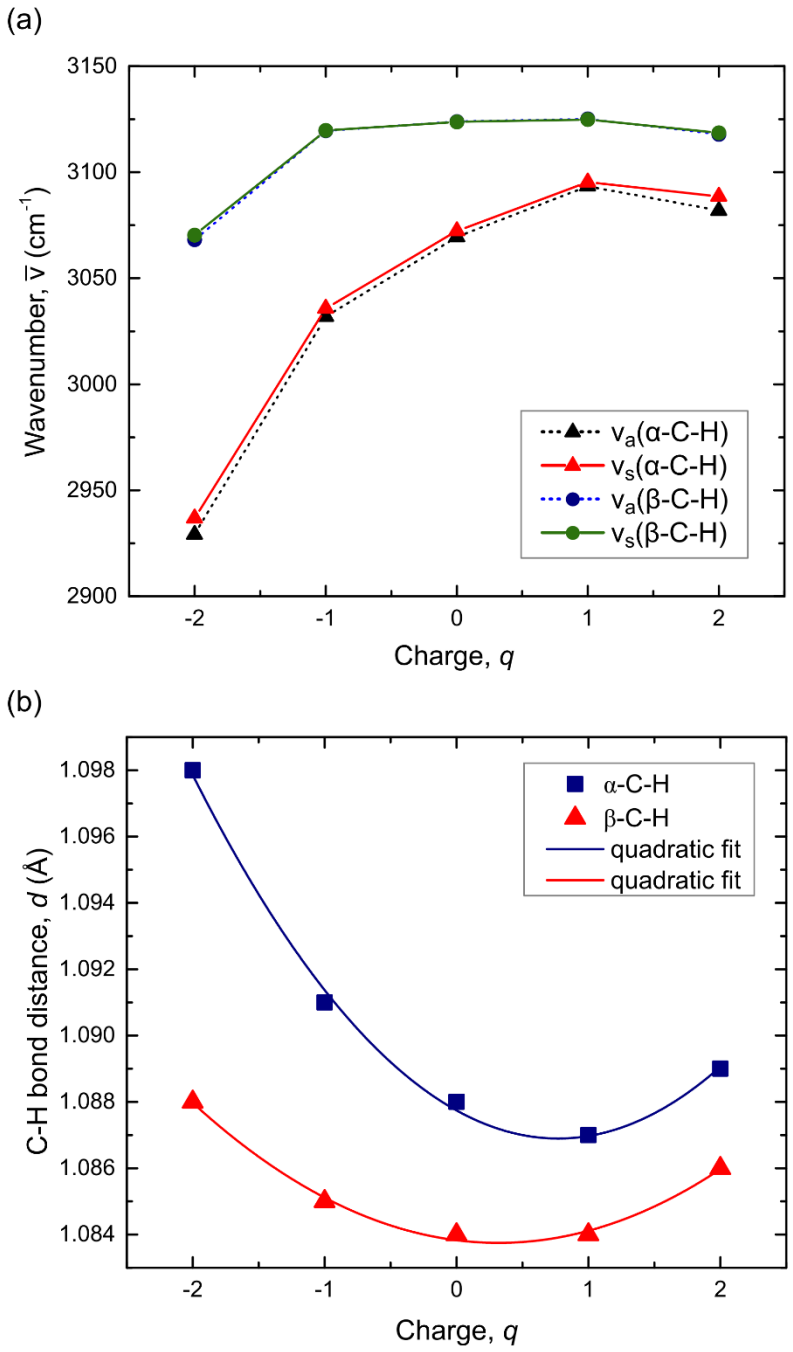

Figure S7. (a) Graph of the DFT-calculated C–H stretching frequencies (symmetric and antisymmetric modes) for the pyridyl CH groups of py-DTDA (compound **2**) as a function of the molecular charge; the α-CH groups are adjacent to the pyridine N atom. (b) Graph of the DFT-calculated C–H bond distance as a function of the molecular charge for py-DTDA in different redox states. Comparing the data from the two plots shows: (i) that longer C–H distances correlate with lower bond stretching frequencies and (ii) that the α- and β-CH groups have intrinsically different bond lengths and hence stretching frequencies due to their slightly different bond orders (or force constants in classical mechanics).

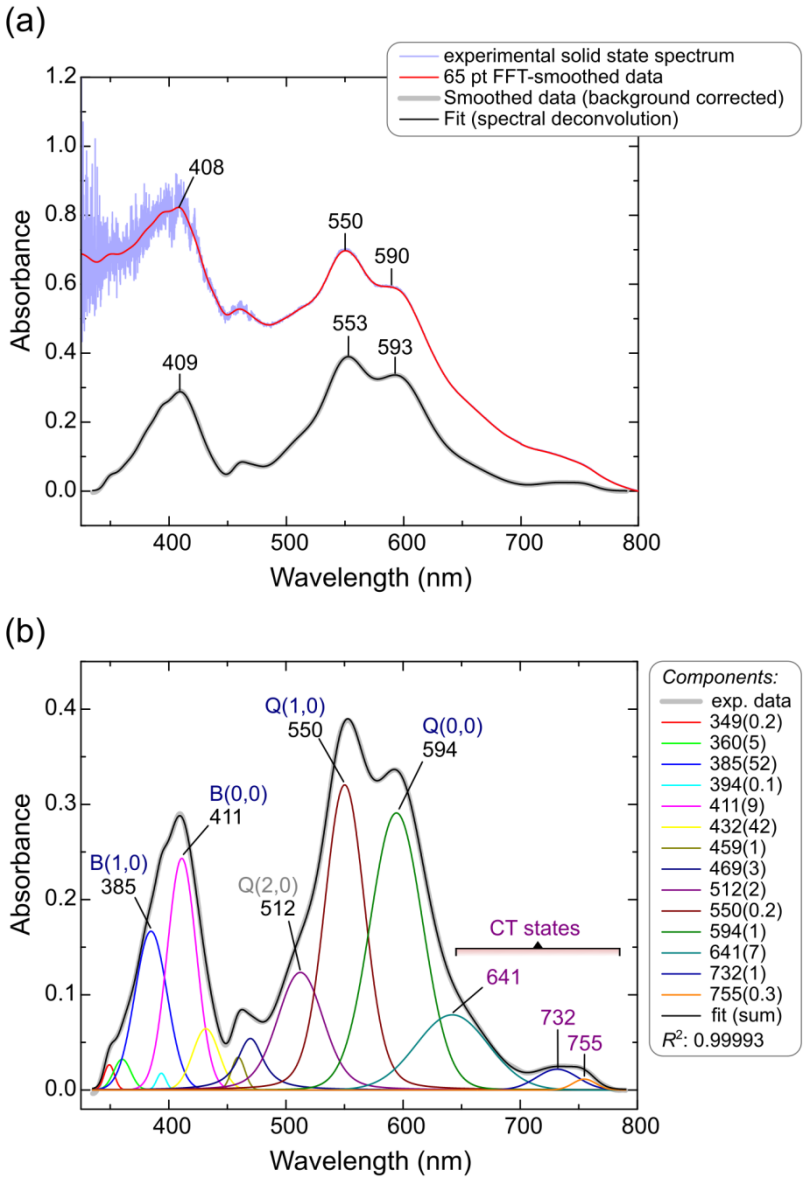

Figure S8. Solid-state UV-visible-NIR absorption spectrum of CP **3**. (a) Details of data smoothing and background subtraction. (b) Deconvoluted (Voigt functions) experimental solid state electronic spectrum of coordination polymer **3**. The band assignments are discussed in the paper.

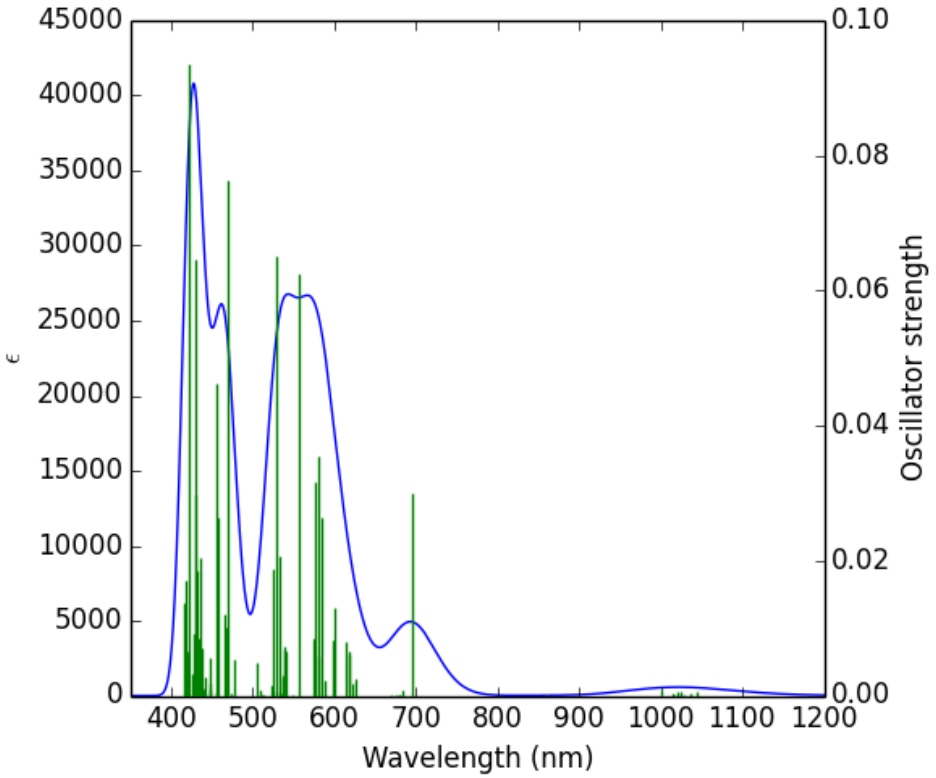

Figure S9. Full range TD-DFT calculated spectrum of solid state tetrameric {**3**}$_4$. A full list of the 140 transitions and their MO components making up the spectrum is given in Table S6. The spectral envelope is plotted as molar absorptivity (left axis, ε, M^{-1} cm^{-1}) with an intrinsic band width of 1400 cm^{-1} (full width at half maximum) for each transition. Transition energies are represented as vertical green lines with heights governed by the oscillator strength (right axis) for the transition.

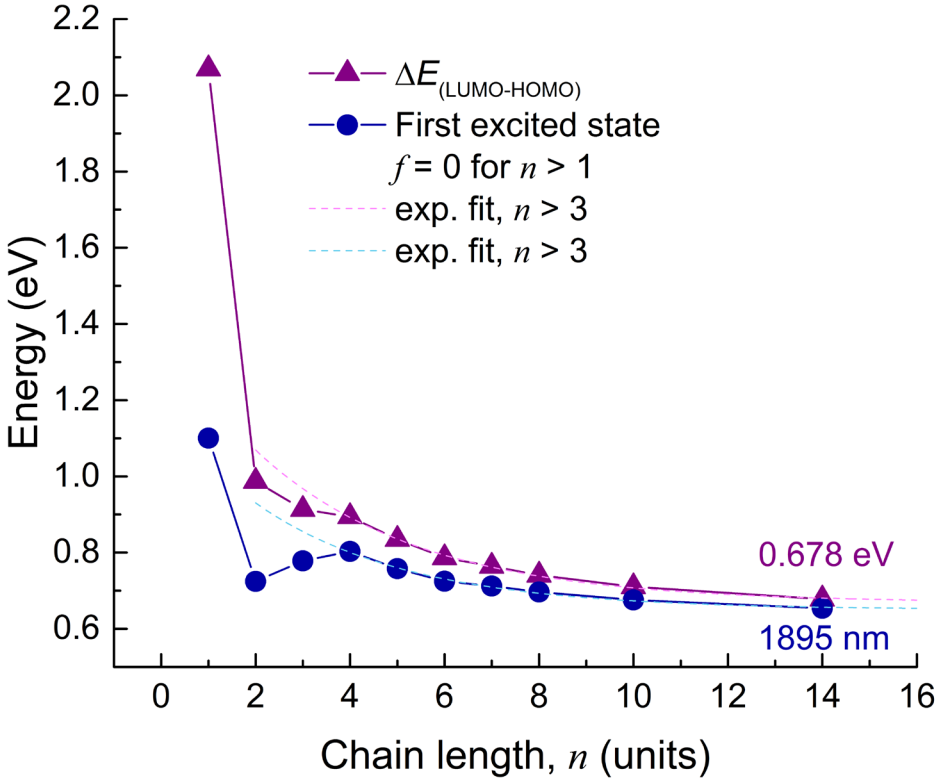

Figure S10. Graph of the DFT-calculated frontier molecular orbital (FMO) energy gap and first excited state energies for 1D CP **3** (X-ray coordinates) vs. chain length. The FMO energy gap at infinite chain length will be equivalent to the band gap of the material.

Curve fitting of Figure S10. Standard exponential decay functions ($E_n = A_1 e^{(n/t_1)} + E_0$) may be used to fit the data in Figure S10 to determine the rate at which the energy changes as a function of the unit increase in polymer chain length, *n*. (Note that *n* could also be viewed as the Co···Co separation in the chain. In the crystalline solid, the Co···Co distance measures 9.594(2) Å, equating to a unit length size, *n*, of 0.96 nm.) The exponential curves fitting the energy terms for the CP (when $n >$ **3**) are as follows.

(i) Frontier molecular orbital (FMO) energy gap:

$\Delta E_{(\text{LUMO–HOMO})} = 0.72(5)e^{(-n/3.4(2))} + 0.669(6)$ eV, $R^2 = 0.996$

(ii) First excited state:

$E_{(1)} = 0.52(6)e^{(-n/3.2(3))} + 0.650(6)$ eV, $R^2 = 0.992$

The "time" constant, τ, governing the exponential decrease of the FMO energy gap with increasing chain length is 2.38(17) unit^{-1}, which yields a "half-life" for the decay of 1.7(1) unit^{-1}. In other words, the value of $\Delta E_{(\text{LUMO–HOMO})}$ is reduced by 50% relative to the limiting energy gap, E_0, of 0.669(6) eV for each 1.7 unit length increase in the CP chain. The limiting energy gap is equivalent to $\Delta E^{\infty}_{(\text{LUMO–HOMO})}$ and is the predicted FMO gap energy for an ordered 1D material comprising chains of **3** of infinite length that are electronically non-interacting (i.e., limited lateral chain···chain MO interactions or overlaps in 2D). The first excited state energy follows a similar pattern to the FMO energy gap.

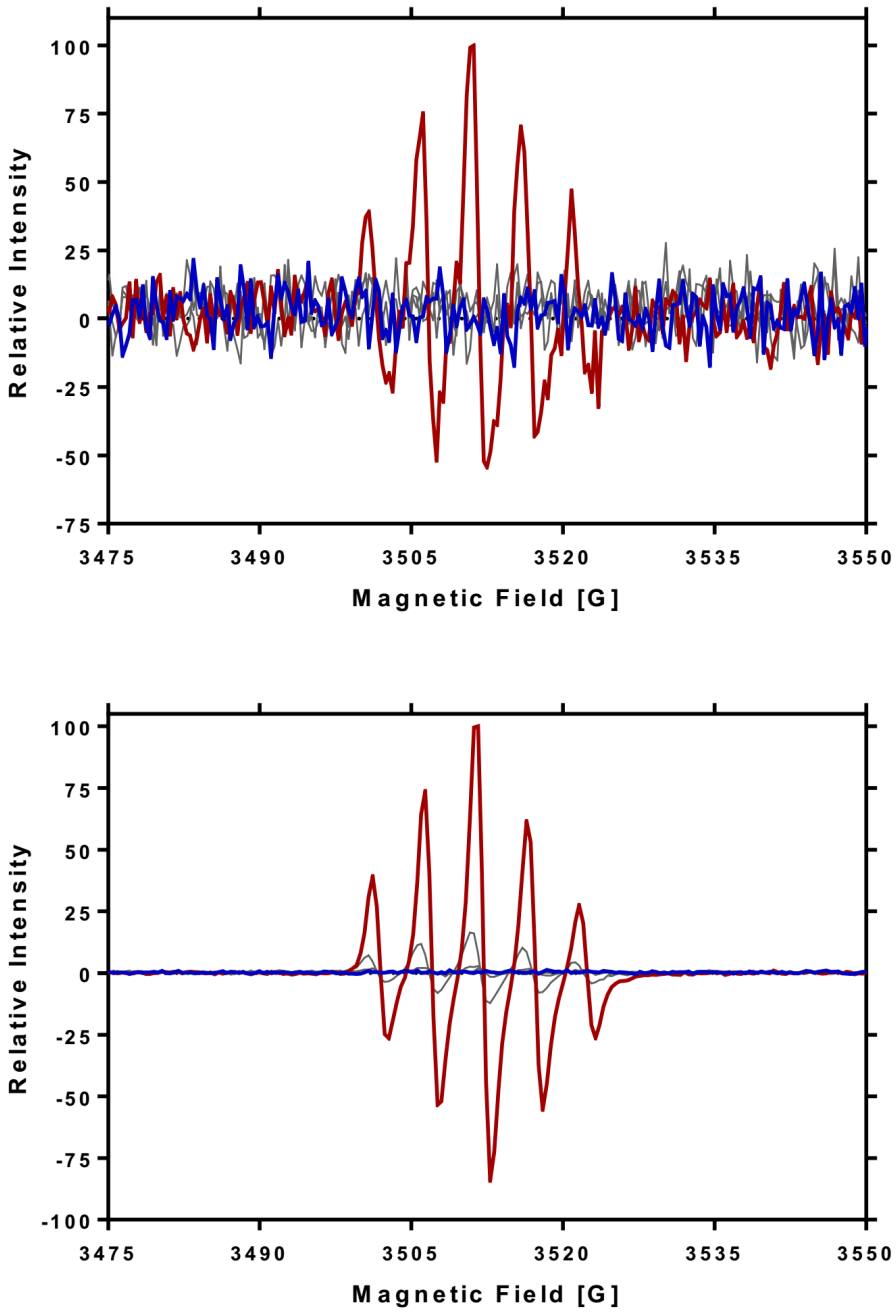

Figure S11. EPR titration spectra (X-band) for py-DTDA$^{\bullet}$ (**2**, top) and Ph-DTDA$^{\bullet}$ (bottom) in DCM with increasing Co^{II}(TPP) (**1**) concentration, at ambient temperature, forming Co^{II}(TPP)(*S*-py-DTDA) and Co^{II}(TPP)(*S*-Ph-DTDA), respectively. The original (starting) dithiadiazolyl radical spectrum is shown in red. The final addition of Co^{II}(TPP) is shown in blue with intermediate additions shown in grey.

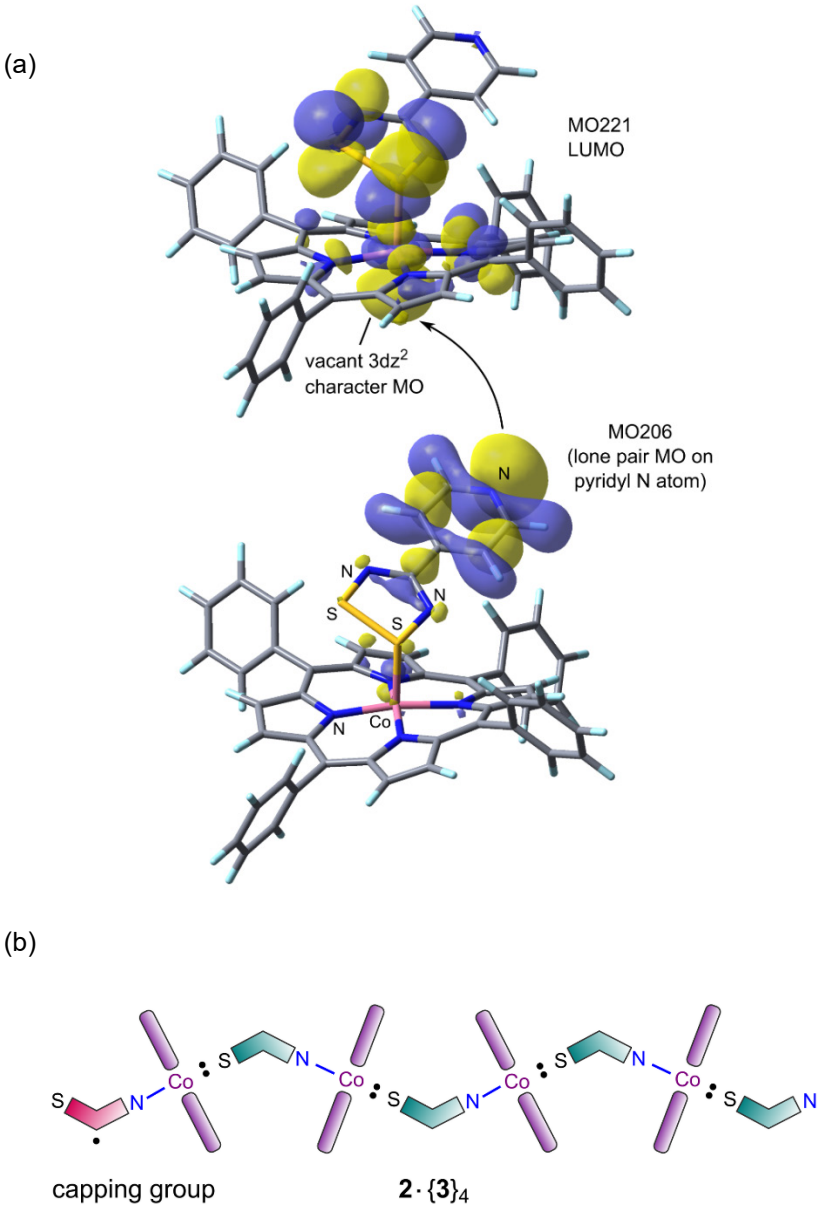

Figure S12. (a) Depiction of the most likely FMO interaction between two 5-coordinate monomeric Co(TPP)(S-py-DTDA) complexes that leads to chain growth by Co–N bond formation and oligomerization to 1D CP **3**. (b) Illustration of a tetramer chain unit for CP **3** in which formerly unpaired spins become spin paired in Co–S bonds of coupled radicals. The Co–N bonds (blue) are normal dative covalent bonds in the 1D metal-organic chain structure. The chain growth direction is from left to right.

Comment on Figure S12. If a slight excess of radical **2** exists in the system, it may cap the chain end to form a 6-coordinate complex. The unpaired spin would be expected to be localized in a MO on the capping ligand's DTDA ring in the ground state and could contribute to a typical EPR signal for the solution phase radical (py-DTDA•) such as that shown in Figure S11 for a solution sample of such a species. In the solid state, the signal from randomly oriented chain ends (powder sample) would likely be broad and centered on g = 2.0. Tight control of reaction stoichiometry and the reagent addition order allows the synthesis of EPR-silent solid CP **3**; the diamagnetic material lacks the capping group. In some preparations, a blue-green

material is produced as a minor component along with CP **3**; this material gives an EPR signal typical of py-DTDA$^{\bullet}$ in solution and may reflect de-polymerization and dissociation of oligomer species such **2**$\cdot\{\mathbf{3}\}_4$. A definitive assignment for the blue-green material is the subject on ongoing work.

Regarding the mechanism of de-polymerization of CP **3**, or the reverse process (oligomerization of monomers **3a** or **3b**), shown in Figure 10 of the main paper, we note that repetitive coupling of monomer **3a**/**3a′** to give $\{\mathbf{3}\}_n$ would yield a growing (or living) chain end with a free pyridyl group; coupling monomer **3b**/**3b′**, in contrast, affords a chain end with a free DTDA ring. The CP chains produced are thus distinct at both chain ends and are unique polymers with specific directionality, namely $\cdots\{\text{Co–S–R–N}\}_n\cdots$, or $\cdots\{\text{Co–N–R–S}\}_n\cdots$. However, because the macromolecule is the chromophore that determines the electronic properties of $\{\mathbf{3}\}_n$, the monomer coupling or de-coupling mechanism cannot be readily delineated from the optical spectrum of the oligomer or the exponential growth model used to fit the data (Figure 9c, main paper).

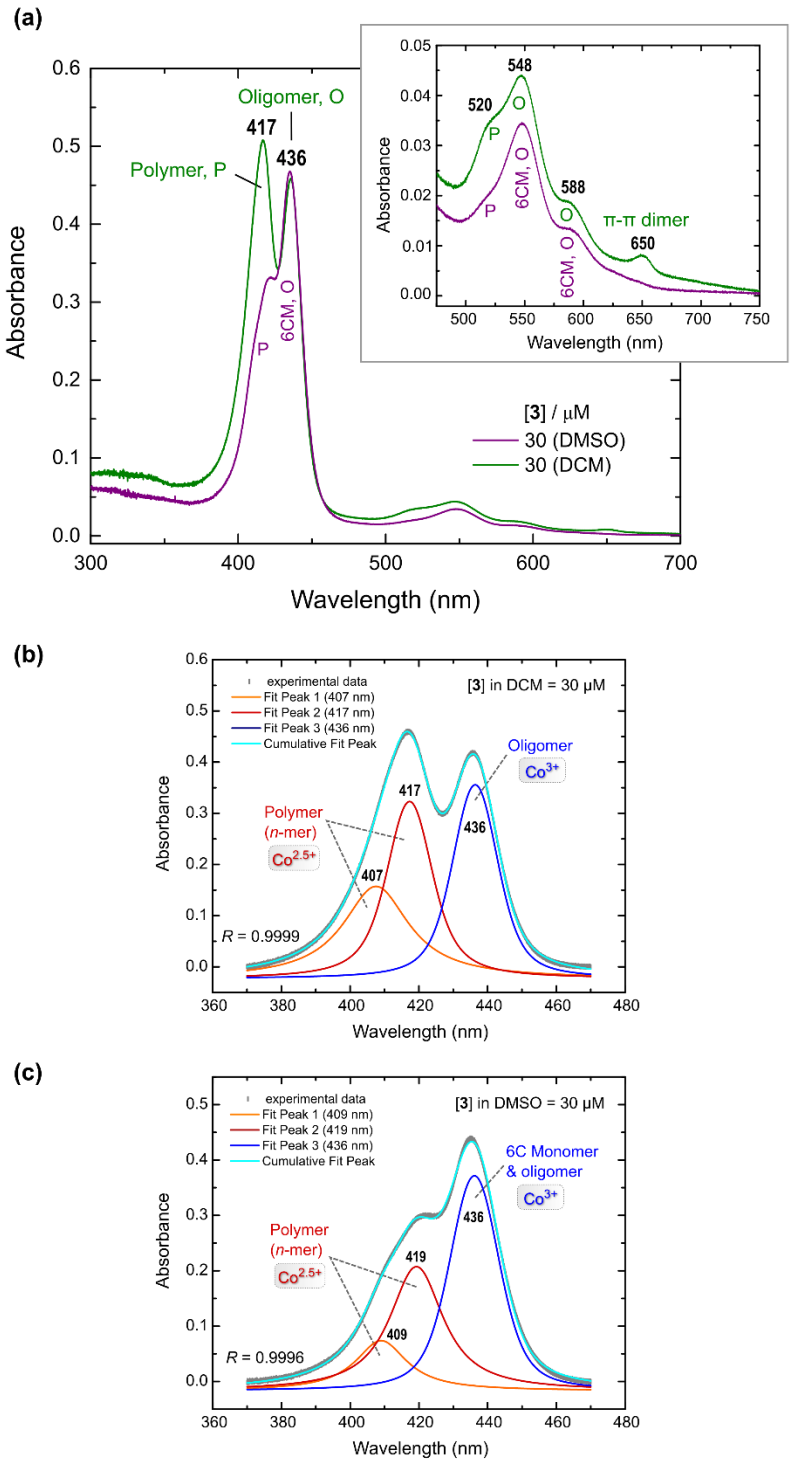

Figure S13. (a) Comparison of the spectra of CP **3** recorded in DMSO and DCM at a concentration of 30 μM (ambient temperature). (b) Deconvoluted (Voigt functions) UV spectrum of 30-μM CP **3** in dichloromethane. (c) Deconvoluted (Voigt functions) UV spectrum of 30-μM CP **3** in DMSO). DMSO clearly monomerizes the coordination polymer to a greater degree than DCM through the formation of 6-coordinate Co^{III}(TPP)(N-py-DTDA)(*O*-DMSO), species **3b**·(*O*-DMSO), as evidenced by ^{1}H NMR spectroscopy (Figure S18). Abbreviations: 6CM, 6-coordinate monomer; M, monomer; O, oligomer; P, polymer.

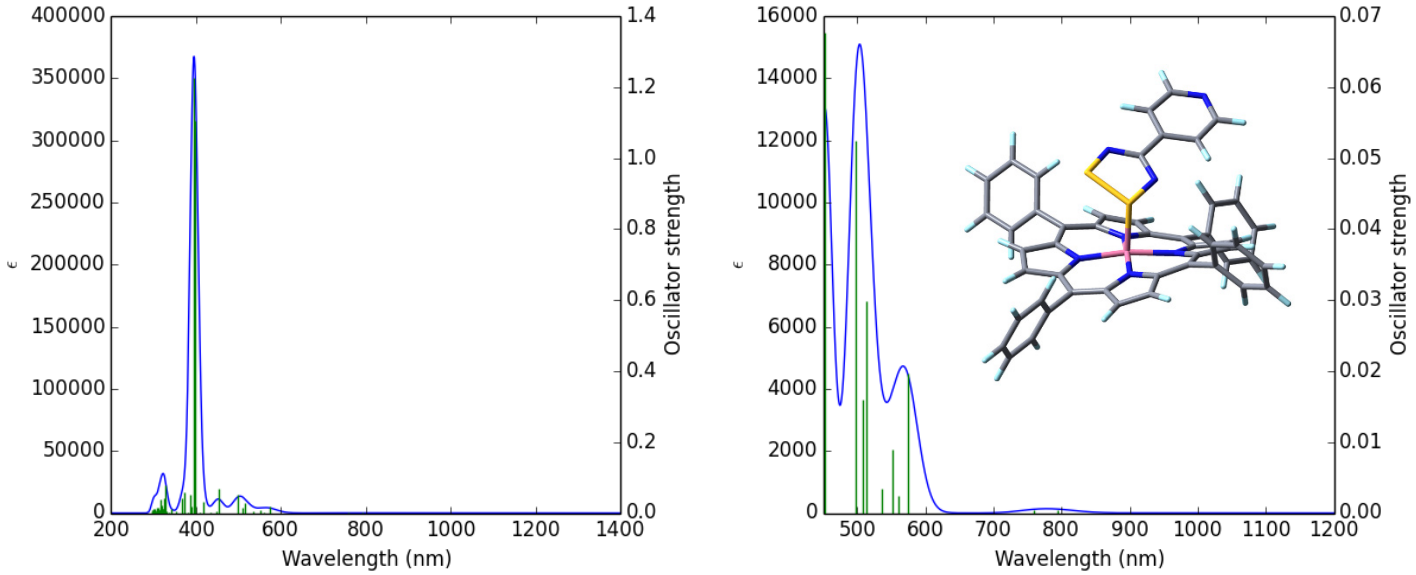

Figure S14. TD-DFT calculated electronic spectra (60 excited singlet states) for 5-coordinate Co(TPP)(*S*-py-DTDA), species **3a**, in 1,2-dichloroethane. Left: full spectral range. Right: visible region. The spectral envelope is plotted as molar absorptivity (left axis, ε, M^{-1} cm^{-1}) with an intrinsic band width of 1400 cm^{-1} (full width at half maximum) for each transition. Transition energies are represented as vertical green lines with heights governed by the oscillator strength (right axis) for the transition.

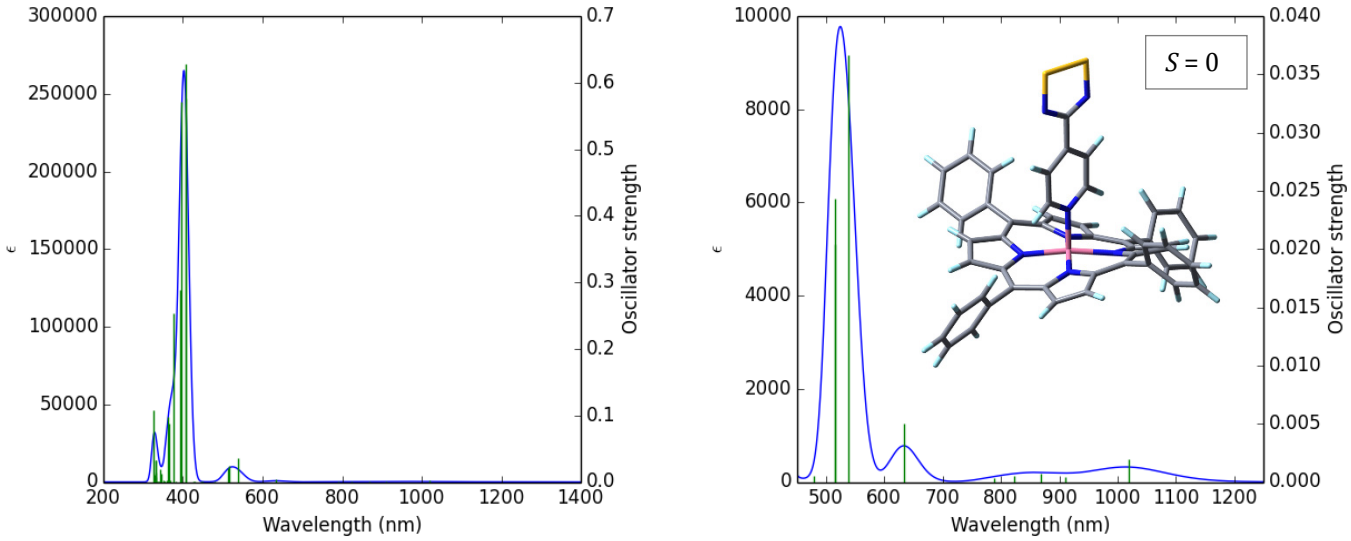

Figure S15a. TD-DFT calculated electronic spectra (60 excited singlet states) for low-spin (*S* = 0) 5-coordinate Co(TPP)(*N*-py-DTDA), species **3b**, in 1,2-dichloroethane. Left: full spectral range. Right: visible region. The spectral envelope is plotted as molar absorptivity (left axis, ε, M^{-1} cm^{-1}) with an intrinsic band width of 1400 cm^{-1} (full width at half maximum) for each transition. Transition energies are represented as vertical green lines with heights governed by the oscillator strength (right axis) for the transition.

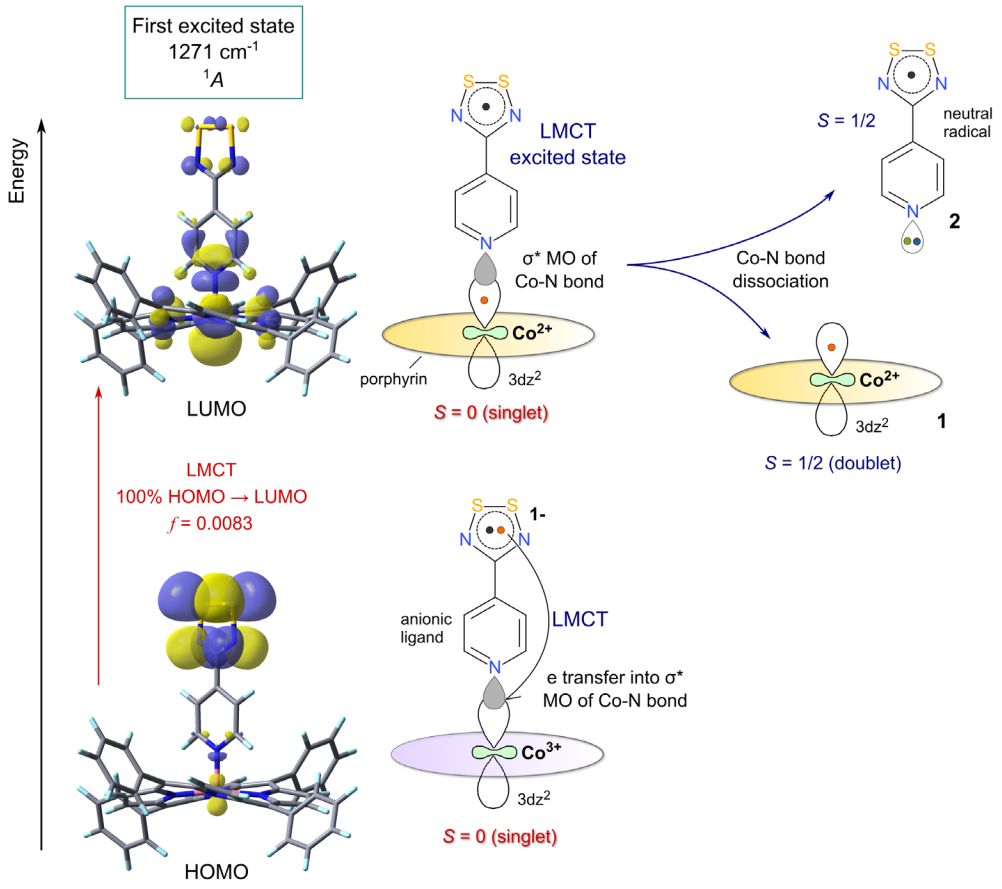

Figure S15b. Illustration of one possible disproportionation pathway (photochemical) for species **3b**. The lowest-energy transition is a LMCT transition from the HOMO to the LUMO of **3b**. Transfer of the electron into the σ* MO of the Co–N bond is expected to enhance bond dissociation by decreasing the Co–N bond order from 1 to 0.5. The first excited state occurs at 7867 nm in the thermal IR region of the spectrum. Dissociation of the axial ligand after electron transfer generates neutral radical **2** and the Co(II) porphyrin **1**. These species are seen in the UV-visible-NIR spectrum of the system at high dilution (Figure 11a of the main paper).

Comment on Figure S15b and disproportionation of 3b. The lowest-energy excited singlet state for **3b** in 1,2-dichloroethane is produced by transfer of an electron from the doubly-occupied HOMO (based almost entirely on the DTDA ring) to the LUMO (the σ* MO for the Co–N bond). The relevant transition is given in Table S9. This LMCT transition occurs at very low energy (1271 cm^{-1}, 7867 nm) and has a moderate oscillator strength (0.083). The transition would, in the limit of complete transfer of an electron, represent the reaction of eq 1:

$$\underset{\textbf{3b}\ (^1A)}{Co^{III}(TPP)(N\text{-py-DTDA}^-)} + h\nu \rightleftharpoons \underset{\textbf{3b*}\ (^1A)}{Co^{II}(TPP)(N\text{-py-DTDA})} \qquad (1)$$

Since the energy of the excited state **3b*** is only 15.2 kJ mol^{-1} above the ground state, the excited state is thermally accessible at 298 K (the Boltzmann factor is 0.0022). Moreover, transfer of the electron to the σ* LUMO with mainly $3d^2$ character and a nodal plane bisecting the Co–N bond is expected to lead to marked elongation and weakening of the Co–N bond resulting in dissociation of the free radical (eq 2).

$$\underset{\textbf{3b*}\ (^1A)}{Co^{II}(TPP)(\textit{N}\text{-py-DTDA})} \rightarrow \underset{\textbf{1}}{Co^{II}(TPP)} + \underset{\textbf{2}}{\text{py-DTDA}} \qquad (2)$$

The mechanism in eqs 1 and 2 amounts to internal electron transfer with concomitant axial ligand dissociation and may be classified as thermally- or electromagnetically-induced disproportionation. Photochemical ligand dissociation mechanisms are known; one of the best examples is the fast intramolecular dissociation of a pyridine axial ligand donor from a flexible tripodal chelator in the complex $[Ru(TPA)(bpy)]X_2$ (X = ClO_4, PF_6),[21] where bpy = 2,2′-bipyridine and TPA = tris(2-pyridylmethl)amine. In this example, visible light MLCT excitation induces the photochemical ligand dissociation. In the case of **3b**, thermal IR radiation would easily excite the broad band at 7.867 μm in the electronic spectrum, promoting ligand dissociation. At higher concentrations, **1** and **2** will combine by radical coupling to generate **3a** (which is more stable than the original species **3b**) and thence $\{\mathbf{3}\}_n$ upon oligomerization. Delineation of this mechanism would require a full study of the photophysical and photochemical behavior of **3b** going forward.

An alternative disproportionation mechanism, which is possibly more complicated, can also be considered. The DFT-calculated energies in 1,2-dichloroethane for **3a** and **3b** (Figure 10 of the main paper) reveal that **3b** is unstable enough (by > 50 kJ mol^{-1}) to isomerize to **3a**. The question is what chemical mechanism might allow this to happen? With **3b** the expectation is that such isomerization would involve dissociation of the anionic axial ligand $\mathbf{2}^-$, with concomitant release of $[Co^{III}(TPP)]^+$. Because DTDA anions are powerful reducing agents,[22] immediate reduction of $[Co^{III}(TPP)]^+$ by the outer-sphere anion (in what would formally be the ion pair or salt $[Co^{III}(TPP)][\mathbf{2}]$) to $Co^{II}(TPP)$, **1**, and free radical **2** is likely. Mechanistically, all that would happen is that the anion $\mathbf{2}^-$ would recombine with the cation through Co–S bond formation, which would give a species isoelectronic with **3a** via intramolecular electron transfer because the doubly-occupied HOMO of the anion would overlap with the vacant $3dz^2$ atomic orbital of $[Co^{III}(TPP)]^+$ to form the Co–S bond. As far as the electrons in the bond are concerned, the end result is identical to radical coupling between **1** and **2**.

The ease with which $\mathbf{2}^-$ might reduce $[Co^{III}(TPP)]^+$ may be estimated by considering the one-electron reduction potential of $Co^{III}(TPP)$ in butyronitrile (+0.40 V)[23] and the estimated oxidation potential of $\mathbf{2}^-$ (ca. +0.8 V in acetonitrile).[24] These half-reactions have potentials that combine to give E = +1.2 V, meaning that reduction of $[Co^{III}(TPP)]^+$ by the py-DTDA^- anion is expected to be spontaneous and rapid in the absence of a kinetic barrier. Under appropriate conditions of high dilution one could, in principle, detect both the Co(II) porphyrin **1** and the free radical **2** if Co–S bond homolysis in **3a** is slow on the NMR timescale (refer to Figure 12 of the main paper). The relevant equilibria and subsequent oligomerization of **3a** are depicted in eqs 3–6 below.

$$\underset{\textbf{3b}}{Co^{III}(TPP)(\textit{N}\text{-py-DTDA}^-)} \rightleftharpoons [Co^{III}(TPP)]^+ + \underset{\mathbf{2}^-}{\text{py-DTDA}^-} \qquad (3)$$

$$[Co^{III}(TPP)]^+ + \underset{\mathbf{2}^-}{\text{py-DTDA}^-} \rightleftharpoons \underset{\textbf{3a}}{Co^{II}(TPP)(\textit{S}\text{-py-DTDA})} \qquad (4)$$

$$\underset{\textbf{3a}}{Co^{II}(TPP)(\textit{S}\text{-py-DTDA})} \rightleftharpoons \underset{\textbf{1}}{Co^{II}(TPP)} + \underset{\textbf{2}}{\text{py-DTDA}} \quad \textit{slow} \qquad (5)$$

$$n\ Co^{II}(TPP)(\textit{S}\text{-py-DTDA}) \rightleftharpoons \{\mathbf{3}\}_n \qquad (6)$$

Since the NMR experiments and electronic spectra identifying the presence of **1** and **2** in solutions containing **3b** are conducted at high dilution (16×10^{-6} M), their recombination to form **3a** as a precursor to oligomerization has a statistically low probability and might allow their observation. In contrast, the synthesis of CP **3** involves the reaction between **1** and **2**

at concentrations ≥ 2.2 × 10^{-2} M. The 1000-fold higher reactant concentrations during the synthetic reaction drives the forward radical coupling reaction to give **3a** through the markedly higher collision probability.

A key question that arises is which mechanistic scheme (if any) might be prevalent? As noted, a full investigation would have to be conducted to answer this with any degree of certainty. That said, ^{1}H NMR evidence for **3a** in dilute solutions of CP **3** dissolved in deuterated 1,2-dichloroethane was distinctly lacking (Figure 12, main paper). Specifically, no normal pyridyl α-CH resonance (δ ~8–9 ppm) unperturbed by ring current shielding anisotropy effects from the porphyrin macrocycle was observed. Consequently, we currently favor the mechanism written in eqs 1 and 2 as the most likely origin of the free radicals **1** and **2** observed by ^{1}H NMR and electronic spectroscopy in dilute 1,2-dichloroethane solutions of (dissociated) CP **3**.

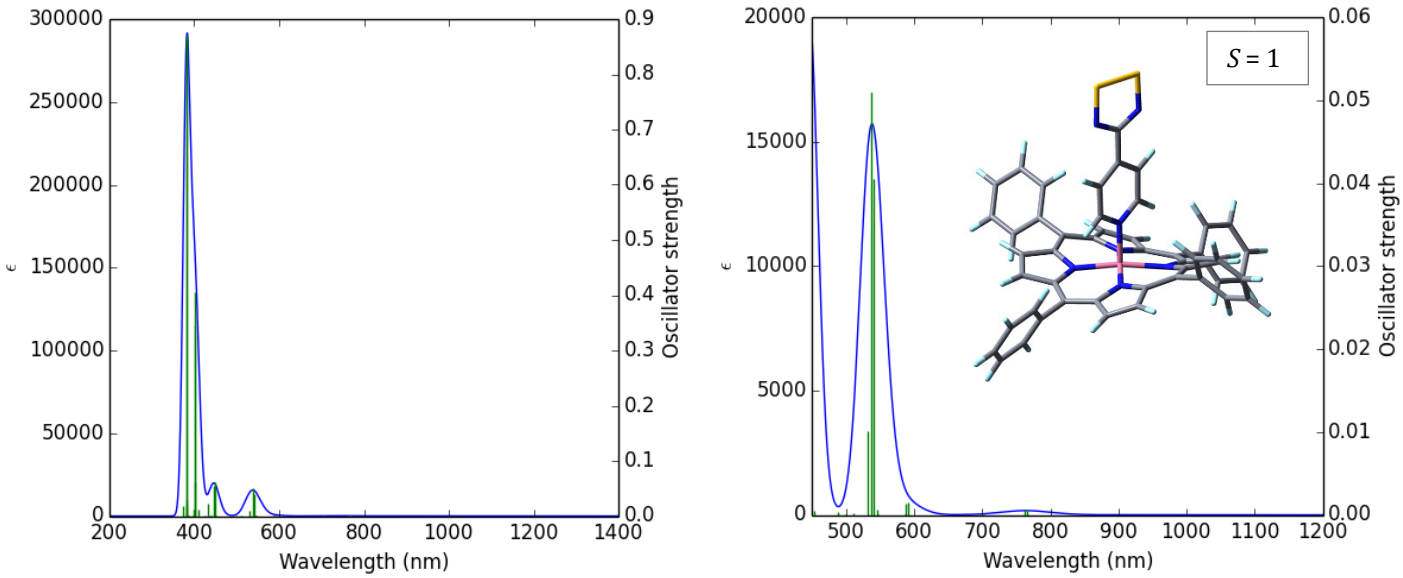

Figure S16. TD-DFT calculated electronic spectra (60 excited states) for high-spin (*S* = 1) triplet state 5-coordinate Co^{II}(TPP)(*N*-py-DTDA$^{\bullet}$), S = 1 species **3b′**, in 1,2-dichloroethane. Left: full spectral range. Right: visible region. The spectral envelope is plotted as molar absorptivity (left axis, ε, M^{-1} cm^{-1}) with an intrinsic band width of 1400 cm^{-1} (full width at half maximum) for each transition. Transition energies are represented as vertical green lines with heights governed by the oscillator strength (right axis) for the transition.

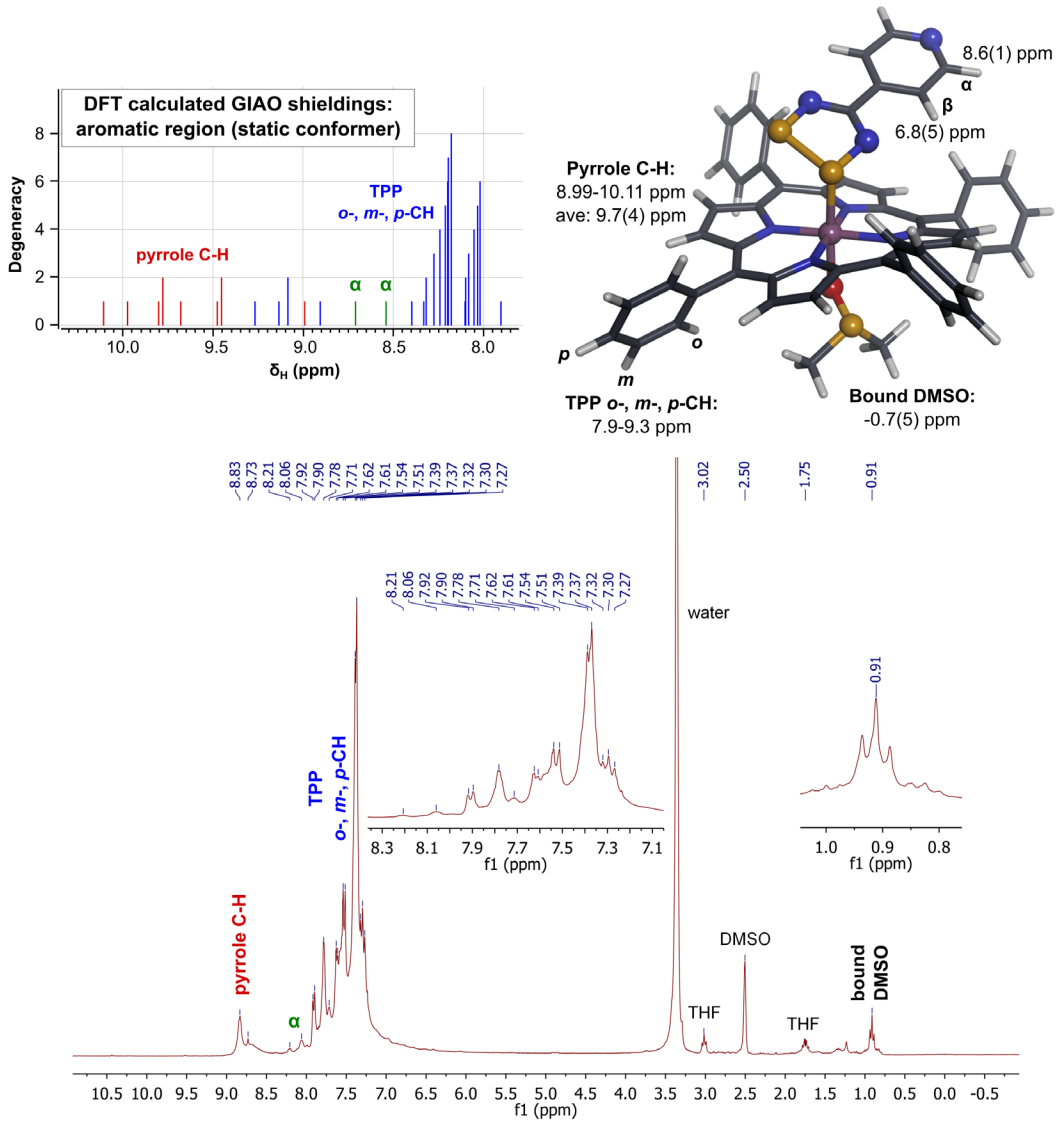

Figure S17. ^{1}H NMR spectrum (300 MHz) of **3a**·(*O*-DMSO)**,** or more formally Co(TPP)(S-py-DTDA)(*O*-DMSO), generated by the reaction of a 1:1.1 mole ratio of Co^{II}(TPP), **1**, and py-DTDA$^{\bullet}$, **2**, in DMSO-d_6. The DFT-calculated structure and GIAO-calculated chemical shift values are given for comparison. The absence of signals in the experimental spectrum between 4.5–6.5 ppm confirms that that axial py-DTDA ligand is not N-bound in this structure.

Comment on Figure S17. The ^{1}H NMR signals are broadened for **3a**·(*O*-DMSO) relative to a typical diamagnetic Co(III) porphyrin. Five-coordinate Co(II) porphyrins axially ligated by pyridines exhibit doublet ground states ($^{2}A_1$) and low-lying ^{2}E excited states which, through spin-orbit coupling, slow the electronic relaxation time (T_{1e}) and commensurately shorten the nuclear spin relaxation times (giving broad signal linewidths).[25,26] Although **3a**·DMSO is diamagnetic, it is still formally a Co(II) porphyrin. For five-coordinate **3a**, our DFT calculations indicate that the ground state (^{1}A) is separated from the

first excited singlet state (^{1}A) by 1.560 eV (795 nm in DMSO). This excited state is thermally inaccessible and inconsequential for the NMR spectrum of ground state **3a**. It is thus possible that the lowest-energy triplet MLCT excited state for **3a** (^{3}A, 0.7325 eV) is partially mixed by spin-orbit coupling with the ^{1}A ground state, thereby increasing the nuclear spin relaxation rate and ^{1}H NMR line widths. Irrespective of the operative mechanism, the broad signals point to a metal oxidation state that is not typical of diamagnetic Co(III).

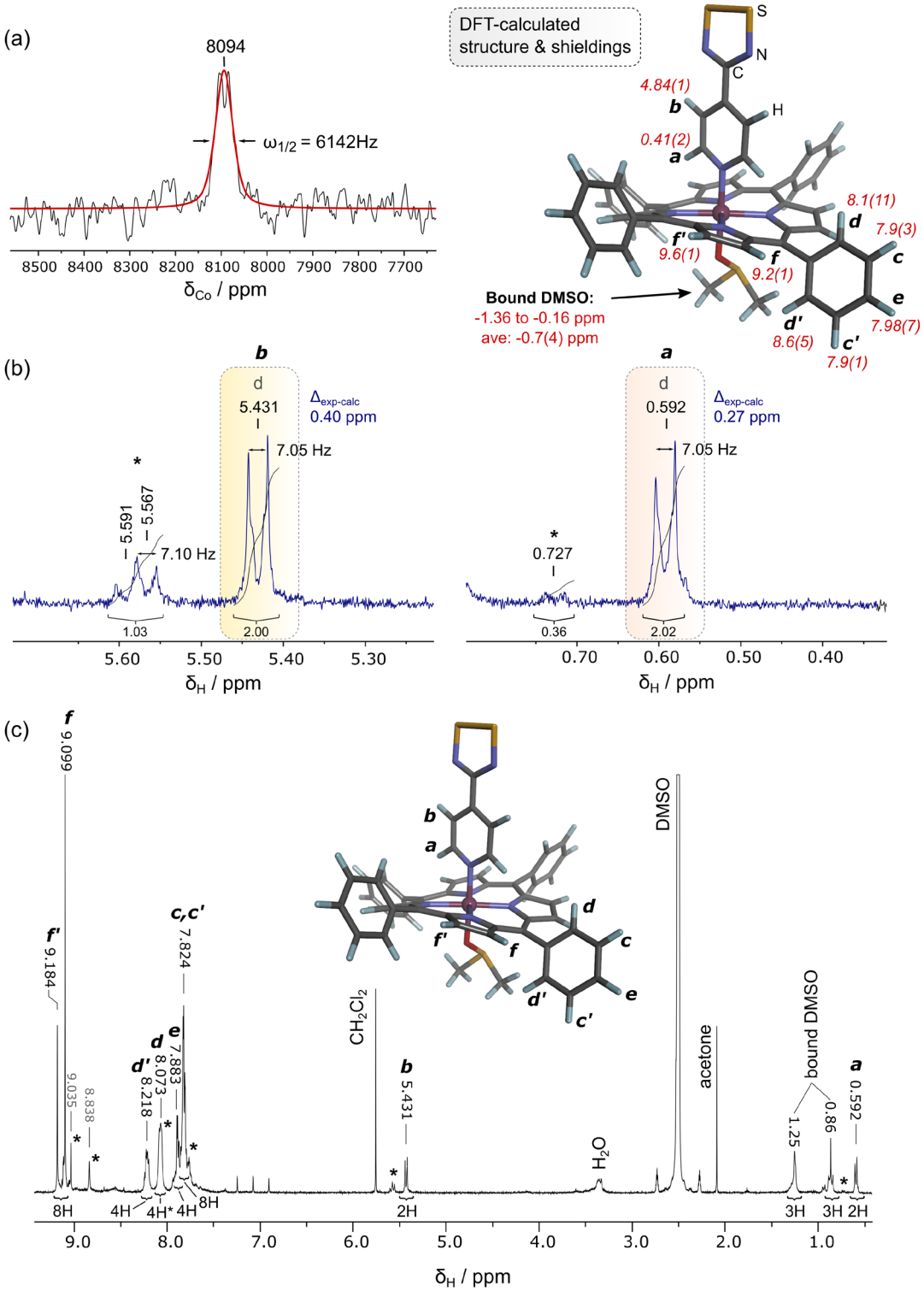

Figure S18. NMR spectra (298 K) of CP **3** dissolved in DMSO-d_6. (a) ^{59}Co NMR spectrum (142.36 MHz). The peak position and linewidth were determined from a least-squares fit of the spectral data to a hybrid Lorentzian-Gaussian function (49% Gaussian). (b) Expansions of the pyridyl proton signals in the ^{1}H NMR spectrum (299.74 MHz). DFT-calculated proton chemical shifts are indicated on the structure (ppm). (c) Full-range ^{1}H NMR spectrum. The coordination polymer **3** dissociates to an equilibrium mixture mostly comprising **3b**·(*O*-DMSO). Evidence for some oligomeric $\{\mathbf{3}\}_n$ is possibly reflected by the additional signals (marked *) that parallel those of **3b**·(*O*-DMSO) in the ^{1}H NMR spectrum. The spectral data confirm that the Co–S bond of CP **3** dissociates when the polymer dissolves.

Comments on the ^{1}H NMR spectra of 3b and $\{3\}_n$ recorded in DCE-d_4. Regarding Figure 12 of the main paper and considering the structure of 1D CP **3** (Scheme S1), perturbation of the magnetic environment close to the py-DTDA ligand is anticipated to be greater than that of the porphyrin peripheral groups in the growing 1D chain. The TPP protons of $\{\mathbf{3}\}_n$ thus exhibit significantly smaller changes in chemical shift upon oligomerization than the bridging py-DTDA ligand relative to monomeric **3b**. The *m*-CH proton signal does shift slightly upfield from 7.77 ppm in monomeric **3b** to 7.75 ppm in $\{\mathbf{3}\}_n$, consistent with increased shielding brought about by *m*-C–H···π(phenyl) interactions (2.90 and 3.25 Å from the X-ray structure of CP **3**) present between the phenyl rings of neighboring TPP molecules in the 1D chain (as evident in Figure 1c).

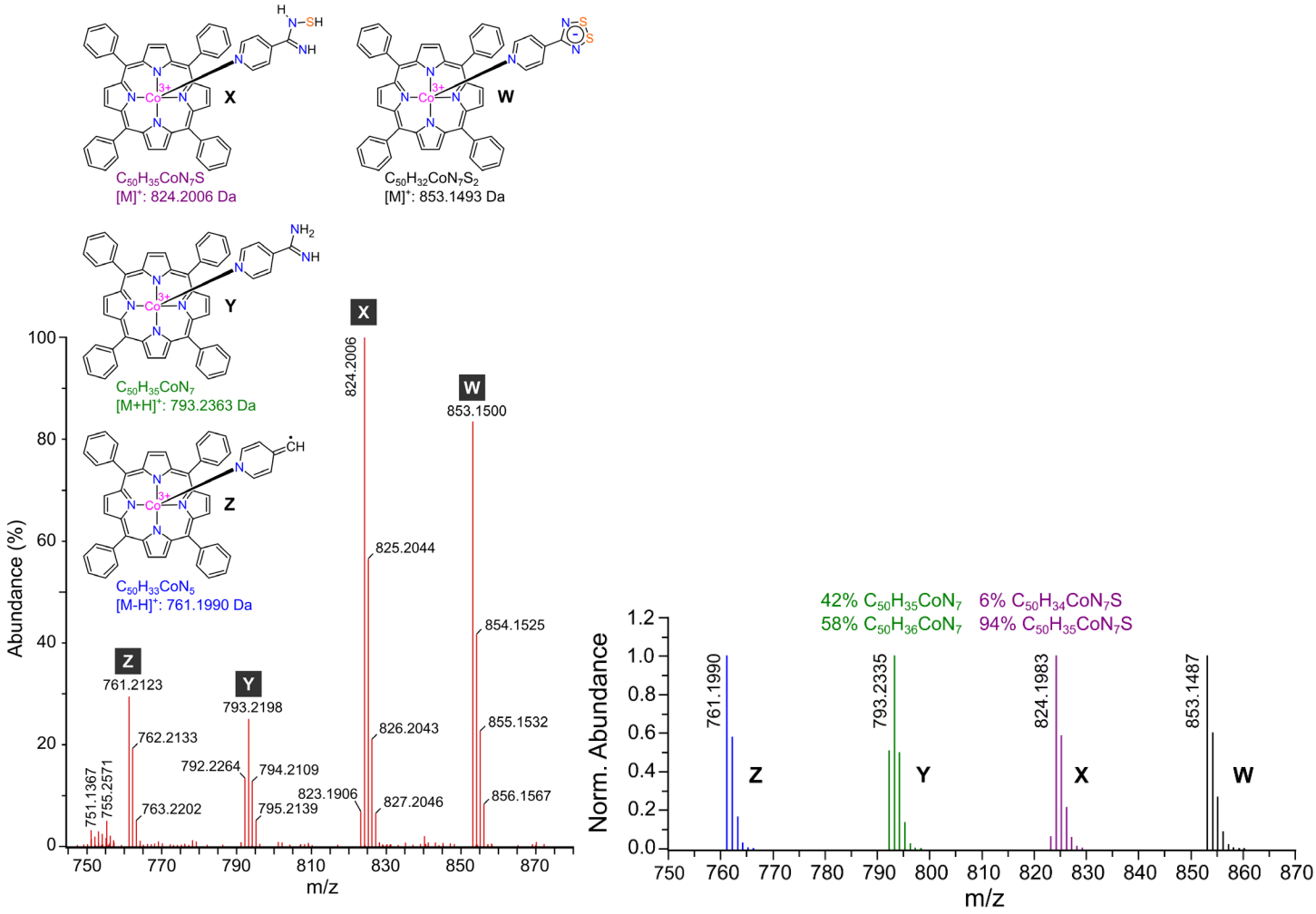

Figure S19. Experimental ESI+ Mass spectrum of CP **3** dissolved in acetonitrile (left) with fragment assignments and calculated monoisotopic masses. The calculated mass spectral signal patterns (IsoPro 3.1) expected from fragments **W** through **Z** are shown at the lower right side of the figure on a normalized abundance scale.

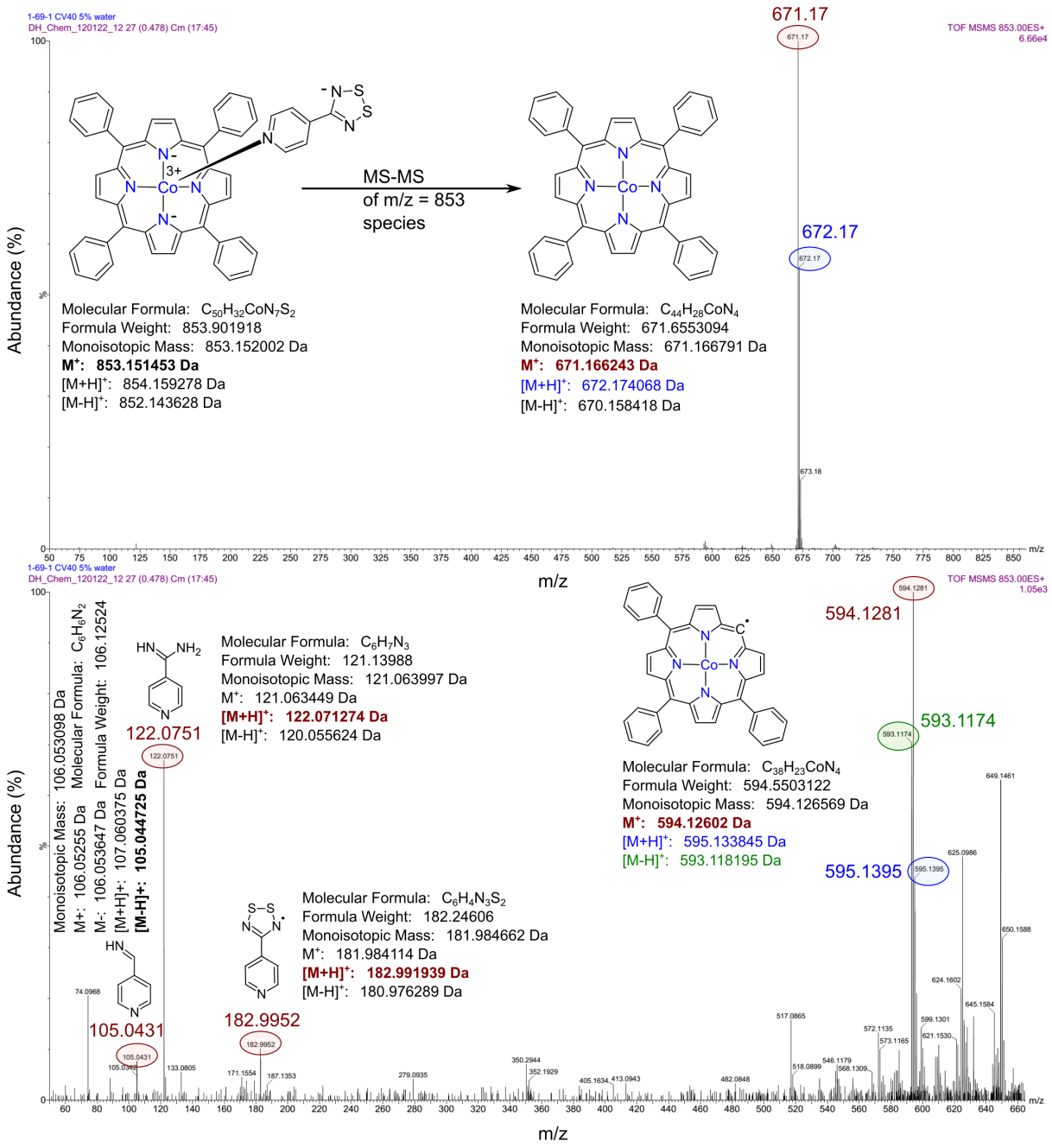

Figure S20. MS-MS spectrum of CP **3** dissolved in acetonitrile confirming that the species at m/z = 853 contains both **1** (m/z = 671) and **2** (m/z = 182).

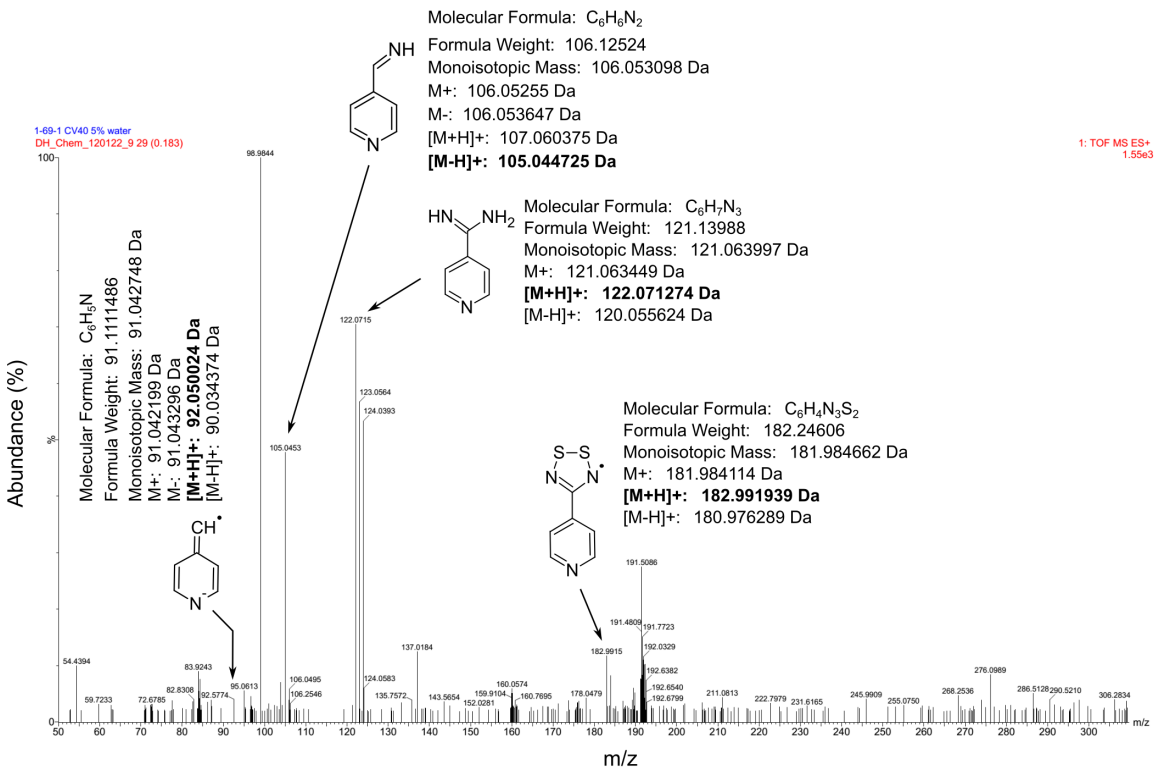

Figure S21. Mass spectrum of CP **3** dissolved in acetonitrile from m/z 50–350 showing relevant assignments.

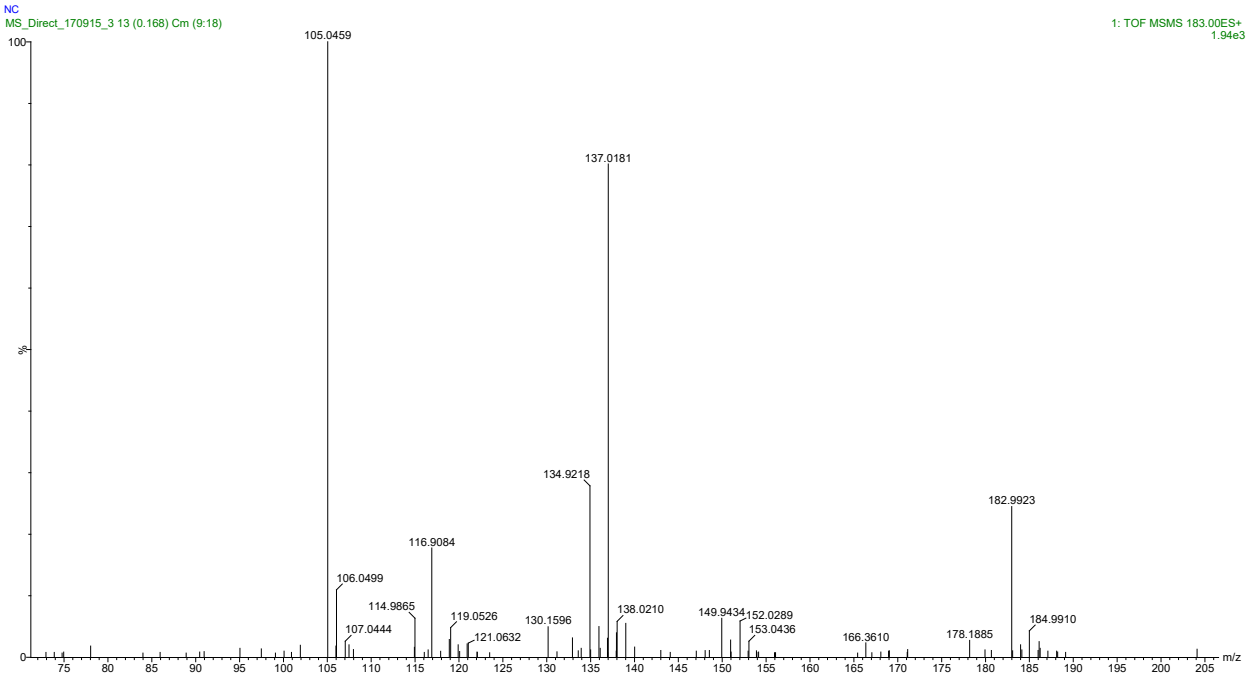

Figure S22. MS-MS spectrum of radical **2**. The signal at m/z = 91 is possibly present but its weak intensity reflects a very low abundance for the fragment C_6H_5N (Figure S21). This is expected since the metalloporphyrin may in fact assist the fragmentation of species **Y** to **Z** (Figure S19), which is the origin of this slightly more abundant low mass fragment in Figure S21.

4. Supporting Tables

Table S1. Experimental details for the X-ray structure determination of CP 3.

Crystal data	
Chemical formula	$[Co(C_{44}H_{28}N_4)(C_6H_4N_3S_2)]\cdot 1.71(C_4H_8O)$
M_r	977.35
Crystal system, space group	Monoclinic, *Pn*
Temperature (K)	100
a, *b*, *c* (Å)	12.834 (3), 24.280 (6), 15.784 (4)
β (°)	101.850 (3)
V (Å^3)	4813.3 (19)
Z	4
Dcalc (g cm^{-3})	1.349
Radiation type	Mo *K*α
μ (mm^{-1})	0.49
Crystal size (mm)	0.53 × 0.20 × 0.06
Data collection	
Diffractometer	Bruker *APEX* CCD area-detector diffractometer
Absorption correction	Multi-scan (*SADABS*; Bruker, 2008)
T_{min}, T_{max}	0.827, 1.000
No. of measured, independent and observed [$I > 2\sigma(I)$] reflections	52661, 20706, 12818
R_{int}	0.088
$(\sin\theta/\lambda)_{max}$ (Å^{-1})	0.658
Refinement	
$R[F^2 > 2\sigma(F^2)]$, $wR(F^2)$, *S*	0.064, 0.137, 1.01
No. of reflections	20706
No. of parameters	1265
No. of restraints	2
H-atom treatment	H atoms treated by constrained refinement
$\Delta\rangle_{max}$, $\Delta\rangle_{min}$ (e Å^{-3})	0.48, -0.63
Absolute structure	Flack, H. D. *Acta Cryst.* **1983**, *A39*, 876-881.
Absolute structure parameter	0.014 (12)

Table S2. Selected geometric parameters (Å, °) for CP 3.

Parameter	Value	Parameter	Value
S31—N31	1.668 (5)	C150—C151	1.396 (8)
S31—S32	2.122 (2)	C151—C152	1.355 (8)
S32—N32	1.616 (4)	C152—C153	1.389 (9)
S32—Co2	2.2590 (16)	C153—C154	1.384 (8)
N31—C30	1.307 (7)	Co2—N211	1.968 (4)
N32—C30	1.345 (6)	Co2—N212	1.975 (4)
C30—C31	1.474 (7)	Co2—N214	1.977 (4)
C31—C32	1.380 (7)	Co2—N213	1.978 (4)
C31—C36	1.393 (7)	Co2—N34^{iv}	2.089 (4)
C32—C33	1.365 (7)	N211—C211	1.374 (6)
C33—N34	1.349 (6)	N211—C214	1.375 (7)
N34—C35	1.338 (7)	C211—C230	1.392 (7)
N34—Co2^{i}	2.089 (4)	C211—C212	1.439 (7)
C35—C36	1.403 (7)	N212—C219	1.385 (6)
S41—N41	1.633 (4)	N212—C216	1.385 (6)
S41—S42	2.119 (2)	C212—C213	1.349 (7)
S41—Co1	2.2512 (15)	N213—C221	1.367 (7)
S42—N42	1.648 (4)	N213—C224	1.377 (6)
N41—C40	1.338 (6)	C213—C214	1.429 (7)
N42—C40	1.346 (7)	N214—C229	1.377 (6)
C40—C41	1.481 (7)	N214—C226	1.384 (6)
C41—C42	1.382 (7)	C214—C215	1.387 (7)
C41—C46	1.390 (7)	C215—C216	1.394 (7)
C42—C43	1.386 (7)	C215—C231	1.514 (7)
C43—N44	1.336 (6)	C216—C217	1.441 (8)
N44—C47	1.351 (6)	C217—C218	1.344 (7)
N44—Co1^{ii}	2.097 (4)	C218—C219	1.443 (7)
C46—C47	1.398 (7)	C219—C220	1.391 (7)
Co1—N113	1.956 (4)	C220—C221	1.395 (7)
Co1—N112	1.962 (4)	C220—C237	1.497 (7)
Co1—N114	1.963 (4)	C221—C222	1.451 (7)
Co1—N111	1.971 (4)	C222—C223	1.353 (7)
Co1—N44^{iii}	2.097 (4)	C223—C224	1.439 (7)
N111—C111	1.375 (6)	C224—C225	1.392 (7)
N111—C114	1.397 (6)	C225—C226	1.389 (7)
C111—C130	1.399 (7)	C225—C243	1.509 (7)
C111—C112	1.429 (7)	C226—C227	1.434 (7)

N112—C116	1.383 (6)	C227—C228	1.344 (7)
N112—C119	1.411 (6)	C228—C229	1.445 (7)
C112—C113	1.348 (7)	C229—C230	1.382 (7)
N113—C124	1.388 (6)	C230—C249	1.491 (7)
N113—C121	1.393 (6)	C231—C236	1.392 (8)
C113—C114	1.446 (7)	C231—C232	1.396 (7)
N114—C126	1.373 (6)	C232—C233	1.405 (8)
N114—C129	1.400 (6)	C233—C234	1.369 (8)
C114—C115	1.382 (7)	C234—C235	1.381 (8)
C115—C116	1.405 (7)	C235—C236	1.380 (7)
C115—C131	1.490 (7)	C237—C242	1.389 (7)
C116—C117	1.429 (7)	C237—C238	1.390 (7)
C117—C118	1.347 (7)	C238—C239	1.388 (8)
C118—C119	1.420 (7)	C239—C240	1.373 (8)
C119—C120	1.387 (7)	C240—C241	1.398 (8)
C120—C121	1.397 (7)	C241—C242	1.386 (7)
C120—C137	1.488 (7)	C243—C244	1.386 (8)
C121—C122	1.428 (7)	C243—C248	1.393 (8)
C122—C123	1.355 (7)	C244—C245	1.359 (8)
C123—C124	1.434 (7)	C245—C246	1.383 (9)
C124—C125	1.397 (7)	C246—C247	1.376 (9)
C125—C126	1.393 (7)	C247—C248	1.378 (8)
C125—C143	1.499 (7)	C249—C250	1.391 (8)
C126—C127	1.439 (7)	C249—C254	1.411 (8)
C127—C128	1.352 (7)	C250—C251	1.412 (8)
C128—C129	1.434 (7)	C251—C252	1.391 (9)
C129—C130	1.375 (7)	C252—C253	1.359 (9)
C130—C149	1.514 (7)	C253—C254	1.396 (8)
C131—C136	1.391 (8)	O1A—C5A	1.420 (9)
C131—C132	1.397 (7)	O1A—C2A	1.432 (9)
C132—C133	1.383 (8)	O1B—C5B	1.444 (8)
C133—C134	1.376 (8)	O1B—C2B	1.447 (8)
C134—C135	1.386 (9)	O1C—C2C	1.432 (8)
C135—C136	1.389 (8)	O1C—C5C	1.455 (7)
C137—C138	1.394 (7)	O1D—C5D	1.430 (9)
C137—C142	1.396 (7)	O1D—C2D	1.441 (9)
C138—C139	1.416 (8)	C2A—C3A	1.497 (11)
C139—C140	1.372 (8)	C2B—C3B	1.523 (10)
C140—C141	1.362 (8)	C2C—C3C	1.480 (11)

C141—C142	1.405 (7)	C2D—C3D	1.534 (9)
C143—C148	1.376 (8)	C3A—C4A	1.445 (12)
C143—C144	1.384 (7)	C3B—C4B	1.502 (9)
C144—C145	1.403 (7)	C3C—C4C	1.496 (10)
C145—C146	1.382 (9)	C3D—C4D	1.509 (9)
C146—C147	1.360 (9)	C4A—C5A	1.487 (11)
C147—C148	1.400 (8)	C4B—C5B	1.500 (9)
C149—C150	1.370 (7)	C4C—C5C	1.532 (9)
C149—C154	1.389 (7)	C4D—C5D	1.527 (9)
N31—S31—S32	93.91 (18)	C143—C148—C147	119.6 (6)
N32—S32—S31	93.36 (17)	C150—C149—C154	118.4 (5)
N32—S32—Co2	109.66 (17)	C150—C149—C130	122.0 (5)
S31—S32—Co2	113.03 (8)	C154—C149—C130	119.6 (5)
C30—N31—S31	112.2 (4)	C149—C150—C151	121.1 (6)
C30—N32—S32	114.2 (4)	C152—C151—C150	119.6 (6)
N31—C30—N32	124.8 (5)	C151—C152—C153	120.8 (6)
N31—C30—C31	118.8 (5)	C154—C153—C152	118.8 (6)
N32—C30—C31	116.4 (5)	C153—C154—C149	121.3 (6)
C32—C31—C36	118.5 (5)	N211—Co2—N212	91.10 (18)
C32—C31—C30	120.4 (5)	N211—Co2—N214	88.85 (18)
C36—C31—C30	121.1 (5)	N212—Co2—N214	179.42 (19)
C33—C32—C31	119.0 (5)	N211—Co2—N213	178.87 (18)
N34—C33—C32	124.2 (5)	N212—Co2—N213	89.54 (18)
C35—N34—C33	117.0 (5)	N214—Co2—N213	90.52 (18)
C35—N34—Co2^{i}	123.0 (4)	N211—Co2—N34^{iv}	90.37 (17)
C33—N34—Co2^{i}	119.9 (4)	N212—Co2—N34^{iv}	88.88 (18)
N34—C35—C36	122.5 (5)	N214—Co2—N34^{iv}	90.54 (18)
C31—C36—C35	118.7 (5)	N213—Co2—N34^{iv}	90.57 (18)
N41—S41—S42	93.56 (16)	N211—Co2—S32	96.22 (14)
N41—S41—Co1	110.51 (17)	N212—Co2—S32	85.52 (13)
S42—S41—Co1	113.90 (7)	N214—Co2—S32	95.05 (13)
N42—S42—S41	94.48 (17)	N213—Co2—S32	82.90 (13)
C40—N41—S41	113.6 (4)	N34^{iv}—Co2—S32	171.42 (13)
C40—N42—S42	112.2 (4)	C211—N211—C214	106.0 (4)
N41—C40—N42	124.3 (5)	C211—N211—Co2	128.0 (4)
N41—C40—C41	118.3 (5)	C214—N211—Co2	125.7 (4)
N42—C40—C41	117.4 (5)	N211—C211—C230	124.9 (5)
C42—C41—C46	119.1 (5)	N211—C211—C212	109.9 (5)

C42—C41—C40	120.2 (5)	C230—C211—C212	125.0 (5)
C46—C41—C40	120.6 (5)	C219—N212—C216	105.8 (4)
C41—C42—C43	118.5 (5)	C219—N212—Co2	127.4 (3)
N44—C43—C42	123.8 (5)	C216—N212—Co2	125.9 (4)
C43—N44—C47	117.3 (5)	C213—C212—C211	106.6 (5)
C43—N44—Co1^{ii}	121.6 (4)	C221—N213—C224	106.4 (4)
C47—N44—Co1^{ii}	121.0 (4)	C221—N213—Co2	127.1 (4)
C41—C46—C47	118.4 (5)	C224—N213—Co2	126.5 (4)
N44—C47—C46	122.8 (5)	C212—C213—C214	107.7 (5)
N113—Co1—N112	89.90 (17)	C229—N214—C226	105.8 (4)
N113—Co1—N114	89.28 (18)	C229—N214—Co2	127.8 (4)
N112—Co1—N114	179.15 (18)	C226—N214—Co2	126.1 (4)
N113—Co1—N111	179.37 (19)	N211—C214—C215	125.7 (5)
N112—Co1—N111	89.98 (17)	N211—C214—C213	109.7 (5)
N114—Co1—N111	90.84 (17)	C215—C214—C213	124.5 (5)
N113—Co1—N44^{iii}	90.07 (17)	C214—C215—C216	124.6 (5)
N112—Co1—N44^{iii}	89.04 (17)	C214—C215—C231	117.5 (5)
N114—Co1—N44^{iii}	91.19 (17)	C216—C215—C231	117.9 (5)
N111—Co1—N44^{iii}	90.54 (17)	N212—C216—C215	123.5 (5)
N113—Co1—S41	95.77 (13)	N212—C216—C217	109.5 (5)
N112—Co1—S41	86.55 (13)	C215—C216—C217	126.6 (5)
N114—Co1—S41	93.31 (13)	C218—C217—C216	107.7 (5)
N111—Co1—S41	83.60 (13)	C217—C218—C219	107.2 (5)
N44^{iii}—Co1—S41	172.66 (13)	N212—C219—C220	125.9 (5)
C111—N111—C114	106.2 (4)	N212—C219—C218	109.7 (5)
C111—N111—Co1	126.4 (3)	C220—C219—C218	123.9 (5)
C114—N111—Co1	127.3 (4)	C219—C220—C221	121.8 (5)
N111—C111—C130	125.6 (5)	C219—C220—C237	117.6 (5)
N111—C111—C112	110.4 (4)	C221—C220—C237	120.3 (5)
C130—C111—C112	123.9 (5)	N213—C221—C220	126.4 (5)
C116—N112—C119	104.2 (4)	N213—C221—C222	109.6 (5)
C116—N112—Co1	127.4 (3)	C220—C221—C222	123.5 (5)
C119—N112—Co1	127.7 (3)	C223—C222—C221	107.0 (5)
C113—C112—C111	107.0 (5)	C222—C223—C224	106.9 (5)
C124—N113—C121	105.0 (4)	N213—C224—C225	125.5 (5)
C124—N113—Co1	128.2 (4)	N213—C224—C223	110.0 (5)
C121—N113—Co1	126.7 (3)	C225—C224—C223	124.5 (5)
C112—C113—C114	108.1 (5)	C226—C225—C224	123.5 (5)
C126—N114—C129	105.7 (4)	C226—C225—C243	118.8 (5)

C126—N114—Co1	127.7 (3)	C224—C225—C243	117.7 (5)
C129—N114—Co1	126.6 (3)	N214—C226—C225	125.2 (5)
C115—C114—N111	124.9 (5)	N214—C226—C227	110.1 (5)
C115—C114—C113	126.6 (5)	C225—C226—C227	124.6 (5)
N111—C114—C113	108.2 (5)	C228—C227—C226	107.1 (5)
C114—C115—C116	122.8 (5)	C227—C228—C229	107.6 (5)
C114—C115—C131	118.9 (5)	N214—C229—C230	125.7 (5)
C116—C115—C131	117.7 (5)	N214—C229—C228	109.4 (4)
N112—C116—C115	125.8 (5)	C230—C229—C228	124.7 (5)
N112—C116—C117	110.6 (5)	C229—C230—C211	122.6 (5)
C115—C116—C117	123.0 (5)	C229—C230—C249	118.1 (5)
C118—C117—C116	107.4 (5)	C211—C230—C249	119.1 (5)
C117—C118—C119	107.5 (5)	C236—C231—C232	119.6 (5)
C120—C119—N112	122.3 (5)	C236—C231—C215	122.1 (5)
C120—C119—C118	127.4 (5)	C232—C231—C215	118.3 (5)
N112—C119—C118	110.1 (4)	C231—C232—C233	119.5 (5)
C119—C120—C121	124.1 (5)	C234—C233—C232	119.4 (6)
C119—C120—C137	118.8 (5)	C233—C234—C235	121.6 (5)
C121—C120—C137	117.0 (4)	C236—C235—C234	119.3 (6)
N113—C121—C120	125.1 (5)	C235—C236—C231	120.6 (6)
N113—C121—C122	110.2 (5)	C242—C237—C238	118.1 (5)
C120—C121—C122	124.6 (5)	C242—C237—C220	119.6 (5)
C123—C122—C121	107.3 (5)	C238—C237—C220	122.3 (5)
C122—C123—C124	107.2 (5)	C239—C238—C237	121.5 (6)
N113—C124—C125	124.6 (5)	C240—C239—C238	119.8 (6)
N113—C124—C123	110.0 (5)	C239—C240—C241	119.8 (6)
C125—C124—C123	125.1 (5)	C242—C241—C240	119.8 (6)
C126—C125—C124	122.1 (5)	C241—C242—C237	121.0 (5)
C126—C125—C143	118.8 (5)	C244—C243—C248	119.5 (5)
C124—C125—C143	118.9 (5)	C244—C243—C225	118.4 (5)
N114—C126—C125	126.2 (5)	C248—C243—C225	122.0 (5)
N114—C126—C127	110.2 (4)	C245—C244—C243	120.5 (6)
C125—C126—C127	123.3 (5)	C244—C245—C246	120.6 (7)
C128—C127—C126	107.0 (5)	C247—C246—C245	119.2 (6)
C127—C128—C129	107.7 (5)	C246—C247—C248	121.1 (6)
C130—C129—N114	124.8 (5)	C247—C248—C243	119.1 (6)
C130—C129—C128	125.9 (5)	C250—C249—C254	118.1 (5)
N114—C129—C128	109.2 (4)	C250—C249—C230	120.2 (5)
C129—C130—C111	123.7 (5)	C254—C249—C230	121.7 (5)

C129—C130—C149	118.7 (5)	C249—C250—C251	120.3 (6)
C111—C130—C149	117.5 (5)	C252—C251—C250	120.5 (6)
C136—C131—C132	118.2 (5)	C253—C252—C251	119.4 (6)
C136—C131—C115	122.1 (5)	C252—C253—C254	121.2 (7)
C132—C131—C115	119.6 (5)	C253—C254—C249	120.5 (6)
C133—C132—C131	121.0 (6)	C5A—O1A—C2A	105.5 (6)
C134—C133—C132	119.9 (6)	C5B—O1B—C2B	107.3 (5)
C133—C134—C135	120.3 (6)	C2C—O1C—C5C	107.4 (5)
C134—C135—C136	119.6 (6)	C5D—O1D—C2D	112.4 (5)
C135—C136—C131	120.9 (6)	O1A—C2A—C3A	104.7 (7)
C138—C137—C142	117.7 (5)	O1B—C2B—C3B	105.6 (6)
C138—C137—C120	123.1 (5)	O1C—C2C—C3C	106.6 (6)
C142—C137—C120	119.2 (5)	O1D—C2D—C3D	104.2 (6)
C137—C138—C139	120.5 (5)	C4A—C3A—C2A	104.9 (7)
C140—C139—C138	119.7 (6)	C4B—C3B—C2B	105.0 (6)
C141—C140—C139	121.2 (5)	C2C—C3C—C4C	103.7 (7)
C140—C141—C142	119.3 (6)	C4D—C3D—C2D	102.8 (6)
C137—C142—C141	121.6 (6)	C3A—C4A—C5A	106.8 (8)
C148—C143—C144	119.3 (5)	C5B—C4B—C3B	99.6 (6)
C148—C143—C125	120.1 (5)	C3C—C4C—C5C	103.2 (6)
C144—C143—C125	120.6 (5)	C3D—C4D—C5D	103.8 (6)
C143—C144—C145	121.0 (6)	O1A—C5A—C4A	106.2 (7)
C146—C145—C144	118.8 (6)	O1B—C5B—C4B	106.0 (6)
C147—C146—C145	120.3 (6)	O1C—C5C—C4C	107.1 (5)
C146—C147—C148	121.0 (6)	O1D—C5D—C4D	104.6 (6)

Symmetry code(s): (i) *x*+1/2, -*y*+1, *z*+1/2; (ii) *x*+1/2, -*y*+2, *z*+1/2; (iii) *x*-1/2, -*y*+2, *z*-1/2; (iv) *x*-1/2, -*y*+1, *z*-1/2.

Table S3. Crystallographic data compiled from the Cambridge Structural Database (CSD) for Co(II/III) porphyrins axially-ligated by ≥ 1 pyridine ligand.

REFCODE	Co-N_{py} (Å)	Co-N_{porph} ave. (Å)	Oxid. State	Coord. No.	Conformation [a]
XIDVUD	2.357	1.972	2+	6	RUF
XIDWAK	1.976	1.962	2+	6	RUF
BIJSAP	2.278	1.973	2+	6	SAD
HUXSIC	2.167	1.946	2+	6	SAD
LIBBUT	2.191	1.982	2+	5	RUF-DOME
MOSFIJ	2.155	1.985	2+	5	FLT-DOME
OBUTIO	2.223	1.985	2+	6	FLT
OEPCOP	2.386	1.993	2+	6	FLT
PIBNUJ	2.203	1.988	2+	5	RUF-DOME
SODBIX	2.186	1.975	2+	5	RUF
	2.089	1.977	2+	5	RUF
VAVWEV	2.189	1.984	2+	5	FLT-DOME
YICHEY	1.958	1.961	2+	6	RUF
GOBLOA	2.178	1.97	2+	6	RUF
	2.288	1.97	2+	6	FLT
GOBHOW	2.276	1.982	2+	6	SAD
	2.259	1.982	2+	6	SAD
ROFXUH	2.286	1.985	2+	6	FLT (slight RUF)
	2.313	1.976	2+	6	FLT (slight RUF)
ROFYAO	2.342	1.993	2+	6	FLT (slight RUF)
LIBCEE	2.214	1.982	3+	6	FLT
NTPOLC	2.037	1.953	3+	6	RUF
NTPOLC01	2.017	1.96	3+	6	RUF
YEQMIQ	2.032	1.969	3+	6	RUF
YEQMOW	2.044	1.955	3+	6	RUF
RIQLUA	1.957	1.944	3+	6	RUF
	1.966	1.944	3+	6	RUF

[a] RUF, S_4-ruffled; SAD, D_{2d} saddled; FLT, flat; DOME, C_{4v}-domed.

Table S4. Experimental and calculated infrared spectra for radical 2 (solid state, sublimed compound).[a]

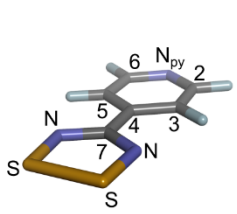

Radical **2**

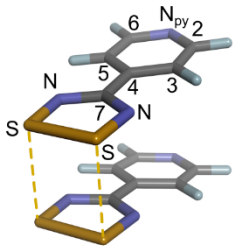

π-π dimer

Exp. Frequency (cm^{-1})	Exp. Intensity	Calc. Frequency (cm^{-1})	Calc. Intensity	Species	Assignment
642	m	647	m	all	$\delta_{ip/s}(C^3\text{-}C^4\text{-}C^5; C^2\text{-}N_{py}\text{-}C^6)$
665	w	691	w	C	$\delta_{oop}(C^{2,6}\text{-H}; C^{3,5}; C7)$
725	m	734	s	D	$\delta_{ip/a}(N\text{-}C^7\text{-}N)$, $\nu_s(N\text{-S})$
777	s	772	vw	D	$\delta_{ip/s}(N\text{-}C^7\text{-}N)$, $\nu_s(N\text{-S})$
816	s	814	m	D	$\nu_a(N\text{-S})$
829	m	826	m	all	$\nu_a(N\text{-S})$; δ_{oop}(C-H, py ring)
906	vw	898	vw	D	$\delta_{ip/a}(C^2\text{-}N_{py}\text{-}C^6; N\text{-}C^7\text{-}N)$
978	w	935	m	C	$\nu_a(N\text{-S})$
1001	m	978	w	all	$\delta_{ip}(C^3\text{-}C^4\text{-}C^5; N_{py}\text{-}C^{2,6})$
1049	w	1053	w	all	$\delta_{ip}(C^4\text{-}C^{3,5}\text{-H})$
1086	w	1083	vw	C	$\delta_{ip/a}$(C-H, py ring, scissor)
1147	m	1139	m	D	$\nu_s(C^4\text{-}C^7;C^7\text{-N})$, $\delta_{ip}(C^3\text{-}C^4\text{-}C^5)$
1188	w	1199	w	D,C	$\delta_{ip/s}$(C-H, py ring, scissor)
1248	w	1247	vw	D	δ_{ip}(C-H, py ring)
1334	m	1345	s	D	$\nu_a(C^4\text{-}C^7;C^7\text{-N})$, $\delta_{ip}(N\text{-}C^7\text{-N})$
1365	s	1355	s	D	$\nu_s(C^4\text{-}C^7;C^7\text{-N})$
1402	s	1380-90	s	M,D,C	$\nu_a(C^{2,6}{=}C^{3,5})$, $\nu(C^4\text{-}C^7)$
1506	m	1486	w	A,C	$\nu_s(N_{py}\text{-}C^{2,6}; C^4\text{-}C^7)$
1520	m	1508	m	A	$\nu_a(C^7\text{-N})$
1608	s	1585	m	M,D	$\nu_a(C^{3,5}{=}C^4; C{=}N_{py})$
1633	s	1604	m	M,A	$\nu_s(C^{2,6}{=}C^{3,5})$
3030	w	3034	w	A	$\nu_a(C^{2,6}\text{-H})$, $\nu_s(C^{2,6}\text{-H})$
3047	w	3047	w	D	$\nu_a(C^{2,6}\text{-H})$, $\nu_s(C^{2,6}\text{-H})$
3069	w	3069	w	M	$\nu_a(C^{2,6}\text{-H})$, $\nu_s(C_{2,6}\text{-H})$
3103	w	3103	vw	D	$\nu_a(C^{3,5}\text{-H})$, $\nu_s(C^{3,5}\text{-H})$
3122	w	3121	vw	all	$\nu_a(C^{3,5}\text{-H})$, $\nu_s(C^{3,5}\text{-H})$

[a] Abbreviations: s, strong; m, medium; w, weak; vw, very weak; M, monomer (radical); D, dimer; A, anion; C, cation; ν_a, antisymmetric stretch; ν_s, symmetric stretch, δ_{ip}, in-plane bend; $\delta_{ip/a}$, antisymmetric in-plane bend; $\delta_{ip/s}$, symmetric in-plane bend; δ_{oop}, out-of-plane bend.

Table S5. DFT-calculated metal orbital populations (NBO 3.0) and energies for 3b and the five-coordinate pyridine analogue, Co(TPP)(py).

$Co^{III}(TPP)(py\text{-}DTDA^{-})^{a}$	$Co^{III}(TPP)(py)^{a}$
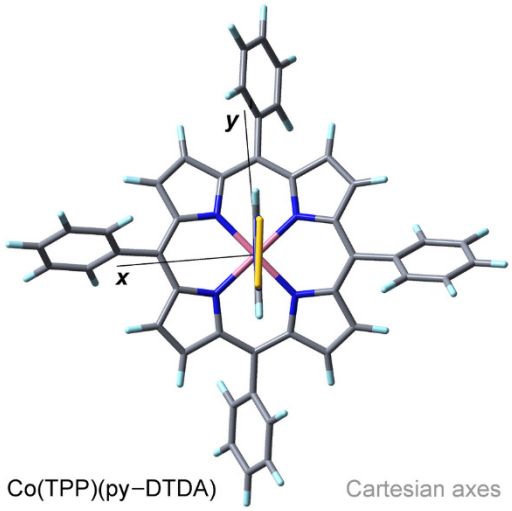	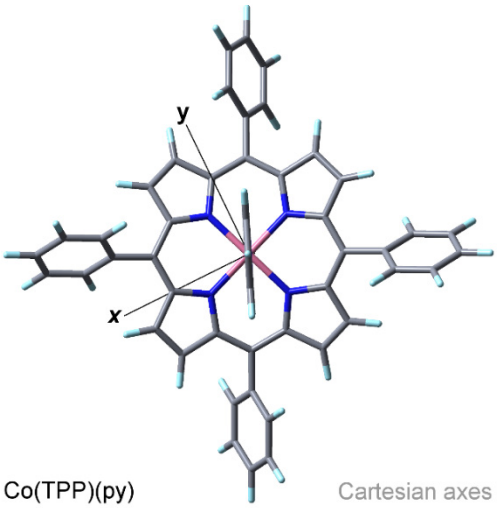

Orbital	Population (*e*)	Energy (eV)	Orbital	Population (e)	Energy (eV)
3dyz	1.960	-8.758	**3dyz**	1.957	-8.851
3dxz	1.943	-8.568	**3dxz**	1.946	-8.701
$3dx^2$-y^2	1.914	-8.471	**3dxy**	1.409	-7.148
$3dz^2$	0.626	-5.130	**$3dx^2$–y^2**	1.225	-6.628
3dxy [a]	0.714	-5.092	**$3dz^2$**	0.620	-5.232
total	7.157		*total*	7.156	
$4p_z$	0.126	4.109	**$4p_z$**	0.125	4.060
$4p_x$	0.159	7.554	**$4p_x$**	0.161	7.623
$4p_y$	0.163	8.345	**$4p_y$**	0.163	8.218
4s	0.277	9.062	**4s**	0.275	9.035
LF splitting, Δ		3.49			2.30
% d^6 low-spin	97			89	

[a] Both structures are solution-phase (DMSO continuum) minimum-energy geometries for illustrative purposes.

Comment on Table S5. The DFT-calculated metal orbital populations indicate that the py-$DTDA^{-}$ anion is a strong field ligand that enforces a low-spin d^6 ground state for [Co^{III}(TPP)(py-$DTDA^{-}$)], complex **3b**, as evidenced by an electron configuration very close (97%) to the ideal low-spin d^6 electron configuration $(dyz)^2(dxz)^2(dx^2–y^2)^2$. Interestingly, the highest-energy $3dz^2$ and 3dxy (or $3dx^2–y^2$) orbitals are not completely vacant in either structure. The ligand field (LF) splitting energy (Δ) for Co(TPP)(py-DTDA) measures 337 kJ mol^{-1} (3.49 eV) and is 52% larger than the LF splitting for Co(TPP)(py). This marked difference in LF splitting for the two complexes is consistent with the py-$DTDA^{-}$ anion being a significantly stronger field ligand than pyridine.

Table S6. TD-DFT calculated singlet excited states and transition components for coordination polymer 3.

The simulations were performed on a tetramer chain, $\{3\}_4$, using the 3D atomic coordinates of the X-ray structure at the B3LYP/6-31G(d,p) level of theory. The HOMO (H) and LUMO (L) orbitals correspond to MOs 860 and 861, respectively. The lowest-energy 140 singlet excited states were calculated; all have ^{1}A symmetry.

No.	Energy (cm^{-1})	Wavelength (nm)	Oscillator Strength	Major contributions	Minor contributions
1	6477	1543.8	0.0	HOMO→LUMO (100%)	
2	8061	1240.6	0.0	HOMO→L+1 (100%)	
3	8194	1220.4	0.0	H-1→LUMO (100%)	
4	8402	1190.2	0.0	HOMO→L+2 (100%)	
5	9573	1044.6	0.0007	H-2→LUMO (95%)	H-2→L+3 (5%)
6	9640	1037.4	0.0003	H-1→L+5 (94%)	H-1→L+6 (4%)
7	9715	1029.3	0.0002	H-2→L+3 (88%)	H-2→LUMO (5%), HOMO→L+3 (4%)
8	9750	1025.6	0.0	HOMO→L+3 (96%)	H-2→L+3 (4%)
9	9767	1023.9	0.0006	H-1→L+6 (94%)	H-1→L+5 (4%)
10	9806	1019.8	0.0006	HOMO→L+8 (73%), HOMO→L+9 (26%)	
11	9813	1019.0	0.0	H-1→L+1 (100%)	
12	9839	1016.3	0.0001	H-2→L+4 (20%), HOMO→L+4 (79%)	
13	9857	1014.5	0.0004	H-2→L+4 (77%), HOMO→L+4 (20%)	
14	9989	1001.1	0.0009	HOMO→L+8 (27%), HOMO→L+9 (73%)	
15	10148	985.4	0.0	H-1→L+2 (100%)	
16	11038	906.0	0.0	H-1→L+3 (94%)	H-1→L+4 (5%)
17	11170	895.3	0.0	H-1→L+4 (41%), HOMO→L+5 (49%)	HOMO→L+6 (6%)
18	11174	894.9	0.0	H-1→L+4 (53%), HOMO→L+5 (38%)	H-1→L+3 (3%), HOMO→L+6 (5%)
19	11277	886.7	0.0	HOMO→L+5 (11%), HOMO→L+6 (87%)	
20	11319	883.5	0.0	H-2→L+1 (99%)	
21	11639	859.2	0.0001	H-2→L+2 (99%)	
22	13390	746.8	0.0	HOMO→L+7 (100%)	
23	14119	708.3	0.0	H-3→LUMO (100%)	
24	14394	694.7	0.0301	H-41→LUMO (12%), H-8→LUMO (61%)	H-37→LUMO (6%), H-8→L+2 (2%), H-8→L+10 (3%)
25	14624	683.8	0.0009	H-2→L+7 (85%), H-1→L+7 (13%)	
26	14699	680.3	0.0002	H-2→L+5 (96%)	H-2→L+6 (3%)
27	14704	680.1	0.0001	H-1→L+8 (96%)	H-1→L+9 (4%)
28	14799	675.7	0.0	H-2→L+6 (97%)	H-2→L+5 (3%)
29	14812	675.1	0.0002	H-1→L+9 (96%)	H-1→L+8 (4%)

30	14944	669.2	0.0001	H-2→L+7 (13%), H-1→L+7 (87%)	
31	15627	639.9	0.0	H-4→LUMO (100%)	
32	15705	636.7	0.0	H-3→L+1 (100%)	
33	15953	626.8	0.0025	H-37→LUMO (31%), H-11→LUMO (11%), H-10→LUMO (12%)	H-93→LUMO (2%), H-11→L+2 (2%), H-8→LUMO (4%), H-8→L+1 (8%), H-8→L+2 (6%)
34	16046	623.2	0.0	H-3→L+2 (100%)	
35	16092	621.4	0.0017	H-8→L+1 (81%)	H-37→LUMO (3%), H-11→L+1 (3%), H-7→L+1 (2%)
36	16118	620.4	0.0	H-5→LUMO (100%)	
37	16159	618.8	0.0066	H-41→LUMO (23%), H-10→LUMO (13%), H-8→L+2 (30%)	H-98→LUMO (7%), H-37→LUMO (2%), H-8→LUMO (4%), H-8→L+1 (4%)
38	16195	617.5	0.0061	H-2→L+11 (14%), H-2→L+15 (66%)	H-2→L+18 (8%)
39	16256	615.2	0.0081	H-1→L+13 (16%), H-1→L+21 (59%)	H-2→L+15 (3%), H-1→L+11 (4%), H-1→L+12 (4%), H-1→L+20 (5%)
40	16548	604.3	0.0	HOMO→L+10 (100%)	
41	16674	599.7	0.0131	H-11→LUMO (30%), H-10→LUMO (18%), H-8→L+2 (37%)	H-41→LUMO (2%), H-8→LUMO (6%)
42	16740	597.4	0.0083	H-1→L+11 (50%), H-1→L+12 (20%), H-1→L+21 (12%), HOMO→L+11 (11%)	
43	16968	589.3	0.0022	HOMO→L+34 (85%)	HOMO→L+19 (4%), HOMO→L+47 (2%)
44	17010	587.9	0.0001	HOMO→L+11 (63%), HOMO→L+13 (13%)	H-1→L+11 (8%), H-1→L+12 (3%), HOMO→L+12 (2%), HOMO→L+16 (6%), HOMO→L+34 (2%)
45	17136	583.6	0.0265	HOMO→L+11 (19%), HOMO→L+13 (46%), HOMO→L+16 (20%)	H-1→L+13 (4%), H-1→L+21 (2%)
46	17200	581.4	0.0355	H-2→L+11 (44%), H-2→L+15 (11%), H-2→L+22 (13%)	H-7→LUMO (9%), H-2→L+12 (6%)
47	17205	581.2	0.0058	H-7→LUMO (88%)	H-2→L+11 (4%)
48	17213	580.9	0.0	H-4→L+1 (100%)	
49	17343	576.6	0.0	H-3→L+3 (100%)	
50	17364	575.9	0.0317	H-1→L+13 (44%), H-1→L+21 (10%)	H-1→L+11 (6%), H-1→L+16 (6%), H-1→L+39 (9%), H-1→L+40 (5%), HOMO→L+13 (4%), HOMO→L+16 (4%)
51	17434	573.6	0.0086	H-41→LUMO (13%), H-10→LUMO (49%)	H-98→LUMO (5%), H-37→LUMO (7%), H-8→LUMO (3%), H-8→L+2 (5%)
52	17439	573.4	0.0	H-3→L+4 (100%)	
53	17452	573.0	0.0	H-6→LUMO (100%)	
54	17554	569.7	0.0	H-4→L+2 (100%)	

55	17752	563.3	0.0	H-5→L+1 (100%)	
56	17951	557.1	0.0624	HOMO→L+19 (62%), HOMO→L+41 (10%)	HOMO→L+13 (3%), HOMO→L+34 (3%), HOMO→L+58 (3%), HOMO→L+60 (3%), HOMO→L+61 (2%)
57	18085	553.0	0.0	H-5→L+2 (100%)	
58	18230	548.6	0.0	H-1→L+10 (98%)	HOMO→L+12 (2%)
59	18248	548.0	0.0002	HOMO→L+12 (94%)	H-1→L+10 (2%), HOMO→L+11 (2%)
60	18316	546.0	0.0	H-2→L+8 (97%)	H-2→L+9 (3%)
61	18398	543.5	0.0	H-2→L+9 (97%)	H-2→L+8 (3%)
62	18483	541.0	0.0065	H-4→L+9 (31%), H-3→L+8 (56%)	H-4→L+8 (3%), H-3→L+5 (3%), H-3→L+9 (5%)
63	18517	540.0	0.0002	H-9→LUMO (95%)	H-7→L+4 (2%)
64	18534	539.6	0.0032	H-6→L+6 (20%), H-5→L+5 (33%), H-3→L+5 (26%)	H-6→L+5 (4%), H-5→L+6 (7%), H-3→L+6 (6%)
65	18546	539.2	0.0025	H-6→L+6 (11%), H-5→L+5 (18%), H-3→L+5 (55%)	H-5→L+6 (2%), H-3→L+6 (9%)
66	18569	538.5	0.0067	H-4→L+8 (31%), H-3→L+9 (57%)	H-4→L+9 (3%), H-3→L+8 (5%)
67	18578	538.3	0.0074	H-9→L+3 (12%), H-9→L+4 (23%), H-7→L+3 (38%), H-7→L+4 (19%)	H-9→LUMO (4%)
68	18625	536.9	0.0024	H-6→L+5 (28%), H-5→L+6 (48%)	H-6→L+6 (5%), H-5→L+5 (9%), H-3→L+6 (3%)
69	18648	536.3	0.0031	H-9→L+3 (20%), H-9→L+4 (12%), H-7→L+3 (21%), H-7→L+4 (35%)	H-2→L+12 (4%)
70	18660	535.9	0.0003	H-3→L+5 (15%), H-3→L+6 (80%)	
71	18727	534.0	0.0001	H-5→L+3 (91%)	H-5→L+4 (8%)
72	18740	533.6	0.0206	H-11→LUMO (42%), H-8→L+10 (14%)	H-37→LUMO (6%), H-37→L+2 (2%), H-10→L+1 (8%), H-8→LUMO (4%), H-8→L+2 (8%)
73	18850	530.5	0.0	H-4→L+3 (100%)	
74	18877	529.8	0.0651	H-2→L+11 (13%), H-2→L+12 (64%)	H-9→L+3 (3%), H-7→L+4 (3%), H-1→L+12 (4%), H-1→L+16 (5%)
75	18887	529.5	0.0005	H-5→L+4 (91%)	H-5→L+3 (8%)
76	18945	527.8	0.0	H-4→L+4 (100%)	
77	18994	526.5	0.0	H-7→L+1 (95%)	H-8→L+1 (3%)
78	19061	524.6	0.0187	H-1→L+13 (13%), H-1→L+16 (71%)	H-2→L+12 (6%)
79	19081	524.1	0.0	H-6→L+1 (100%)	
80	19126	522.9	0.0015	H-1→L+11 (27%), H-1→L+12 (66%)	H-2→L+12 (5%)
81	19310	517.9	0.0	H-7→L+2 (95%)	H-8→L+2 (3%), H-7→L+1 (2%)
82	19415	515.1	0.0	H-6→L+2 (100%)	

83	19469	513.6	0.0001	HOMO→L+13 (30%), HOMO→L+16 (67%)	H-1→L+16 (2%)
84	19545	511.6	0.0001	H-2→L+10 (98%)	
85	19612	509.9	0.0008	H-11→L+1 (46%), H-10→L+2 (48%)	
86	19810	504.8	0.005	H-11→L+2 (45%), H-10→L+1 (41%)	H-10→L+2 (2%), H-8→L+10 (3%)
87	20055	498.6	0.0	H-4→L+5 (82%), H-4→L+6 (18%)	
88	20095	497.6	0.0	H-6→L+3 (94%)	H-6→L+4 (6%)
89	20167	495.9	0.0	HOMO→L+14 (100%)	
90	20179	495.6	0.0	H-4→L+5 (18%), H-4→L+6 (82%)	
91	20237	494.1	0.0	H-6→L+4 (94%)	H-6→L+3 (6%)
92	20310	492.4	0.0	H-9→L+1 (98%)	
93	20397	490.3	0.0	HOMO→L+15 (100%)	
94	20636	484.6	0.0	H-9→L+2 (98%)	
95	20944	477.5	0.0053	H-8→L+3 (93%)	H-8→L+4 (2%)
96	21009	476.0	0.0	H-3→L+7 (100%)	
97	21086	474.3	0.0004	H-8→L+4 (95%)	H-8→L+3 (2%)
98	21270	470.1	0.0	HOMO→L+17 (100%)	
99	21300	469.5	0.0764	H-2→L+22 (28%)	H-29→L+11 (4%), H-29→L+12 (3%), H-26→L+15 (2%), H-2→L+11 (4%), H-2→L+20 (7%), H-1→L+39 (5%), H-1→L+40 (3%)
100	21358	468.2	0.0102	H-1→L+39 (18%), H-1→L+40 (10%)	H-17→L+13 (3%), H-17→L+16 (3%), H-16→L+21 (2%), H-2→L+22 (6%), H-1→L+13 (4%), H-1→L+29 (7%)
101	21460	466.0	0.0121	HOMO→L+41 (32%)	H-89→L+19 (3%), H-38→L+19 (3%), H-14→L+19 (7%), H-13→L+19 (5%), H-13→L+34 (2%), HOMO→L+19 (5%), HOMO→L+43 (3%), HOMO→L+58 (4%), HOMO→L+60 (3%), HOMO→L+61 (3%)
102	21704	460.7	0.0	H-1→L+15 (98%)	
103	21833	458.0	0.0264	H-8→L+7 (13%), H-7→L+7 (69%)	H-8→L+10 (9%)
104	21904	456.5	0.0462	H-8→L+7 (42%), H-8→L+10 (16%), H-7→L+7 (28%)	H-11→LUMO (3%), H-8→LUMO (3%)
105	21916	456.3	0.0001	H-1→L+14 (97%)	
106	21929	456.0	0.0	HOMO→L+18 (99%)	
107	21978	455.0	0.0006	H-11→L+14 (10%), H-8→L+14 (74%)	
108	22075	453.0	0.0	HOMO→L+21 (90%)	HOMO→L+20 (9%)

109	22348	447.5	0.0009	H-83→L+21 (17%)	H-96→L+21 (3%), H-18→L+21 (3%), H-17→L+21 (7%), H-16→L+13 (5%), H-16→L+16 (4%), H-5→L+21 (8%), H-2→L+13 (6%)
110	22377	446.9	0.0056	H-14→L+19 (10%), H-14→L+34 (13%)	H-89→L+34 (4%), H-75→L+34 (6%), H-67→L+19 (5%), H-67→L+34 (3%), H-38→L+34 (3%), H-13→L+19 (7%), H-13→L+34 (3%), H-12→L+19 (2%), H-1→L+19 (4%), HOMO→L+34 (2%)
111	22384	446.7	0.0019	H-91→L+15 (13%), H-29→L+15 (10%)	H-91→L+18 (2%), H-29→L+12 (2%), H-26→L+11 (6%), H-26→L+12 (5%), H-7→L+15 (8%)
112	22517	444.1	0.0	H-4→L+7 (100%)	
113	22604	442.4	0.0001	H-95→L+14 (24%), H-94→L+14 (47%)	H-92→L+14 (8%), H-80→L+14 (4%), H-11→L+14 (4%)
114	22644	441.6	0.0002	H-75→L+34 (62%), H-3→L+34 (10%)	H-75→L+47 (3%), H-72→L+34 (2%), H-28→L+34 (2%)
115	22653	441.4	0.0027	H-83→L+21 (22%), H-2→L+13 (39%)	H-82→L+21 (5%), H-5→L+21 (5%), H-2→L+16 (5%)
116	22733	439.9	0.0	H-5→L+7 (100%)	
117	22762	439.3	0.0011	H-91→L+15 (28%), H-90→L+15 (10%)	H-95→L+15 (2%), H-91→L+18 (5%), H-29→L+15 (4%), H-26→L+11 (3%), H-26→L+12 (3%), H-7→L+15 (5%), H-2→L+15 (2%), H-2→L+18 (4%)
118	22813	438.4	0.0	HOMO→L+20 (91%)	HOMO→L+21 (9%)
119	22844	437.8	0.0071	H-83→L+21 (10%), H-2→L+13 (42%)	H-82→L+21 (3%), H-17→L+21 (3%), H-16→L+13 (4%), H-16→L+16 (3%), H-2→L+16 (4%)
120	22894	436.8	0.0008	H-2→L+18 (77%)	H-2→L+15 (8%), H-1→L+18 (5%)
121	22942	435.9	0.0204	HOMO→L+19 (10%), HOMO→L+41 (36%)	H-89→L+19 (3%), H-14→L+19 (5%), H-13→L+19 (7%), H-13→L+34 (4%), H-4→L+8 (2%), H-3→L+19 (2%)
122	23024	434.3	0.0	H-1→L+17 (99%)	
123	23031	434.2	0.0085	H-8→L+7 (38%), H-8→L+10 (42%)	H-11→LUMO (2%), H-8→LUMO (3%)
124	23128	432.4	0.0184	H-1→L+19 (84%)	H-1→L+29 (4%)
125	23218	430.7	0.0647	H-1→L+29 (49%)	H-2→L+20 (3%), H-1→L+13 (2%), H-1→L+19 (9%)
126	23259	429.9	0.0001	H-7→L+5 (97%)	
127	23274	429.7	0.0297	H-9→L+7 (10%), H-2→L+20 (31%)	H-29→L+11 (2%), H-29→L+12 (2%), H-26→L+15 (2%), H-9→L+3 (4%), H-7→L+4 (2%), H-2→L+11 (3%), H-2→L+12 (3%), H-2→L+21 (3%), H-1→L+29 (9%)
128	23297	429.2	0.0001	H-5→L+8 (93%)	H-5→L+9 (7%)
129	23339	428.5	0.0	H-7→L+6 (99%)	
130	23391	427.5	0.0	H-5→L+9 (93%)	H-5→L+8 (7%)
131	23409	427.2	0.0002	H-2→L+14 (43%), H-1→L+18 (51%)	H-9→L+7 (3%)

132	23413	427.1	0.0092	H-9→L+7 (78%)	H-2→L+20 (9%), H-1→L+18 (4%)
133	23431	426.8	0.0001	H-2→L+14 (54%), H-1→L+18 (39%)	H-2→L+18 (4%)
134	23507	425.4	0.0033	HOMO→L+43 (89%)	HOMO→L+41 (7%)
135	23659	422.7	0.0	H-12→LUMO (99%)	
136	23682	422.3	0.0936	H-2→L+20 (10%), H-1→L+29 (19%), H-1→L+39 (14%)	H-2→L+22 (5%), H-1→L+13 (4%), H-1→L+16 (2%), H-1→L+40 (8%)
137	23777	420.6	0.0065	H-2→L+20 (23%), H-2→L+22 (22%)	H-9→L+7 (2%), H-2→L+11 (3%), H-2→L+12 (2%), H-2→L+21 (2%), H-1→L+20 (2%), H-1→L+29 (3%), H-1→L+39 (4%), H-1→L+40 (2%)
138	23912	418.2	0.0	HOMO→L+22 (94%)	HOMO→L+23 (4%)
139	23949	417.6	0.0172	H-5→L+11 (55%), H-5→L+12 (28%)	H-5→L+13 (4%), H-5→L+16 (3%)
140	24018	416.3	0.0138	H-3→L+13 (53%), H-3→L+16 (28%)	H-4→L+9 (3%), H-3→L+11 (2%), H-3→L+19 (7%)

Table S7. Selected TD-DFT calculated Vis-NIR electronic transitions and assignments for tetrameric 3.[a]

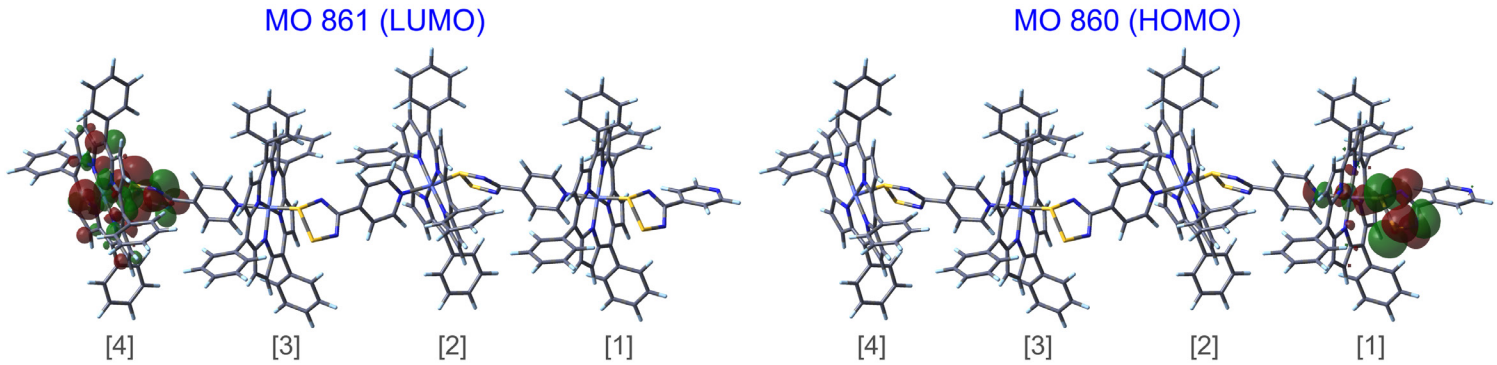

λ/nm	*E*/eV	MOs	Coeff. [b]	*f* [c]	Transition Assignment [d]
1544	0.803	860, H → 861, L	0.707	0	dz^2, π(DTDA) [1] → dz^2*, π*(DTDA, porphyrin) [4]
1220	1.016	859, H–1 → 861, L	0.707	0	dz^2, π(DTDA) [2] → dz^2*, π*(DTDA, porphyrin) [4]
1045	1.187	858, H–2 → 861, L	0.688	0.0007	dz^2, π(DTDA) [3] → dz^2*, π*(DTDA, porphyrin) [4]
1020	1.216	860, H → 869, L+8	0.605	0.0006	dz^2, π(DTDA) [1] → π*(e_{gx}, porphyrin) [1]
1001	1.239	860, H → 870, L+9	0.604	0.0009	dz^2, π(DTDA) [1] → π*(e_{gy}, porphyrin) [1]
859	1.443	858, H–2 → 863, L+2	0.702	0.0001	dz^2, π(DTDA) [3] → π*(e_{gx}, porphyrin) [4]
695	1.785	852, H–8 → 861, L	0.550	0.0301	dz^2, π(DTDA, porphyrin) [4] → dz^2*, π*(DTDA, porphyrin) [4]
615	2.016	859, H–1 → 882, L+21	0.544	0.0081	dz^2, π(DTDA) [2] → dx^2-y^2*, σ*(porphyrin), π*(py) [2]
581	2.133	858, H–2 → 872, L+11	0.468	0.0354	dz^2, π(DTDA) [3] → dz^2*, π*(py-DTDA, porphyrin) [3], dπ* [2]
530	2.341	858, H–2 → 873, L+12	0.566	0.0651	dz^2, π(DTDA) [3] → dz^2*, π*(py-DTDA, porphyrin) [3], dπ* [2]

[a] Eleven out of the lowest 80 calculated excited states are listed specifically for comparison with the deconvoluted experimental spectrum of **3** shown in Figure 5b of the main paper. Abbreviations: H, HOMO; L, LUMO. [b] Where multiple transitions contribute to an excited state, only that with the largest transition coefficient has been listed. [c] Oscillator strength. [d] The number in the square bracket denotes the position of the MO and metal center in the 1D polymer chain (see Figure 6b of the main paper and the structure above).

Table S8. TD-DFT calculated singlet excited states and transition components for 3a, Co^{II}(TPP)(*S*-py-DTDA), in 1,2-dichloroethane.
The simulations were performed on the geometry-optimized structure at the hseh1pbe /6-31G(d,p) level of theory. The HOMO (H) and LUMO (L) orbitals correspond to MOs 220 and 221, respectively. The lowest-energy 60 singlet excited states were calculated.

No.	Energy (cm^{-1})	Wavelength (nm)	Oscillator Strength	Symmetry	Major contributions	Minor contributions
1	12602	793.5	0.0005	Singlet-A	H-3→LUMO (54%), H-3→L+2 (13%)	H-25→LUMO (2%), H-19→LUMO (6%), H-18→LUMO (5%), H-4→L+6 (3%)
2	13175	759.0	0.0004	Singlet-A	H-22→LUMO (11%), H-4→LUMO (52%), H-4→L+2 (12%)	H-23→LUMO (3%), H-22→L+2 (3%), H-3→L+6 (4%)
3	17419	574.1	0.0196	Singlet-A	HOMO→LUMO (69%)	H-1→LUMO (6%), H-1→L+2 (9%), HOMO→L+2 (7%)
4	17820	561.2	0.0024	Singlet-A	H-1→LUMO (14%), HOMO→L+1 (78%)	H-1→L+1 (5%)
5	18141	551.2	0.0089	Singlet-A	H-1→LUMO (37%), HOMO→L+2 (44%)	H-1→L+1 (5%), HOMO→L+1 (7%)
6	18665	535.8	0.0035	Singlet-A	H-2→LUMO (60%), H-1→LUMO (11%), HOMO→L+2 (13%)	H-2→L+2 (5%), H-1→L+2 (3%), HOMO→LUMO (3%)
7	19451	514.1	0.0298	Singlet-A	H-2→LUMO (14%), H-2→L+2 (12%), H-1→L+1 (32%), HOMO→L+2 (10%)	H-2→L+1 (4%), H-1→LUMO (9%), HOMO→L+1 (6%), HOMO→L+3 (7%)
8	19670	508.4	0.0159	Singlet-A	H-2→L+1 (39%), H-1→L+2 (48%)	H-1→LUMO (2%), H-1→L+1 (5%)
9	20108	497.3	0.0525	Singlet-A	H-2→L+2 (29%), H-1→L+1 (16%), HOMO→L+3 (20%)	H-2→LUMO (6%), H-1→L+2 (5%), HOMO→LUMO (3%), HOMO→L+2 (8%), HOMO→L+4 (4%)
10	20757	481.8	0.0	Singlet-A	H-19→L+6 (32%), H-18→L+6 (31%), H-16→L+6 (15%)	H-17→L+6 (9%), H-1→L+6 (4%)
11	22078	452.9	0.0677	Singlet-A	HOMO→LUMO (12%), HOMO→L+3 (37%)	H-19→LUMO (4%), H-18→LUMO (4%), H-3→L+1 (3%), H-2→LUMO (4%), H-2→L+2 (4%), H-1→L+3 (3%), HOMO→L+2 (6%), HOMO→L+4 (6%)
12	22371	447.0	0.0046	Singlet-A	H-19→LUMO (17%), H-18→LUMO (20%), H-16→LUMO (12%)	H-19→L+2 (4%), H-18→L+2 (6%), H-17→LUMO (6%), H-16→L+2 (3%), H-4→L+2 (2%), H-1→LUMO (7%), H-1→L+2 (3%), HOMO→L+3 (7%)
13	23031	434.2	0.0014	Singlet-A	H-18→L+6 (12%), H-3→L+6 (53%)	H-25→L+6 (4%), H-19→L+6 (5%), H-4→LUMO (5%), H-4→L+6 (8%)

14	23882	418.7	0.0319	Singlet-A	H-22→L+6 (15%), H-4→L+6 (51%), H-3→L+6 (10%)	H-23→L+6 (4%), H-21→L+6 (2%), H-3→LUMO (6%)
15	24437	409.2	0.0016	Singlet-A	H-1→L+6 (28%), HOMO→L+6 (52%)	H-4→L+1 (3%), H-3→L+2 (3%), H-2→L+6 (4%)
16	25203	396.8	1.1044	Singlet-A	H-2→L+1 (49%), H-1→L+2 (27%)	H-1→LUMO (6%), HOMO→L+1 (2%), HOMO→L+2 (4%)
17	25339	394.7	1.2264	Singlet-A	H-2→LUMO (11%), H-2→L+2 (40%), H-1→L+1 (31%)	H-4→L+6 (2%), HOMO→L+1 (5%), HOMO→L+2 (3%)
18	25740	388.5	0.019	Singlet-A	H-4→L+1 (37%), H-3→L+1 (11%), H-3→L+2 (34%)	H-4→LUMO (4%), H-4→L+2 (5%), H-3→LUMO (7%)
19	25864	386.6	0.0526	Singlet-A	H-1→L+3 (82%), HOMO→L+3 (10%)	H-1→L+4 (3%)
20	26281	380.5	0.003	Singlet-A	H-4→L+2 (32%), H-3→L+1 (44%)	H-4→LUMO (7%), H-4→L+1 (5%), H-3→LUMO (4%), H-3→L+2 (4%)
21	26906	371.7	0.003	Singlet-A	H-4→L+1 (39%), H-3→L+2 (31%)	H-4→LUMO (3%), H-4→L+2 (4%), H-3→LUMO (6%), H-3→L+1 (4%), H-1→L+6 (2%), HOMO→L+6 (6%)
22	26934	371.3	0.0598	Singlet-A	H-2→L+3 (56%), HOMO→L+3 (10%), HOMO→L+4 (21%)	H-2→L+4 (2%), H-1→L+3 (6%)
23	27170	368.0	0.0421	Singlet-A	H-2→L+3 (37%), HOMO→L+4 (53%)	HOMO→L+3 (3%)
24	28337	352.9	0.0058	Singlet-A	H-4→L+2 (28%), H-3→L+1 (27%)	H-4→LUMO (5%), H-4→L+1 (8%), H-3→LUMO (3%), H-3→L+2 (4%), H-1→L+4 (4%), HOMO→L+4 (5%)
25	29349	340.7	0.0106	Singlet-A	H-1→L+4 (87%)	H-1→L+3 (3%)
26	29753	336.1	0.0021	Singlet-A	H-12→LUMO (11%), H-8→LUMO (25%), H-7→LUMO (49%)	H-6→LUMO (3%)
27	30252	330.6	0.005	Singlet-A	H-2→L+4 (93%)	
28	30595	326.9	0.0797	Singlet-A	H-5→LUMO (81%)	H-8→LUMO (2%), H-6→L+1 (2%), H-3→LUMO (2%)
29	30671	326.0	0.0428	Singlet-A	H-6→LUMO (81%)	H-8→LUMO (5%), H-4→LUMO (2%)
30	30957	323.0	0.0017	Singlet-A	H-5→L+1 (17%), HOMO→L+5 (57%)	H-8→LUMO (6%), H-7→LUMO (5%), H-1→L+6 (3%)
31	31041	322.2	0.0105	Singlet-A	H-8→LUMO (34%), H-7→LUMO (25%), HOMO→L+5 (15%)	H-7→L+1 (4%), H-7→L+2 (4%), H-6→L+1 (2%), H-5→LUMO (6%), H-5→L+2 (2%)
32	31100	321.5	0.0051	Singlet-A	H-1→L+6 (44%), HOMO→L+6 (29%)	H-18→L+6 (2%), H-5→L+1 (4%), HOMO→L+5 (9%)

33	31170	320.8	0.0112	Singlet-A	H-5→L+1 (61%)	H-5→LUMO (4%), H-5→L+2 (6%), H-1→L+6 (7%), HOMO→L+5 (6%), HOMO→L+6 (5%)
34	31214	320.4	0.0053	Singlet-A	H-8→L+1 (19%), H-7→L+1 (48%)	H-12→L+1 (2%), H-8→LUMO (2%), H-8→L+2 (4%), H-6→L+1 (7%), H-6→L+2 (3%), H-5→L+2 (3%), HOMO→L+5 (4%)
35	31355	318.9	0.0221	Singlet-A	H-8→L+2 (23%), H-7→L+2 (44%)	H-12→L+2 (3%), H-8→LUMO (8%), H-7→L+1 (6%), H-6→L+2 (3%), H-5→L+1 (3%), H-5→L+2 (2%)
36	31404	318.4	0.0085	Singlet-A	H-7→L+1 (10%), H-6→L+1 (42%), H-5→L+2 (31%)	H-7→L+2 (3%), H-5→L+1 (5%)
37	31520	317.3	0.0395	Singlet-A	H-8→L+1 (33%), H-8→L+2 (15%), H-7→L+2 (12%), H-6→L+2 (18%)	H-7→L+1 (4%), H-5→L+2 (6%)
38	31566	316.8	0.0106	Singlet-A	H-8→L+1 (30%), H-7→L+1 (13%), H-6→L+2 (27%)	H-8→LUMO (4%), H-7→LUMO (2%), H-7→L+2 (3%), H-6→L+1 (8%), H-5→L+2 (4%)
39	31787	314.6	0.0077	Singlet-A	H-6→L+1 (22%), H-6→L+2 (25%), H-5→L+2 (25%)	H-8→LUMO (3%), H-8→L+2 (6%), H-5→L+1 (3%), H-2→L+5 (3%)
40	31930	313.2	0.0074	Singlet-A	H-8→L+2 (28%), H-7→L+2 (13%), H-6→L+2 (10%)	H-19→LUMO (2%), H-9→LUMO (9%), H-8→L+1 (4%), H-7→L+1 (4%), H-6→L+1 (3%), H-5→LUMO (2%), H-3→LUMO (3%)
41	32031	312.2	0.0144	Singlet-A	H-10→LUMO (11%), H-9→LUMO (23%), H-8→L+2 (11%), H-5→L+2 (13%)	H-19→LUMO (4%), H-16→LUMO (3%), H-13→LUMO (2%), H-7→LUMO (2%), H-7→L+2 (7%), H-6→L+1 (2%), H-3→LUMO (3%)
42	32150	311.0	0.0026	Singlet-A	H-10→LUMO (43%), H-9→LUMO (11%)	H-22→LUMO (5%), H-18→LUMO (2%), H-13→LUMO (2%), H-6→LUMO (4%), H-6→L+2 (2%), H-4→LUMO (5%), H-4→L+3 (5%)
43	32404	308.6	0.0164	Singlet-A	H-9→LUMO (26%), H-9→L+2 (10%)	H-19→LUMO (5%), H-17→LUMO (2%), H-16→LUMO (5%), H-13→LUMO (4%), H-12→LUMO (5%), H-11→LUMO (4%), H-10→LUMO (3%), H-10→L+2 (4%), H-4→L+3 (3%), H-3→L+3 (7%)
44	32489	307.8	0.0009	Singlet-A	H-10→LUMO (10%), H-10→L+1 (12%), H-4→L+3 (41%)	H-13→LUMO (2%), H-11→LUMO (2%), H-9→LUMO (6%), H-9→L+1 (4%), H-4→L+4 (4%), H-3→L+3 (5%)
45	32600	306.7	0.003	Singlet-A	H-11→LUMO (21%), H-10→L+1 (16%), H-4→L+3 (11%), H-2→L+6 (19%)	H-12→LUMO (6%), H-9→LUMO (3%), H-9→L+1 (9%), H-1→L+5 (3%)
46	32622	306.5	0.0005	Singlet-A	H-2→L+6 (69%)	H-12→LUMO (3%), H-11→LUMO (8%), H-10→L+1 (5%), H-1→L+6 (5%)

47	32735	305.5	0.0018	Singlet-A	H-12→LUMO (13%), H-11→LUMO (22%), H-10→L+1 (19%), H-9→L+1 (21%)	H-12→L+1 (7%), H-11→L+1 (5%)
48	32828	304.6	0.004	Singlet-A	H-12→LUMO (30%), H-11→LUMO (15%), H-3→L+3 (16%)	H-18→LUMO (3%), H-17→LUMO (4%), H-16→LUMO (3%), H-13→LUMO (7%), H-12→L+2 (2%), H-11→L+2 (3%), H-8→LUMO (2%)
49	32890	304.0	0.0048	Singlet-A	H-10→L+1 (17%), H-9→L+1 (26%), H-1→L+5 (36%)	H-11→L+1 (2%), H-9→LUMO (3%), H-9→L+2 (2%)
50	32911	303.9	0.0016	Singlet-A	H-12→LUMO (10%), H-10→L+2 (16%), H-9→L+2 (10%), H-3→L+3 (17%)	H-18→LUMO (5%), H-17→LUMO (4%), H-13→LUMO (5%), H-11→LUMO (4%), H-11→L+2 (4%), H-10→LUMO (4%), H-10→L+1 (4%), H-9→L+1 (2%), H-1→L+5 (2%)
51	33051	302.6	0.0068	Singlet-A	H-10→L+2 (14%), H-4→L+3 (12%), H-3→L+3 (13%), H-1→L+5 (10%)	H-17→LUMO (7%), H-15→LUMO (7%), H-13→LUMO (8%), H-12→LUMO (3%), H-11→LUMO (2%), H-10→L+1 (4%), H-9→LUMO (4%)
52	33099	302.1	0.0111	Singlet-A	H-11→L+1 (34%), H-9→L+1 (12%), H-1→L+5 (12%)	H-12→LUMO (3%), H-12→L+1 (4%), H-11→LUMO (4%), H-10→L+1 (7%), H-4→L+3 (2%)
53	33151	301.7	0.0079	Singlet-A	H-13→LUMO (13%), H-12→L+1 (16%), H-11→L+1 (10%), H-9→L+1 (14%), H-1→L+5 (11%)	H-16→L+1 (3%), H-13→L+1 (3%), H-9→L+2 (8%), H-7→L+1 (2%)
54	33230	300.9	0.0104	Singlet-A	H-11→L+1 (12%), H-9→L+2 (30%), H-1→L+5 (11%)	H-12→LUMO (2%), H-12→L+2 (3%), H-11→L+2 (3%), H-10→LUMO (6%), H-10→L+1 (5%), H-10→L+2 (8%)
55	33274	300.5	0.0023	Singlet-A	H-12→L+1 (19%), H-12→L+2 (10%), H-11→L+2 (12%), H-9→L+2 (12%)	H-16→L+1 (5%), H-13→LUMO (3%), H-13→L+1 (5%), H-12→LUMO (3%), H-11→LUMO (5%), H-11→L+1 (7%), H-10→L+1 (3%), H-10→L+2 (6%)
56	33369	299.7	0.0068	Singlet-A	H-13→LUMO (18%), H-13→L+1 (11%), H-9→L+2 (15%)	H-22→LUMO (3%), H-16→L+1 (2%), H-16→L+2 (3%), H-15→LUMO (6%), H-13→L+2 (9%), H-11→L+1 (3%), H-11→L+2 (4%), H-9→LUMO (4%)
57	33395	299.4	0.0011	Singlet-A	H-10→L+2 (22%)	H-18→LUMO (4%), H-16→L+1 (7%), H-14→LUMO (9%), H-13→LUMO (5%), H-13→L+1 (9%), H-12→L+2 (3%), H-11→L+2 (6%), H-10→LUMO (5%), H-9→L+1 (3%), H-9→L+2 (4%)
58	33516	298.4	0.0018	Singlet-A	H-13→L+1 (11%), H-11→L+1 (11%), H-11→L+2 (32%)	H-16→L+2 (3%), H-13→L+2 (7%), H-12→L+2 (8%), H-11→LUMO (3%), H-10→L+2 (8%)
59	33570	297.9	0.0096	Singlet-A	H-13→L+1 (13%), H-12→L+1 (35%)	H-16→L+1 (5%), H-14→LUMO (8%), H-13→LUMO (7%), H-11→L+1 (3%), H-10→L+2 (7%)

60	33749	296.3	0.0065	Singlet-A	H-14→LUMO (31%), H-12→L+2 (12%), H-11→L+2 (18%)	H-16→LUMO (4%), H-13→LUMO (5%), H-13→L+1 (4%), H-13→L+2 (6%), H-12→L+1 (4%), HOMO→L+16 (4%)

Table S9. TD-DFT calculated singlet excited states and transition components for 3b, Co^{III}(TPP)(*N*-py-$DTDA^-$), in 1,2-dichloroethane.
The simulations were performed on the geometry-optimized structure at the hseh1pbe /6-31G(d,p) level of theory. The HOMO (H) and LUMO (L) orbitals correspond to MOs 220 and 221, respectively. The lowest-energy 60 singlet excited states were calculated.

No.	Energy (cm^{-1})	Wavelength (nm)	Oscillator Strength	Symmetry	Major contributions	Minor contributions
1	1271	7867.0	0.0083	Singlet-A	HOMO→LUMO (100%)	
2	3079	3247.4	0.0001	Singlet-B	HOMO→L+1 (100%)	
3	3171	3153.2	0.0001	Singlet-B	HOMO→L+2 (100%)	
4	9816	1018.8	0.002	Singlet-B	HOMO→L+3 (98%)	
5	10982	910.6	0.0004	Singlet-B	H-27→LUMO (12%), H-22→LUMO (18%), H-8→LUMO (12%), H-5→LUMO (12%), H-3→LUMO (10%)	H-37→LUMO (2%), H-29→LUMO (4%), H-20→LUMO (6%), H-13→LUMO (8%), H-7→LUMO (6%), HOMO→L+3 (2%)
6	11519	868.1	0.0007	Singlet-A	HOMO→L+4 (100%)	
7	12159	822.4	0.0005	Singlet-B	H-25→LUMO (34%), H-4→LUMO (30%)	H-28→LUMO (4%), H-11→LUMO (8%), H-8→LUMO (2%), H-7→LUMO (8%)
8	12676	788.9	0.0003	Singlet-B	HOMO→L+6 (100%)	
9	15779	633.7	0.005	Singlet-A	H-1→LUMO (89%)	H-23→LUMO (6%)
10	16056	622.8	0.0	Singlet-A	HOMO→L+5 (100%)	
11	16211	616.9	0.0	Singlet-A	H-2→LUMO (98%)	
12	18541	539.3	0.0367	Singlet-A	HOMO→L+7 (99%)	
13	19382	515.9	0.0243	Singlet-B	H-2→L+2 (34%), H-1→L+1 (52%)	H-2→L+1 (6%), H-1→L+2 (7%)
14	19425	514.8	0.0204	Singlet-B	H-2→L+1 (35%), H-1→L+2 (52%)	H-2→L+2 (5%), H-1→L+1 (7%)
15	20848	479.7	0.0005	Singlet-A	H-23→LUMO (69%), H-17→LUMO (13%)	H-32→LUMO (4%), H-1→LUMO (8%)
16	21962	455.3	0.0	Singlet-A	H-23→L+4 (56%), H-17→L+4 (10%), H-1→L+4 (23%)	H-32→L+4 (4%)
17	22140	451.7	0.0	Singlet-A	HOMO→L+8 (100%)	
18	22253	449.4	0.0003	Singlet-B	HOMO→L+9 (100%)	
19	22424	446.0	0.0002	Singlet-B	HOMO→L+10 (100%)	
20	23026	434.3	0.0	Singlet-A	HOMO→L+11 (56%), HOMO→L+12 (43%)	
21	23046	433.9	0.0	Singlet-A	HOMO→L+11 (43%), HOMO→L+12 (56%)	
22	23257	430.0	0.0002	Singlet-B	HOMO→L+13 (100%)	

23	23354	428.2	0.0	Singlet-A	HOMO→L+14 (100%)	
24	23386	427.6	0.0001	Singlet-B	HOMO→L+15 (100%)	
25	24510	408.0	0.6278	Singlet-B	H-3→LUMO (14%), H-2→L+1 (19%), H-2→L+2 (17%), H-1→L+1 (10%), H-1→L+2 (13%)	H-8→LUMO (2%), H-5→LUMO (8%)
26	24631	406.0	0.577	Singlet-B	H-2→L+1 (19%), H-2→L+2 (13%), H-1→L+2 (13%)	H-27→L+4 (5%), H-22→L+4 (7%), H-20→L+4 (2%), H-13→L+4 (3%), H-8→L+4 (4%), H-7→L+4 (3%), H-5→L+4 (5%), H-4→LUMO (5%), H-3→L+4 (4%), H-1→L+1 (9%)
27	24981	400.3	0.0	Singlet-A	HOMO→L+17 (99%)	
28	25210	396.7	0.5704	Singlet-B	H-2→L+2 (19%), H-1→L+1 (13%)	H-37→L+4 (2%), H-27→L+4 (4%), H-22→L+4 (6%), H-20→L+4 (3%), H-13→L+4 (4%), H-8→L+4 (8%), H-7→L+4 (3%), H-5→L+4 (8%), H-4→L+4 (2%), H-3→LUMO (3%), H-3→L+4 (5%), H-2→L+1 (6%), H-1→L+2 (4%)
29	25512	392.0	0.2886	Singlet-B	H-3→LUMO (59%)	H-25→L+4 (4%), H-7→L+4 (2%), H-4→L+4 (4%), H-2→L+1 (6%), H-2→L+2 (6%), H-1→L+1 (4%), H-1→L+2 (4%)
30	26108	383.0	0.0002	Singlet-A	H-23→L+4 (21%), H-1→L+4 (73%)	
31	26615	375.7	0.2533	Singlet-B	H-25→L+4 (20%), H-4→L+4 (29%)	H-28→L+4 (3%), H-11→L+4 (7%), H-7→L+4 (8%), H-5→LUMO (5%), H-2→L+1 (6%), H-1→L+2 (4%)
32	26670	375.0	0.0	Singlet-A	H-14→LUMO (35%), H-9→LUMO (58%)	H-6→LUMO (2%)
33	27158	368.2	0.0018	Singlet-B	H-1→L+3 (97%)	
34	27433	364.5	0.0885	Singlet-B	H-7→LUMO (23%), H-5→LUMO (59%)	H-8→LUMO (8%)
35	27459	364.2	0.0002	Singlet-A	H-2→L+4 (94%)	H-23→L+4 (2%)
36	27604	362.3	0.0984	Singlet-B	H-8→LUMO (34%), H-7→LUMO (20%), H-4→LUMO (35%)	H-11→LUMO (4%), H-5→LUMO (3%)
37	27800	359.7	0.0024	Singlet-A	H-6→LUMO (94%)	H-9→LUMO (3%)
38	28055	356.4	0.0	Singlet-A	H-3→L+1 (70%)	H-7→L+1 (4%), H-5→L+1 (7%), H-4→L+1 (4%), H-4→L+2 (5%), H-3→L+2 (5%)
39	28214	354.4	0.0003	Singlet-A	H-3→L+2 (79%)	H-8→L+2 (3%), H-5→L+2 (3%), H-4→L+2 (4%), H-3→L+1 (9%)
40	28289	353.5	0.0005	Singlet-B	H-2→L+3 (100%)	

41	28559	350.1	0.0029	Singlet-B	H-10→LUMO (99%)	
42	28584	349.8	0.0	Singlet-A	H-5→L+1 (10%), H-4→L+1 (14%), H-4→L+2 (33%), H-3→L+1 (16%)	H-8→L+2 (4%), H-7→L+1 (5%), H-5→L+2 (4%), H-3→L+2 (9%)
43	28854	346.6	0.0	Singlet-A	H-7→L+1 (11%), H-5→L+2 (10%), H-4→L+1 (32%), H-4→L+2 (19%)	H-8→L+2 (8%), H-5→L+1 (7%), H-3→L+1 (3%), H-3→L+2 (5%)
44	28892	346.1	0.0131	Singlet-B	H-11→LUMO (64%), H-7→LUMO (15%)	H-8→LUMO (8%), H-4→LUMO (8%)
45	29040	344.4	0.0185	Singlet-B	H-13→LUMO (61%), H-8→LUMO (18%), H-7→LUMO (10%)	H-5→LUMO (3%)
46	29188	342.6	0.0002	Singlet-A	H-14→LUMO (24%), H-12→LUMO (48%), H-9→LUMO (23%)	
47	29370	340.5	0.0002	Singlet-A	H-14→LUMO (29%), H-12→LUMO (49%), H-9→LUMO (13%)	H-5→L+1 (2%)
48	29655	337.2	0.0001	Singlet-A	H-5→L+1 (33%), H-4→L+1 (22%)	H-14→LUMO (7%), H-8→L+1 (8%), H-7→L+1 (3%), H-7→L+2 (9%), H-5→L+2 (4%), H-4→L+2 (7%)
49	29808	335.5	0.0016	Singlet-A	H-8→L+1 (10%), H-5→L+1 (10%), H-5→L+2 (53%), H-4→L+2 (11%)	H-15→LUMO (5%), H-7→L+2 (2%), H-4→L+1 (6%)
50	30023	333.1	0.0334	Singlet-B	H-6→L+1 (93%)	
51	30039	332.9	0.0003	Singlet-A	H-15→LUMO (12%), H-7→L+1 (40%), H-7→L+2 (13%), H-4→L+1 (11%)	H-17→LUMO (3%), H-8→L+1 (4%), H-5→L+1 (7%), H-5→L+2 (5%)
52	30092	332.3	0.0147	Singlet-A	H-15→LUMO (35%), H-8→L+1 (11%), H-7→L+1 (25%)	H-17→LUMO (3%), H-11→L+1 (3%), H-7→L+2 (4%), H-5→L+1 (8%), H-5→L+2 (5%)
53	30102	332.2	0.0324	Singlet-B	H-6→L+2 (90%)	H-9→L+1 (5%)
54	30214	331.0	0.0081	Singlet-A	H-8→L+1 (10%), H-8→L+2 (57%)	H-15→LUMO (4%), H-7→L+2 (3%), H-5→L+1 (3%), H-5→L+2 (8%), H-4→L+2 (5%)
55	30383	329.1	0.0106	Singlet-B	H-9→L+1 (82%)	H-14→L+1 (4%), H-9→L+2 (5%), H-6→L+2 (5%)
56	30462	328.3	0.0092	Singlet-B	H-9→L+2 (73%)	H-22→LUMO (4%), H-14→L+2 (3%), H-12→L+1 (4%), H-9→L+1 (3%), H-6→L+1 (3%)

57	30470	328.2	0.0082	Singlet-A	H-15→LUMO (40%), H-8→L+1 (23%), H-7→L+2 (22%)	H-17→LUMO (4%), H-8→L+2 (4%), H-7→L+1 (3%)
58	30526	327.6	0.0	Singlet-A	H-8→L+1 (24%), H-8→L+2 (14%), H-7→L+2 (39%)	H-5→L+1 (9%), H-5→L+2 (2%), H-4→L+2 (8%)
59	30656	326.2	0.1073	Singlet-B	H-22→LUMO (22%), H-13→LUMO (21%), H-9→L+2 (12%)	H-27→LUMO (5%), H-20→LUMO (9%), H-8→LUMO (6%), H-5→LUMO (2%), H-3→LUMO (6%)
60	30706	325.7	0.0	Singlet-A	HOMO→L+16 (100%)	

Table S10. Selected TD-DFT calculated Vis-NIR electronic transitions and assignments for 3b.[a]

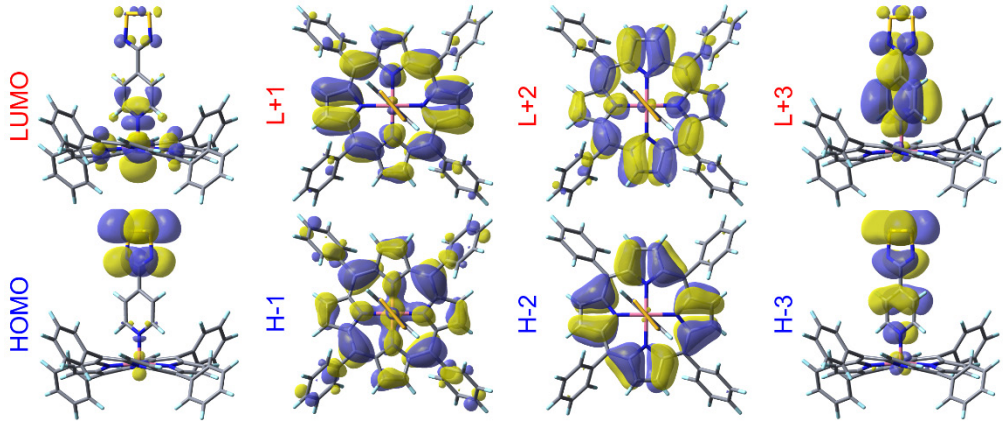

λ (nm)[b]	f[c]	Symm.	Contribution	Assignment[d]
3286	0.0001	^1B	H → L+1 (100%)	**A**; MLCT: dz^2,π(DTDA) → π*(porphyrin, e_g)
3192	0.0001	^1B	H → L+2 (100%)	**A**; MLCT: dz^2,π(DTDA) → π*(porphyrin, e_g)
1058 (**a**)	0.0020	^1B	H → L+3 (100%)	**B**; π-π* IL (A): dz^2,π(DTDA) → dπ*,π*(DTDA)
950 (**b**)	0.0004	^1B	H-27 → L (12%)	**N**; LMCT: dπ,π(porphyrin, py-DTDA) → dz^{2*},π*(porphyrin, a_{2u})
			H-22 → L (18%)	**O;**, LMCT: dπ,π(py-DTDA) → dz^{2*},π*(porphyrin, a_{2u})
			H-8 → L (12%)	**C**; LMCT: dπ,π(porphyrin) → dz^{2*},π*(porphyrin, a_{2u})
			H-5 → L (12%)	**C**; LMCT: dπ,π(porphyrin) → dz^{2*},π*(porphyrin, a_{2u})
			H-3 → L (10%)	**D**; LMCT: dπ,π(DTDA) → dz^{2*},π*(porphyrin, a_{2u})
907 (**c**)	0.0007	^1A	H → L+4 (100%)	**E**; d-d, LMCT: dz^2,π(DTDA) → σ*(dx^2-y^2, porphyrin)
861 (**d**)	0.0005	^1B	H-25 → L (34%)	**P**; LMCT: σ(porphyrin) → dz^{2*},π*(porphyrin, a_{2u})
			H-4 → L (30%)	**C**; LMCT: dπ,π(porphyrin) → dz^{2*},π*(porphyrin, a_{2u})
			H-11 → L (8%)	**C**; LMCT: dπ,π(porphyrin) → dz^{2*},π*(porphyrin, a_{2u})
			H-7 → L (8%)	**C**; LMCT: dπ,π(porphyrin) → dz^{2*},π*(porphyrin, a_{2u})
828 (**d**)	0.0003	^1B	H → L+6 (100%)	**F**; π-σ* (A): dz^2,π(DTDA) → σ*(DTDA, S–S)
673 (**g**)	0.0050	^1A	H-1 → L (89%)	**C**; LMCT: dπ,π(porphyrin) → dz^{2*},π*(porphyrin, a_{2u})
			H-23 → L (6%)	**Q;** d-d, MLCT: dxy,σ(porphyrin) → dz^{2*},π*(porphyrin, a_{2u})
662 (**g**)	0	^1A	H → L+5 (100%)	**G**; π-π* (A-P): dz^2,π(DTDA) → π*(porphyrin, e_u)
656 (**g**)	0	^1A	H-2 → L (98%)	**H**; LMCT: π(porphyrin, a_{2u}) → dz^{2*},π*(porphyrin)
578 (**h**)	0.0367	^1A	H → L+7 (99%)	**I**; π-π* (A): π(porphyrin, a_{1u}) → π*(porphyrin, e_g)
555 (**h**)	0.0243	^1B	H-2 → L+2 (34%)	**J**; π-π* (P): π(porphyrin, a_{1u}) → π*(porphyrin, e_g)
			H-1 → L+1 (52%)	**K**; π-π* (P): dπ,π(porphyrin, a_{2u}) → π*(porphyrin, e_g)
554 (**h**)	0.0204	^1B	H-2 → L+1 (35%)	**L**; π-π* (P): π(porphyrin, a_{1u}) → π*(porphyrin, e_g)
			H-1 → L+2 (52%)	**M**; π-π* (P): dπ,π(porphyrin, a_{2u}) → π*(porphyrin, e_g)
519	0.0005	^1A	H-23 → L (69%)	**Q;** d-d, MLCT: dxy,σ(porphyrin) → dz^{2*},π*(porphyrin, a_{2u})
			H-17 → L (13%)	**R**; MLCT: π(porphyrin) → dz^{2*},π*(porphyrin, a_{2u})

[a] Fourteen out of the lowest 60 calculated excited states are listed. Abbreviations: A, axial ligand (py-DTDA); H, HOMO (MO 220); L, LUMO (MO 221); LMCT, ligand-to-metal charge transfer; MLCT, metal-to-ligand charge transfer; P, porphyrin (TPP). [b] The calculated wavelength has been corrected by +39 nm to match the energy of the experimental spectrum (Soret band, UV region). Transitions (**a**, **b**, **c**, **d**, **g**, and **h**) making up key bands in the experimentally deconvoluted electronic spectrum of **3b** displayed in Figure 11 of the main paper are indicated. [c] Oscillator strength. [d] Symmetry labels for porphyrin MOs are those appropriate for D_{4h} symmetry (as per convention in the field); the actual point group symmetry of **3b** is C_2. Bold capital letters (arbitrary order) for specific transitions are used to facilitate straightforward discussion of assignments where necessary (next page).

Comments on Selected Bands Listed in Table S10. Band **a** has been discussed within the context of Figure 11 of the paper. Band **b** (939 nm) in the experimental spectrum of **3b** correlates with the transition at 950 nm in the calculated spectrum, is a composite LMCT band (^1B state) derived from multiple single-electron excitations from filled porphyrin-based MOs (transitions **N**, **O**, and **C**) as well as a filled π-symmetry py-DTDA orbital admixed with significant dπ character (transition **D**) to the LUMO, which has mainly mixed dz^{2*} and π*(porphyrin, a_{2u}) character. Band **c** (901 nm) in the experimental spectrum of **3b** is matched by the calculated transition at 907 nm (Table S10), which involves a ^1A excited state generated exclusively by an excitation from the HOMO to the LUMO+4 level. The LUMO+4 level (σ*) is the antibonding MO for the in-plane Co–$N_{pyrrole}$ σ bonds ($3dx^2$–y^2 mixed with the pyrrole nitrogen atom lone pairs). Consequently, the transition has substantial LMCT character. Band **d** (846 nm) in the experimental spectrum of **3b** is assigned to the closely-spaced ^1B states at 861 and 828 nm in the DFT-calculated spectrum. The band at 861 nm is a combination MLCT state involving excitations from filled mixed dπ,π(porphyrin) MOs as well as a porphyrin-based σ-bonding MO to the LUMO with mixed dz^{2*},π*(porphyrin, a_{2u}) character. The calculated band at 828 nm is derived from a single transition originating in the HOMO (π-symmetry, DTDA ring) and terminating in L+6, the σ* MO of the S–S bond in the DTDA ring. The distinct band at 672 nm in the DFT-calculated spectrum of **3b** matches the experimental band (673 nm, **g**) and is of mixed LMCT and d-d character. The remaining bands in the spectrum (Table S10) are mostly π-π* transitions of the metalloporphyrin, the notable exception being the intense band at 578 nm in the calculated spectrum (preceding the porphyrin Q states), which is due to a strongly allowed π-π* transition of the axial py-DTDA$^-$ ligand. This important diagnostic band for the axial ligand is unfortunately difficult to resolve in the experimental spectrum due to overlap with the intense Q bands.

5. Cartesian Coordinates: DFT Structures

Typical Gaussian 09 keywords used to run jobs (with a solvent continuum):

```
# opt freq=vcd uhseh1pbe/6-31g(d,p)/auto
scrf=(solvent=dichloromethane) pop=npa
geom=connectivity
```

The atomic Cartesian coordinates of geometry-optimized structures presented in the following sections may be copied into a text editor and saved as **file_name.xyz** in order to produce an input file for import into any open-source molecular modelling or molecular graphics application, e.g. Avogadro 1.2.0,[27] for 3D viewing or re-use in a calculation. All listed energies are in Hartrees. Structures listed throughout Section 5 have C_1 symmetry unless otherwise noted.

5.1. py-DTDA in Five Redox States

Point group symmetry: Sections 6.1.1 through 6.1.5, C_{2v}.

5.1.1. Neutral Radical 2

A. Gas Phase

```
15
Energy: -747334.4505475
S          0.00000        1.06916       -2.68143
S          0.00000       -1.06916       -2.68143
N          0.00000        1.17145       -1.04920
N          0.00000       -1.17145       -1.04920
C          0.00000        0.00000       -0.41013
C          0.00000        0.00000        1.06654
C          0.00000       -1.19709        1.78243
H          0.00000       -2.14756        1.26078
C          0.00000       -1.13695        3.17119
H          0.00000       -2.05613        3.75370
N          0.00000        0.00000        3.86910
C          0.00000        1.13695        3.17119
H          0.00000        2.05613        3.75370
C          0.00000        1.19709        1.78243
H          0.00000        2.14756        1.26078
```

B. DCM Solution

```
15
Energy: -747337.9116512
S          0.00000        1.06594       -2.68327
S          0.00000       -1.06594       -2.68327
N          0.00000        1.17141       -1.04902
N          0.00000       -1.17141       -1.04902
C          0.00000        0.00000       -0.41070
C          0.00000        0.00000        1.06688
C          0.00000       -1.19672        1.78380
H          0.00000       -2.14953        1.26693
C          0.00000       -1.13838        3.17247
H          0.00000       -2.05946        3.75144
N          0.00000        0.00000        3.87169
C          0.00000        1.13838        3.17247
H          0.00000        2.05946        3.75144
C          0.00000        1.19672        1.78380
H          0.00000        2.14953        1.26693
```

C. DMSO Solution

```
15
Energy: -747338.5137215
S          0.00000        1.06585       -2.68359
S          0.00000       -1.06585       -2.68359
N          0.00000        1.17119       -1.04926
N          0.00000       -1.17119       -1.04926
C          0.00000        0.00000       -0.41074
C          0.00000        0.00000        1.06700
C          0.00000       -1.19671        1.78415
H          0.00000       -2.15001        1.26825
C          0.00000       -1.13872        3.17278
H          0.00000       -2.06018        3.75106
N          0.00000        0.00000        3.87216
C          0.00000        1.13872        3.17278
H          0.00000        2.06018        3.75106
C          0.00000        1.19671        1.78415
H          0.00000        2.15001        1.26825
```

D. DCE Solution

```
15
Energy: -747337.9981973
S          0.00000        1.06594       -2.68327
S          0.00000       -1.06594       -2.68327
N          0.00000        1.17141       -1.04902
N          0.00000       -1.17141       -1.04902
C          0.00000        0.00000       -0.41070
C          0.00000        0.00000        1.06688
C          0.00000       -1.19672        1.78380
H          0.00000       -2.14953        1.26693
C          0.00000       -1.13838        3.17247
H          0.00000       -2.05946        3.75144
N          0.00000        0.00000        3.87169
C          0.00000        1.13838        3.17247
H          0.00000        2.05946        3.75144
C          0.00000        1.19672        1.78380
H          0.00000        2.14953        1.26693
```

5.1.2. Cationic py-DTDA, 2^+

A. Gas Phase

```
15
Energy: -747158.5395442
N          0.00000        0.00000        3.85055
S          0.00000        1.03760       -2.66119
S          0.00000       -1.03760       -2.66119
N          0.00000        1.15350       -1.08648
N          0.00000       -1.15350       -1.08648
C          0.00000        0.00000       -0.38575
C          0.00000        0.00000        1.06981
C          0.00000        1.20676        1.77477
H          0.00000        2.16267        1.26290
C          0.00000        1.14310        3.16521
H          0.00000        2.05763        3.75251
C          0.00000       -1.20676        1.77477
H          0.00000       -2.16267        1.26290
C          0.00000       -1.14310        3.16521
H          0.00000       -2.05763        3.75251
```

B. DCM Solution

```
15
Energy: -747207.6492573
N          0.00000        0.00000        3.85620
S          0.00000        1.03069       -2.66050
S          0.00000       -1.03069       -2.66050
N          0.00000        1.15295       -1.08503
N          0.00000       -1.15295       -1.08503
C          0.00000        0.00000       -0.39512
C          0.00000        0.00000        1.06862
C          0.00000        1.20306        1.77537
H          0.00000        2.15818        1.26281
```

C	0.00000	1.14164	3.16431
H	0.00000	2.06026	3.74524
C	0.00000	-1.20306	1.77537
H	0.00000	-2.15818	1.26281
C	0.00000	-1.14164	3.16431
H	0.00000	-2.06026	3.74524

C. DMSO Solution

15
Energy: -747213.2591731

N	0.00000	0.00000	3.85703
S	0.00000	1.03078	-2.65999
S	0.00000	-1.03078	-2.65999
N	0.00000	1.15273	-1.08499
N	0.00000	-1.15273	-1.08499
C	0.00000	0.00000	-0.39679
C	0.00000	0.00000	1.06805
C	0.00000	1.20243	1.77525
H	0.00000	2.15729	1.26241
C	0.00000	1.14152	3.16397
H	0.00000	2.06104	3.74369
C	0.00000	-1.20243	1.77525
H	0.00000	-2.15729	1.26241
C	0.00000	-1.14152	3.16397
H	0.00000	-2.06104	3.74369

5.1.3. Anionic py-DTDA, 2^-

A. Gas Phase

15
Energy: -747366.8347361

N	0.00000	0.00000	3.88413
S	0.00000	1.10602	-2.70225
S	0.00000	-1.10602	-2.70225
N	0.00000	1.19483	-1.00058
N	0.00000	-1.19483	-1.00058
C	0.00000	0.00000	-0.42720
C	0.00000	0.00000	1.05682
C	0.00000	1.19164	1.78560
H	0.00000	2.13358	1.24788
C	0.00000	1.13329	3.17354
H	0.00000	2.05663	3.75408
C	0.00000	-1.19164	1.78560
H	0.00000	-2.13358	1.24788
C	0.00000	-1.13329	3.17354
H	0.00000	-2.05663	3.75408

B. DCM Solution

15
Energy: -747410.7944978

N	0.00000	0.00000	3.88417
S	0.00000	1.10308	-2.70745
S	0.00000	-1.10308	-2.70745
N	0.00000	1.19230	-1.00397
N	0.00000	-1.19230	-1.00397
C	0.00000	0.00000	-0.42352
C	0.00000	0.00000	1.06347
C	0.00000	1.19225	1.78995
H	0.00000	2.14086	1.26528
C	0.00000	1.13623	3.17847
H	0.00000	2.05920	3.75662
C	0.00000	-1.19225	1.78995
H	0.00000	-2.14086	1.26528
C	0.00000	-1.13623	3.17847
H	0.00000	-2.05920	3.75662

C. DMSO Solution

15
Energy: -747415.6642474

N	0.00000	0.00000	3.88505
S	0.00000	1.10299	-2.70917
S	0.00000	-1.10299	-2.70917
N	0.00000	1.19151	-1.00516
N	0.00000	-1.19151	-1.00516
C	0.00000	0.00000	-0.42274
C	0.00000	0.00000	1.06519
C	0.00000	1.19258	1.79164
H	0.00000	2.14223	1.26892
C	0.00000	1.13684	3.18018
H	0.00000	2.05970	3.75807
C	0.00000	-1.19258	1.79164
H	0.00000	-2.14223	1.26892
C	0.00000	-1.13684	3.18018
H	0.00000	-2.05970	3.75807

5.1.4. Di-cationic py-DTDA, 2^{2+}

A. Gas Phase

15
Energy: -746865.7739409

N	0.00000	0.00000	3.69445
S	0.00000	1.04058	-2.64790
S	0.00000	-1.04058	-2.64790
N	0.00000	1.15323	-1.07074
N	0.00000	-1.15323	-1.07074
C	0.00000	0.00000	-0.38980
C	0.00000	0.00000	1.08942
C	0.00000	1.21945	1.77899
H	0.00000	2.17936	1.27079
C	0.00000	1.20180	3.17774
H	0.00000	2.08051	3.82100
C	0.00000	-1.21945	1.77899
H	0.00000	-2.17936	1.27079
C	0.00000	-1.20180	3.17774
H	0.00000	-2.08051	3.82100

B. DMSO Solution

15
Energy: -747031.7710790

N	0.00000	0.00000	3.91567
S	0.00000	1.03254	-2.67531
S	0.00000	-1.03254	-2.67531
N	0.00000	1.15449	-1.09972
N	0.00000	-1.15449	-1.09972
C	0.00000	0.00000	-0.42781
C	0.00000	0.00000	1.04332
C	0.00000	1.18506	1.76850
H	0.00000	2.15517	1.28231
C	0.00000	1.12594	3.21489
H	0.00000	2.06038	3.76916
C	0.00000	-1.18506	1.76850
H	0.00000	-2.15517	1.28231
C	0.00000	-1.12594	3.21489
H	0.00000	-2.06038	3.76916

5.1.5. Di-anionic py-DTDA, 2^{2-}

A. Gas Phase

```
15
Energy: -747265.9293561
N           0.00000         0.00000         3.97022
S           0.00000         1.11757        -2.73214
S           0.00000        -1.11757        -2.73214
N           0.00000         1.19896        -1.03724
N           0.00000        -1.19896        -1.03724
C           0.00000         0.00000        -0.41596
C           0.00000         0.00000         1.03545
C           0.00000         1.19727         1.82568
H           0.00000         2.15798         1.31532
C           0.00000         1.13555         3.19791
H           0.00000         2.07663         3.76374
C           0.00000        -1.19727         1.82568
H           0.00000        -2.15798         1.31532
C           0.00000        -1.13555         3.19791
H           0.00000        -2.07663         3.76374
```

B. DMSO Solution

```
15
Energy: -747438.8603483
N           0.00000         0.00000         3.95328
S           0.00000         1.10482        -2.73076
S           0.00000        -1.10482        -2.73076
N           0.00000         1.19910        -1.03240
N           0.00000        -1.19910        -1.03240
C           0.00000         0.00000        -0.40732
C           0.00000         0.00000         1.03696
C           0.00000         1.20092         1.82332
H           0.00000         2.16556         1.32240
C           0.00000         1.14052         3.19494
H           0.00000         2.07570         3.76167
C           0.00000        -1.20092         1.82332
H           0.00000        -2.16556         1.32240
C           0.00000        -1.14052         3.19494
H           0.00000        -2.07570         3.76167
```

5.1.6. π-π dimer, $\{py\text{-}DTDA\}_2$

A. Gas Phase

```
30
Energy: -1495433.1448772
S          -2.67625         1.57362        -1.08688
S          -2.67604         1.57312         1.08752
N          -1.04396         1.68539        -1.17515
N          -1.04373         1.68483         1.17555
C          -0.40459         1.74710         0.00015
C           1.06855         1.91662         0.00006
C           1.78185         2.01027         1.19961
H           1.26700         1.94265         2.15069
C           3.16160         2.19682         1.14080
H           3.73817         2.27480         2.06039
N           3.85610         2.29337        -0.00011
C           3.16142         2.19710        -1.14094
H           3.73786         2.27537        -2.06059
C           1.78167         2.01063        -1.19958
H           1.26665         1.94334        -2.15059
S          -2.67731        -1.57263         1.08686
S          -2.67716        -1.57211        -1.08748
N          -1.04506        -1.68489         1.17514
N          -1.04483        -1.68452        -1.17558
C          -0.40575        -1.74695        -0.00017
C           1.06734        -1.91704        -0.00007
C           1.78041        -2.01130         1.19957
H           1.26542        -1.94379         2.15059
C           3.16010        -2.19829         1.14093
H           3.73650        -2.27674         2.06060
N           3.85475        -2.29479         0.00011
C           3.16029        -2.19800        -1.14080
H           3.73685        -2.27617        -2.06038
C           1.78061        -2.01097        -1.19961
H           1.26577        -1.94320        -2.15069
```

5.2. Five-Coordinate Co(TPP)(L) Complexes

5.2.1. Co(TPP)(*S*-py-DTDA), compound 3a

A. Gas Phase

```
92
Energy: -2813751.6218733
S           0.06463        -1.75856        -2.54355
S          -0.23147         0.18008        -1.66511
N           1.71076        -1.60590        -2.57397
N           1.31996         0.60750        -1.88583
C           2.13307        -0.39841        -2.26381
C           3.58054        -0.10860        -2.33192
C           4.06111         1.18532        -2.12831
H           3.37052         1.99447        -1.91825
C           5.43389         1.40078        -2.18669
H           5.83203         2.40149        -2.02944
N           6.33295         0.44190        -2.41720
C           5.85810        -0.79121        -2.61409
H           6.60072        -1.56434        -2.80334
C           4.50824        -1.11959        -2.58713
H           4.17165        -2.13709        -2.75143
Co         -0.65120         0.07444         0.47175
N          -1.76987        -1.53451         0.43839
C          -1.34118        -2.83571         0.30950
N          -2.26102         1.18146         0.30387
C          -2.44488        -3.71826         0.07299
H          -2.36125        -4.78064        -0.10035
N           0.39451         1.69326         0.79529
C          -3.56693        -2.95979         0.12788
H          -4.59417        -3.26902         0.00374
N           0.88065        -1.02683         0.95173
C          -3.14218        -1.60825         0.34502
C          -4.02383        -0.53272         0.37771
C          -3.57783         0.78507         0.34914
C          -4.45421         1.91681         0.26101
H          -5.53099         1.87028         0.32669
C          -3.66742         3.00532         0.08091
H          -3.96194         4.03902        -0.02438
C          -2.31152         2.54202         0.11484
C          -1.21511         3.39941         0.06320
C           0.06190         2.97344         0.41282
C           1.19277         3.84818         0.51594
H           1.19262         4.89349         0.24542
C           2.21036         3.10776         1.01807
H           3.22094         3.41627         1.24116
C           1.71226         1.77150         1.17090
C           2.51616         0.70592         1.56850
C           2.09555        -0.61433         1.45124
C           2.92910        -1.74078         1.75791
H           3.90812        -1.67887         2.20860
C           2.24922        -2.84504         1.36796
H           2.54861        -3.88015         1.43789
C           0.98057        -2.39426         0.87453
C          -0.02833        -3.26671         0.47476
C          -5.48472        -0.81165         0.38405
C          -6.07055        -1.46061         1.47734
H          -5.44618        -1.74428         2.31962
C          -7.43499        -1.73149         1.49393
H          -7.87453        -2.22951         2.35317
C          -8.23463        -1.36205         0.41578
H          -9.29951        -1.57445         0.42815
C          -7.66198        -0.72131        -0.67969
H          -8.27755        -0.43811        -1.52846
C          -6.29789        -0.44806        -0.69592
H          -5.84933         0.04179        -1.55529
C          -1.44738         4.82371        -0.29283
C          -1.90783         5.16100        -1.57093
H          -2.07393         4.37122        -2.29776
C          -2.13880         6.48942        -1.91336
H          -2.48805         6.73488        -2.91196
```

C	-1.91912	7.50047	-0.98176
H	-2.10062	8.53726	-1.24888
C	-1.46823	7.17598	0.29495
H	-1.30400	7.95830	1.03017
C	-1.23396	5.84811	0.63733
H	-0.89506	5.59331	1.63729
C	3.88676	0.99700	2.06531
C	4.06656	1.74282	3.23646
H	3.19365	2.08688	3.78385
C	5.34487	2.03361	3.70204
H	5.46720	2.60628	4.61676
C	6.46268	1.59104	2.99935
H	7.46042	1.82290	3.36011
C	6.29554	0.85406	1.82997
H	7.15955	0.51820	1.26436
C	5.01784	0.55583	1.36739
H	4.89077	-0.00544	0.44686
C	0.31500	-4.69963	0.28538
C	1.22427	-5.06404	-0.71571
H	1.65276	-4.28916	-1.34573
C	1.56431	-6.39935	-0.90721
H	2.26426	-6.66823	-1.69290
C	1.00844	-7.38751	-0.09887
H	1.27611	-8.42930	-0.24847
C	0.11120	-7.03393	0.90538
H	-0.31705	-7.79804	1.54753
C	-0.23326	-5.69963	1.09704
H	-0.92076	-5.42174	1.89069

B. DCM Solution

92
Energy: -2813768.9546010

S	0.02668	-1.68893	-2.58535
S	-0.21390	0.22382	-1.63773
N	1.67775	-1.56508	-2.65184
N	1.34972	0.62531	-1.86108
C	2.13102	-0.37954	-2.30261
C	3.58222	-0.11565	-2.41589
C	4.11021	1.14045	-2.11360
H	3.46114	1.94281	-1.78190
C	5.48100	1.33620	-2.24429
H	5.91137	2.30897	-2.01449
N	6.33686	0.38998	-2.63999
C	5.81822	-0.80891	-2.92588
H	6.52275	-1.57353	-3.24702
C	4.46573	-1.11192	-2.83473
H	4.09841	-2.10166	-3.08114
Co	-0.64524	0.07320	0.49136
N	-1.67728	-1.58736	0.47425
C	-1.18446	-2.86517	0.34056
N	-2.30245	1.09308	0.28070
C	-2.24932	-3.80659	0.15742
H	-2.11966	-4.86649	-0.00265
N	0.30594	1.74365	0.81120
C	-3.40714	-3.10632	0.24729
H	-4.42015	-3.47263	0.16931
N	0.93910	-0.94344	0.96983
C	-3.04663	-1.73022	0.42517
C	-3.98071	-0.69816	0.43720
C	-3.59929	0.63743	0.33837
C	-4.52489	1.72129	0.17697
H	-5.59959	1.63098	0.23132
C	-3.78617	2.83346	-0.06069
H	-4.12872	3.84361	-0.23050
C	-2.41045	2.43839	0.01884
C	-1.35402	3.34631	-0.03501
C	-0.07450	2.99900	0.39007
C	0.99968	3.93468	0.54875
H	0.96144	4.97657	0.26776
C	2.02253	3.25744	1.12706
H	2.99702	3.62779	1.40951
C	1.59459	1.89484	1.25964
C	2.44448	0.87175	1.67511
C	2.11956	-0.46972	1.49628
C	3.02530	-1.55053	1.76096
H	3.99808	-1.44526	2.21742
C	2.42229	-2.68159	1.32067
H	2.79318	-3.69542	1.35082
C	1.12375	-2.29884	0.84643
C	0.15620	-3.22308	0.45716
C	-5.42584	-1.04832	0.48342
C	-5.95960	-1.66456	1.62180
H	-5.31038	-1.87028	2.46804
C	-7.30847	-2.00287	1.67769
H	-7.70841	-2.47440	2.57040
C	-8.14219	-1.73528	0.59438
H	-9.19426	-2.00053	0.63733
C	-7.61990	-1.12880	-0.54573
H	-8.26178	-0.92529	-1.39768
C	-6.27173	-0.78745	-0.60150
H	-5.86396	-0.32529	-1.49585
C	-1.64075	4.73974	-0.46673
C	-2.05669	4.99035	-1.78018
H	-2.14994	4.16080	-2.47514
C	-2.33737	6.28751	-2.19892
H	-2.65132	6.46612	-3.22300
C	-2.21382	7.35203	-1.30915
H	-2.43442	8.36390	-1.63548
C	-1.80958	7.11260	0.00229
H	-1.72082	7.93619	0.70446
C	-1.52488	5.81629	0.42123
H	-1.22360	5.63017	1.44798
C	3.76002	1.24061	2.26221
C	3.80798	1.93530	3.47741
H	2.87982	2.18602	3.98302
C	5.02891	2.29284	4.04150
H	5.04916	2.82446	4.98820
C	6.21960	1.96832	3.39553
H	7.17224	2.24938	3.83437
C	6.18276	1.28492	2.18218
H	7.10607	1.03745	1.66685
C	4.96256	0.92231	1.61924
H	4.93631	0.40285	0.66605
C	0.57513	-4.63288	0.24303
C	1.46131	-4.93610	-0.79875
H	1.81561	-4.13475	-1.44177
C	1.87473	-6.24740	-1.01454
H	2.55623	-6.46915	-1.83049
C	1.41613	-7.27148	-0.18906
H	1.74104	-8.29399	-0.35654
C	0.54279	-6.97792	0.85583
H	0.19019	-7.76938	1.51049
C	0.12472	-5.66790	1.07141
H	-0.54358	-5.43922	1.89656

C. DMSO Solution

92
Energy: -2813770.6963413

S	-0.01222	-1.67074	2.59595
S	0.21388	0.23488	1.63045
N	-1.66415	-1.55369	2.67244
N	-1.35221	0.63031	1.85695
C	-2.12524	-0.37381	2.31447
C	-3.57727	-0.11670	2.43682
C	-4.12006	1.12339	2.09670
H	-3.48343	1.91916	1.72727
C	-5.49046	1.31336	2.23988
H	-5.93166	2.27374	1.98069
N	-6.33245	0.37574	2.68352
C	-5.80005	-0.80816	3.00521
H	-6.49294	-1.56597	3.36523
C	-4.44665	-1.10382	2.90444
H	-4.06865	-2.08108	3.18243
Co	0.64348	0.07321	-0.49792
N	1.65655	-1.59820	-0.48018
C	1.14941	-2.87008	-0.34338
N	2.31046	1.07432	-0.28282
C	2.20437	-3.82302	-0.16162
H	2.06428	-4.88152	-0.00090
N	-0.28872	1.75407	-0.81435
C	3.36971	-3.13575	-0.25598
H	4.37858	-3.51393	-0.18123
N	-0.95091	-0.92518	-0.97820
C	3.02423	-1.75576	-0.43445
C	3.96967	-0.73372	-0.44869
C	3.60247	0.60568	-0.34486
C	4.53879	1.67963	-0.17840
H	5.61254	1.57988	-0.23442
C	3.81134	2.79737	0.06858
H	4.16476	3.80261	0.24511
C	2.43156	2.41664	-0.01162
C	1.38377	3.33467	0.04858

C	0.10209	3.00330	-0.38410
C	-0.96186	3.95024	-0.54505
H	-0.91610	4.99055	-0.25937
C	-1.98719	3.28639	-1.13510
H	-2.95525	3.66906	-1.42319
C	-1.57258	1.92006	-1.27139
C	-2.43082	0.90675	-1.69454
C	-2.12296	-0.43848	-1.51171
C	-3.04030	-1.50938	-1.77698
H	-4.00961	-1.39482	-2.23861
C	-2.45319	-2.64626	-1.32940
H	-2.83680	-3.65542	-1.35828
C	-1.15191	-2.27789	-0.85110
C	-0.19547	-3.21268	-0.45842
C	5.41066	-1.09961	-0.50054
C	5.93217	-1.72381	-1.64043
H	5.27703	-1.92429	-2.48337
C	7.27708	-2.07695	-1.70204
H	7.66758	-2.55449	-2.59570
C	8.11877	-1.81661	-0.62297
H	9.16764	-2.09345	-0.67037
C	7.60846	-1.20265	0.51871
H	8.25643	-1.00478	1.36733
C	6.26433	-0.84632	0.58022
H	5.86622	-0.37852	1.47596
C	1.68320	4.72032	0.49611
C	2.10738	4.94963	1.81108
H	2.19849	4.11002	2.49421
C	2.39951	6.23875	2.24669
H	2.71994	6.40055	3.27152
C	2.27950	7.31655	1.37237
H	2.50903	8.32213	1.71166
C	1.86768	7.09829	0.05945
H	1.78194	7.93212	-0.63084
C	1.57155	5.81004	-0.37639
H	1.26490	5.64133	-1.40452
C	-3.73637	1.29155	-2.29357
C	-3.76372	1.98924	-3.50786
H	-2.82775	2.23079	-4.00344
C	-4.97457	2.36167	-4.08408
H	-4.97870	2.89548	-5.02970
C	-6.17571	2.04943	-3.45128
H	-7.12041	2.34204	-3.89955
C	-6.15931	1.36365	-2.23869
H	-7.09090	1.12578	-1.73388
C	-4.94921	0.98618	-1.66370
H	-4.93936	0.46515	-0.71098
C	-0.63140	-4.61690	-0.24153
C	-1.52291	-4.90676	0.79967
H	-1.86797	-4.10001	1.44104
C	-1.95332	-6.21230	1.01775
H	-2.63891	-6.42366	1.83302
C	-1.50656	-7.24389	0.19491
H	-1.84478	-8.26179	0.36391
C	-0.62784	-6.96358	-0.84929
H	-0.28419	-7.76076	-1.50169
C	-0.19278	-5.65937	-1.06705
H	0.47964	-5.44160	-1.89178

E. DCE Solution

92
Energy: -2813769.2263565

S	0.02579	-1.68793	-2.58573
S	-0.21425	0.22447	-1.63727
N	1.67694	-1.56432	-2.65258
N	1.34948	0.62590	-1.86105
C	2.13050	-0.37898	-2.30308
C	3.58177	-0.11543	-2.41684
C	4.11035	1.14036	-2.11432
H	3.46186	1.94293	-1.78201
C	5.48113	1.33577	-2.24560
H	5.91185	2.30833	-2.01563
N	6.33647	0.38940	-2.64216
C	5.81732	-0.80927	-2.92821
H	6.52137	-1.57405	-3.24999
C	4.46478	-1.11186	-2.83646
H	4.09718	-2.10143	-3.08308
Co	-0.64511	0.07320	0.49183
N	-1.67706	-1.58745	0.47427
C	-1.18418	-2.86524	0.34040
N	-2.30234	1.09308	0.28118
C	-2.24904	-3.80664	0.15707
H	-2.11948	-4.86656	-0.00298
N	0.30600	1.74370	0.81171
C	-3.40688	-3.10639	0.24700
H	-4.41985	-3.47278	0.16902
N	0.93939	-0.94347	0.96980
C	-3.04641	-1.73031	0.42511
C	-3.98055	-0.69829	0.43736
C	-3.59917	0.63734	0.33872
C	-4.52479	1.72119	0.17731
H	-5.59950	1.63090	0.23147
C	-3.78610	2.83339	-0.06035
H	-4.12876	3.84348	-0.23025
C	-2.41036	2.43838	0.01921
C	-1.35394	3.34634	-0.03472
C	-0.07442	2.99906	0.39050
C	0.99979	3.93470	0.54925
H	0.96165	4.97663	0.26841
C	2.02257	3.25746	1.12773
H	2.99698	3.62791	1.41032
C	1.59464	1.89486	1.26028
C	2.44456	0.87173	1.67565
C	2.11979	-0.46974	1.49642
C	3.02559	-1.55055	1.76092
H	3.99836	-1.44538	2.21741
C	2.42262	-2.68160	1.32044
H	2.79363	-3.69540	1.35054
C	1.12406	-2.29888	0.84625
C	0.15650	-3.22316	0.45699
C	-5.42567	-1.04852	0.48358
C	-5.95928	-1.66522	1.62180
H	-5.31001	-1.87131	2.46792
C	-7.30816	-2.00356	1.67771
H	-7.70799	-2.47545	2.57028
C	-8.14199	-1.73557	0.59456
H	-9.19406	-2.00085	0.63753
C	-7.61984	-1.12867	-0.54541
H	-8.26180	-0.92483	-1.39721
C	-6.27167	-0.78726	-0.60120
H	-5.86406	-0.32476	-1.49544
C	-1.64065	4.73963	-0.46694
C	-2.05728	4.98961	-1.78032
H	-2.15117	4.15972	-2.47482
C	-2.33790	6.28660	-2.19963
H	-2.65242	6.46471	-3.22362
C	-2.21365	7.35159	-1.31049
H	-2.43424	8.36333	-1.63725
C	-1.80877	7.11279	0.00089
H	-1.71947	7.93674	0.70256
C	-1.52411	5.81664	0.42040
H	-1.22235	5.63112	1.44711
C	3.75992	1.24062	2.26317
C	3.80741	1.93529	3.47841
H	2.87908	2.18605	3.98371
C	5.02812	2.29283	4.04298
H	5.04800	2.82445	4.98968
C	6.21908	1.96833	3.39746
H	7.17154	2.24938	3.83667
C	6.18272	1.28496	2.18405
H	7.10625	1.03749	1.66913
C	4.96272	0.92237	1.62063
H	4.93689	0.40290	0.66743
C	0.57546	-4.63296	0.24287
C	1.46191	-4.93617	-0.79871
H	1.81637	-4.13485	-1.44167
C	1.87542	-6.24746	-1.01446
H	2.55715	-6.46917	-1.83023
C	1.41661	-7.27157	-0.18911
H	1.74159	-8.29407	-0.35652
C	0.54298	-6.97804	0.85558
H	0.19020	-7.76952	1.51010
C	0.12483	-5.66803	1.07111
H	-0.54371	-5.43948	1.89609

5.2.2. Co(TPP)(*N*-py-DTDA), compound 3b

The structures listed here for **3b** all have C_2 symmetry.

A. Gas Phase

```
92
Energy: -2813739.8801859
Co          0.00000         0.00000         1.10369
N          -1.34372        -1.40111         1.27836
C          -2.69375        -1.26728         1.07828
N           1.41096        -1.33875         1.25620
C          -3.36971        -2.50675         1.33283
H          -4.43884        -2.64791         1.27227
N           1.34372         1.40111         1.27836
C          -2.42063        -3.39872         1.70998
H          -2.55008        -4.42666         2.01422
N          -1.41096         1.33875         1.25620
C          -1.15855        -2.72078         1.62015
C           0.07692        -3.35510         1.73514
C           1.27322        -2.68824         1.46556
C           2.52139        -3.36395         1.25295
H           2.66768        -4.43022         1.34375
C           3.41941        -2.41863         0.87995
H           4.45676        -2.54982         0.61023
C           2.73486        -1.15901         0.92774
C           3.36346         0.07641         0.79654
C           2.69375         1.26728         1.07828
C           3.36971         2.50675         1.33283
H           4.43884         2.64791         1.27227
C           2.42063         3.39872         1.70998
H           2.55008         4.42666         2.01422
C           1.15855         2.72078         1.62015
C          -0.07692         3.35510         1.73514
C          -1.27322         2.68824         1.46556
C          -2.52139         3.36395         1.25295
H          -2.66768         4.43022         1.34375
C          -3.41941         2.41863         0.87995
H          -4.45676         2.54982         0.61023
C          -2.73486         1.15901         0.92774
C          -3.36346        -0.07641         0.79654
C           0.13579        -4.80217         2.06937
C          -0.42401        -5.76915         1.22557
H          -0.90751        -5.45486         0.30521
C          -0.34893        -7.12024         1.54827
H          -0.78203        -7.85789         0.87922
C           0.28657        -7.52598         2.71873
H           0.34417        -8.58071         2.97030
C           0.85105        -6.57366         3.56300
H           1.34697        -6.88239         4.47847
C           0.77934        -5.22265         3.23958
H           1.21576        -4.47819         3.89911
C           4.80803         0.14454         0.45496
C           5.78582        -0.38551         1.30535
H           5.48160        -0.85244         2.23762
C           7.13404        -0.29947         0.97323
H           7.88126        -0.70948         1.64630
C           7.52486         0.31654        -0.21278
H           8.57728         0.38122        -0.47227
C           6.56109         0.85167        -1.06302
H           6.85793         1.33123        -1.99094
C           5.21292         0.77031        -0.73005
H           4.45944         1.18231        -1.39501
C          -0.13579         4.80217         2.06937
C           0.42401         5.76915         1.22557
H           0.90751         5.45486         0.30521
C           0.34893         7.12024         1.54827
H           0.78203         7.85789         0.87922
C          -0.28657         7.52598         2.71873
H          -0.34417         8.58071         2.97030
C          -0.85105         6.57366         3.56300
H          -1.34697         6.88239         4.47847
C          -0.77934         5.22265         3.23958
H          -1.21576         4.47819         3.89911
C          -4.80803        -0.14454         0.45496
C          -5.78582         0.38551         1.30535
H          -5.48160         0.85244         2.23762
C          -7.13404         0.29947         0.97323
H          -7.88126         0.70948         1.64630
C          -7.52486        -0.31654        -0.21278
H          -8.57728        -0.38122        -0.47227
C          -6.56109        -0.85167        -1.06302
H          -6.85793        -1.33123        -1.99094
C          -5.21292        -0.77031        -0.73005
H          -4.45944        -1.18231        -1.39501
N           0.00000         0.00000        -0.84035
S           0.18802        -1.07096        -7.36472
S          -0.18802         1.07096        -7.36472
N           0.18670        -1.17110        -5.69623
N          -0.18670         1.17110        -5.69623
C           0.00000         0.00000        -5.10188
C           0.00000         0.00000        -3.62559
C          -0.01225        -1.19578        -2.90649
H          -0.02423        -2.13957        -3.43963
C           0.00000        -1.15500        -1.52426
H           0.01289        -2.06231        -0.93129
C           0.01225         1.19578        -2.90649
H           0.02423         2.13957        -3.43963
C           0.00000         1.15500        -1.52426
H          -0.01289         2.06231        -0.93129
```

B. DCM Solution

```
92
Energy: -2813756.1138371
Co          0.00000         0.00000         1.10807
N          -1.31863        -1.41141         1.28151
C          -2.66832        -1.30482         1.05008
N           1.42906        -1.30682         1.25856
C          -3.32312        -2.55225         1.30852
H          -4.38759        -2.71639         1.22843
N           1.31863         1.41141         1.28151
C          -2.36526        -3.42138         1.71891
H          -2.48372        -4.44791         2.03192
N          -1.42906         1.30682         1.25856
C          -1.11412        -2.72636         1.64122
C           0.12909        -3.34110         1.76791
C           1.31116        -2.65898         1.47852
C           2.56232        -3.31721         1.24476
H           2.72641        -4.37996         1.34499
C           3.43939        -2.36454         0.83853
H           4.47198        -2.48800         0.54804
C           2.74453        -1.11334         0.89255
C           3.35319         0.12906         0.74407
C           2.66832         1.30482         1.05008
C           3.32312         2.55225         1.30852
H           4.38759         2.71639         1.22843
C           2.36526         3.42138         1.71891
H           2.48372         4.44791         2.03192
C           1.11412         2.72636         1.64122
C          -0.12909         3.34110         1.76791
C          -1.31116         2.65898         1.47852
C          -2.56232         3.31721         1.24476
H          -2.72641         4.37996         1.34499
C          -3.43939         2.36454         0.83853
H          -4.47198         2.48800         0.54804
C          -2.74453         1.11334         0.89255
C          -3.35319        -0.12906         0.74407
C           0.21276        -4.78142         2.12409
C          -0.32842        -5.77049         1.29362
H          -0.81470        -5.48225         0.36629
C          -0.22889        -7.11458         1.63982
H          -0.64707        -7.87106         0.98276
C           0.41061        -7.48829         2.81960
H           0.48617        -8.53730         3.08927
C           0.95642        -6.51208         3.64977
H           1.45586        -6.79634         4.57101
C           0.86271        -5.16781         3.30283
H           1.28585        -4.40635         3.95160
C           4.78528         0.22329         0.36187
C           5.79497        -0.30698         1.17447
H           5.52931        -0.79270         2.10883
C           7.13114        -0.19525         0.80225
H           7.90417        -0.60505         1.44525
C           7.47607         0.44525        -0.38579
H           8.51888         0.52936        -0.67614
C           6.47911         0.98071        -1.19779
H           6.74059         1.48041        -2.12556
C           5.14275         0.87549        -0.82473
H           4.36480         1.28909        -1.45995
C          -0.21276         4.78142         2.12409
C           0.32842         5.77049         1.29362
```

H	0.81470	5.48225	0.36629
C	0.22889	7.11458	1.63982
H	0.64707	7.87106	0.98276
C	-0.41061	7.48829	2.81960
H	-0.48617	8.53730	3.08927
C	-0.95642	6.51208	3.64977
H	-1.45586	6.79634	4.57101
C	-0.86271	5.16781	3.30283
H	-1.28585	4.40635	3.95160
C	-4.78528	-0.22329	0.36187
C	-5.79497	0.30698	1.17447
H	-5.52931	0.79270	2.10883
C	-7.13114	0.19525	0.80225
H	-7.90417	0.60505	1.44525
C	-7.47607	-0.44525	-0.38579
H	-8.51888	-0.52936	-0.67614
C	-6.47911	-0.98071	-1.19779
H	-6.74059	-1.48041	-2.12556
C	-5.14275	-0.87549	-0.82473
H	-4.36480	-1.28909	-1.45995
N	0.00000	0.00000	-0.77230
S	0.16956	-1.08693	-7.31402
S	-0.16956	1.08693	-7.31402
N	0.13204	-1.18508	-5.61743
N	-0.13204	1.18508	-5.61743
C	0.00000	0.00000	-5.03880
C	0.00000	0.00000	-3.55900
C	0.00000	-1.19431	-2.83589
H	-0.00093	-2.14240	-3.35968
C	0.00491	-1.15932	-1.45489
H	0.01417	-2.06963	-0.86952
C	0.00000	1.19431	-2.83589
H	0.00093	2.14240	-3.35968
C	-0.00491	1.15932	-1.45489
H	-0.01417	2.06963	-0.86952

C. DMSO Solution

92
Energy: -2813759.9408604

Co	0.00000	0.00000	1.10603
N	-1.23503	-1.48241	1.28032
C	-2.58790	-1.45465	1.04426
N	1.50168	-1.22120	1.25577
C	-3.17013	-2.73551	1.31095
H	-4.22316	-2.96149	1.23109
N	1.23503	1.48241	1.28032
C	-2.16499	-3.54521	1.73038
H	-2.22606	-4.57436	2.05095
N	-1.50168	1.22120	1.25577
C	-0.95535	-2.78132	1.64938
C	0.32087	-3.32364	1.77802
C	1.46102	-2.57722	1.47921
C	2.74547	-3.16391	1.23760
H	2.97052	-4.21524	1.33937
C	3.56461	-2.16444	0.82223
H	4.60044	-2.23137	0.52504
C	2.80185	-0.95394	0.87980
C	3.33782	0.32140	0.72928
C	2.58790	1.45465	1.04426
C	3.17013	2.73551	1.31095
H	4.22316	2.96149	1.23109
C	2.16499	3.54521	1.73038
H	2.22606	4.57436	2.05095
C	0.95535	2.78132	1.64938
C	-0.32087	3.32364	1.77802
C	-1.46102	2.57722	1.47921
C	-2.74547	3.16391	1.23760
H	-2.97052	4.21524	1.33937
C	-3.56461	2.16444	0.82223
H	-4.60044	2.23137	0.52504
C	-2.80185	0.95394	0.87980
C	-3.33782	-0.32140	0.72928
C	0.48910	-4.75351	2.14527
C	0.00000	-5.78003	1.32802
H	-0.50960	-5.52976	0.40222
C	0.18179	-7.11276	1.68501
H	-0.19658	-7.89845	1.03820
C	0.85233	-7.43754	2.86219
H	0.99217	-8.47778	3.13995
C	1.34655	-6.42334	3.67922
H	1.86994	-6.66907	4.59821
C	1.17079	-5.09010	3.32156
H	1.55431	-4.29951	3.96003
C	4.75843	0.50109	0.33621
C	5.80526	0.01615	1.13013
H	5.57850	-0.49881	2.05898
C	7.12897	0.21181	0.74788
H	7.93056	-0.16325	1.37687
C	7.42469	0.89234	-0.43125
H	8.45800	1.04264	-0.72874
C	6.39030	1.38353	-1.22447
H	6.61318	1.91514	-2.14456
C	5.06606	1.19408	-0.84153
H	4.25932	1.57452	-1.46144
C	-0.48910	4.75351	2.14527
C	0.00000	5.78003	1.32802
H	0.50960	5.52976	0.40222
C	-0.18179	7.11276	1.68501
H	0.19658	7.89845	1.03820
C	-0.85233	7.43754	2.86219
H	-0.99217	8.47778	3.13995
C	-1.34655	6.42334	3.67922
H	-1.86994	6.66907	4.59821
C	-1.17079	5.09010	3.32156
H	-1.55431	4.29951	3.96003
C	-4.75843	-0.50109	0.33621
C	-5.80526	-0.01615	1.13013
H	-5.57850	0.49881	2.05898
C	-7.12897	-0.21181	0.74788
H	-7.93056	0.16325	1.37687
C	-7.42469	-0.89234	-0.43125
H	-8.45800	-1.04264	-0.72874
C	-6.39030	-1.38353	-1.22447
H	-6.61318	-1.91514	-2.14456
C	-5.06606	-1.19408	-0.84153
H	-4.25932	-1.57452	-1.46144
N	0.00000	0.00000	-0.76302
S	0.12442	-1.09620	-7.31001
S	-0.12442	1.09620	-7.31001
N	0.09286	-1.18953	-5.60797
N	-0.09286	1.18953	-5.60797
C	0.00000	0.00000	-5.03133
C	0.00000	0.00000	-3.55001
C	0.06290	-1.19231	-2.82611
H	0.11385	-2.14059	-3.34665
C	0.06152	-1.15839	-1.44521
H	0.11042	-2.06785	-0.86105
C	-0.06290	1.19231	-2.82611
H	-0.11385	2.14059	-3.34665
C	-0.06152	1.15839	-1.44521
H	-0.11042	2.06785	-0.86105

E. DCE Solution

92
Energy: -2813756.6508471

Co	0.00000	0.00000	1.10824
N	-1.31623	-1.41303	1.28128
C	-2.66584	-1.30888	1.04797
N	1.43102	-1.30408	1.25866
C	-3.31862	-2.55724	1.30662
H	-4.38267	-2.72344	1.22533
N	1.31623	1.41303	1.28128
C	-2.35975	-3.42432	1.71913
H	-2.47687	-4.45078	2.03281
N	-1.43102	1.30408	1.25866
C	-1.10972	-2.72739	1.64233
C	0.13438	-3.33999	1.77022
C	1.31522	-2.65627	1.47971
C	2.56708	-3.31269	1.24508
H	2.73294	-4.37508	1.34621
C	3.44224	-2.35911	0.83676
H	4.47467	-2.48143	0.54523
C	2.74580	-1.10888	0.89062
C	3.35228	0.13438	0.74075
C	2.66584	1.30888	1.04797
C	3.31862	2.55724	1.30662
H	4.38267	2.72344	1.22533
C	2.35975	3.42432	1.71913
H	2.47687	4.45078	2.03281
C	1.10972	2.72739	1.64233
C	-0.13438	3.33999	1.77022
C	-1.31522	2.65627	1.47971

C	-2.56708	3.31269	1.24508
H	-2.73294	4.37508	1.34621
C	-3.44224	2.35911	0.83676
H	-4.47467	2.48143	0.54523
C	-2.74580	1.10888	0.89062
C	-3.35228	-0.13438	0.74075
C	0.22060	-4.77961	2.12839
C	-0.31849	-5.77095	1.29930
H	-0.80510	-5.48514	0.37139
C	-0.21631	-7.11431	1.64762
H	-0.63285	-7.87264	0.99166
C	0.42367	-7.48491	2.82814
H	0.50126	-8.53335	3.09944
C	0.96740	-6.50635	3.65694
H	1.46723	-6.78819	4.57870
C	0.87115	-5.16281	3.30788
H	1.29270	-4.39955	3.95556
C	4.78344	0.23121	0.35593
C	5.79565	-0.29815	1.16598
H	5.53285	-0.78514	2.10048
C	7.13086	-0.18373	0.79113
H	7.90588	-0.59281	1.43217
C	7.47228	0.45856	-0.39699
H	8.51437	0.54478	-0.68933
C	6.47276	0.99318	-1.20642
H	6.73151	1.49437	-2.13414
C	5.13735	0.88530	-0.83074
H	4.35743	1.29833	-1.46392
C	-0.22060	4.77961	2.12839
C	0.31849	5.77095	1.29930
H	0.80510	5.48514	0.37139
C	0.21631	7.11431	1.64762
H	0.63285	7.87264	0.99166
C	-0.42367	7.48491	2.82814
H	-0.50126	8.53335	3.09944
C	-0.96740	6.50635	3.65694
H	-1.46723	6.78819	4.57870
C	-0.87115	5.16281	3.30788
H	-1.29270	4.39955	3.95556
C	-4.78344	-0.23121	0.35593
C	-5.79565	0.29815	1.16598
H	-5.53285	0.78514	2.10048
C	-7.13086	0.18373	0.79113
H	-7.90588	0.59281	1.43217
C	-7.47228	-0.45856	-0.39699
H	-8.51437	-0.54478	-0.68933
C	-6.47276	-0.99318	-1.20642
H	-6.73151	-1.49437	-2.13414
C	-5.13735	-0.88530	-0.83074
H	-4.35743	-1.29833	-1.46392
N	0.00000	0.00000	-0.76933
S	0.14725	-1.09103	-7.31198
S	-0.14725	1.09103	-7.31198
N	0.11189	-1.18743	-5.61405
N	-0.11189	1.18743	-5.61405
C	0.00000	0.00000	-5.03613
C	0.00000	0.00000	-3.55614
C	0.00000	-1.19423	-2.83282
H	-0.00058	-2.14254	-3.35612
C	0.00443	-1.15951	-1.45187
H	0.01269	-2.06996	-0.86684
C	0.00000	1.19423	-2.83282
H	0.00058	2.14254	-3.35612
C	-0.00443	1.15951	-1.45187
H	-0.01269	2.06996	-0.86684

F. Triplet State DCE Solution

92
Energy: -2813770.2557983

Co	0.00000	0.00000	1.16192
N	-1.24386	-1.51374	1.28962
C	-2.60610	-1.47037	1.13926
N	1.51519	-1.24718	1.27346
C	-3.18675	-2.76306	1.38097
H	-4.24415	-2.98225	1.35006
N	1.24386	1.51374	1.28962
C	-2.16493	-3.59599	1.69845
H	-2.21427	-4.63994	1.97100
N	-1.51519	1.24718	1.27346
C	-0.95691	-2.82282	1.59600
C	0.32543	-3.36519	1.69115
C	1.47465	-2.60616	1.45406
C	2.77734	-3.18390	1.26450
H	3.00402	-4.23781	1.33435
C	3.61351	-2.16369	0.94936
H	4.66731	-2.21211	0.71778
C	2.83048	-0.95907	1.00025
C	3.36793	0.32449	0.89869
C	2.60610	1.47037	1.13926
C	3.18675	2.76306	1.38097
H	4.24415	2.98225	1.35006
C	2.16493	3.59599	1.69845
H	2.21427	4.63994	1.97100
C	0.95691	2.82282	1.59600
C	-0.32543	3.36519	1.69115
C	-1.47465	2.60616	1.45406
C	-2.77734	3.18390	1.26450
H	-3.00402	4.23781	1.33435
C	-3.61351	2.16369	0.94936
H	-4.66731	2.21211	0.71778
C	-2.83048	0.95907	1.00025
C	-3.36793	-0.32449	0.89869
C	0.48796	-4.81261	1.99232
C	0.00000	-5.79784	1.12434
H	-0.50470	-5.49767	0.21058
C	0.16878	-7.14842	1.41555
H	-0.21127	-7.89848	0.72814
C	0.82877	-7.53701	2.57923
H	0.95971	-8.59082	2.80632
C	1.32214	-6.56673	3.44845
H	1.83625	-6.86084	4.35877
C	1.15526	-5.21628	3.15608
H	1.53670	-4.46050	3.83669
C	4.81839	0.49480	0.61628
C	5.79732	0.02592	1.50165
H	5.49087	-0.47061	2.41775
C	7.14966	0.20525	1.22499
H	7.89490	-0.15982	1.92563
C	7.54611	0.85732	0.05946
H	8.60133	0.99645	-0.15596
C	6.58188	1.33332	-0.82600
H	6.88219	1.84237	-1.73717
C	5.22966	1.15600	-0.54818
H	4.47821	1.52442	-1.24076
C	-0.48796	4.81261	1.99232
C	0.00000	5.79784	1.12434
H	0.50470	5.49767	0.21058
C	-0.16878	7.14842	1.41555
H	0.21127	7.89848	0.72814
C	-0.82877	7.53701	2.57923
H	-0.95971	8.59082	2.80632
C	-1.32214	6.56673	3.44845
H	-1.83625	6.86084	4.35877
C	-1.15526	5.21628	3.15608
H	-1.53670	4.46050	3.83669
C	-4.81839	-0.49480	0.61628
C	-5.79732	-0.02592	1.50165
H	-5.49087	0.47061	2.41775
C	-7.14966	-0.20525	1.22499
H	-7.89490	0.15982	1.92563
C	-7.54611	-0.85732	0.05946
H	-8.60133	-0.99645	-0.15596
C	-6.58188	-1.33332	-0.82600
H	-6.88219	-1.84237	-1.73717
C	-5.22966	-1.15600	-0.54818
H	-4.47821	-1.52442	-1.24076
N	0.00000	0.00000	-0.98195
S	0.07083	-1.06368	-7.52084
S	-0.07083	1.06368	-7.52084
N	0.07665	-1.16905	-5.88666
N	-0.07665	1.16905	-5.88666
C	0.00000	0.00000	-5.24921
C	0.00000	0.00000	-3.77195
C	0.06222	-1.19610	-3.05621
H	0.11218	-2.14666	-3.57420
C	0.05936	-1.14489	-1.67045
H	0.10583	-2.05332	-1.07731
C	-0.06222	1.19610	-3.05621
H	-0.11218	2.14666	-3.57420
C	-0.05936	1.14489	-1.67045
H	-0.10583	2.05332	-1.07731

5.3. Six-Coordinate Co(TPP)(L) Complexes

5.3.1. Co(TPP)(*S*-py-DTDA)(DMSO)

A. Co(TPP)(S-py-DTDA)(O-DMSO)

102
Energy: -3160726.0457902

S	0.01576	-1.74483	-2.79872
S	-0.14941	0.18848	-1.86433
N	1.68100	-1.66223	-2.90010
N	1.41988	0.56556	-2.16619
C	2.16070	-0.47680	-2.59026
C	3.61685	-0.25251	-2.74232
C	4.16580	1.02381	-2.60664
H	3.52701	1.87218	-2.38901
C	5.53829	1.18246	-2.76202
H	5.98169	2.17171	-2.66426
N	6.38051	0.18028	-3.03069
C	5.84316	-1.03761	-3.15763
H	6.53550	-1.84866	-3.37490
C	4.48607	-1.30644	-3.02857
H	4.10569	-2.31549	-3.13912
N	-2.44465	0.35440	-0.10426
C	-3.03648	1.53224	-0.49900
N	-0.84417	-1.86854	0.37495
C	-4.42989	1.32742	-0.76789
H	-5.11406	2.09296	-1.10242
N	1.34059	-0.21452	0.83947
C	-4.69477	0.02561	-0.49389
H	-5.64048	-0.49133	-0.56008
N	-0.24880	2.01294	0.34112
C	-3.45101	-0.58132	-0.11892
C	-3.29569	-1.94709	0.10535
C	-2.04341	-2.52880	0.28879
C	-1.83987	-3.94975	0.30906
H	-2.62834	-4.68561	0.25263
C	-0.50209	-4.15180	0.38632
H	0.03639	-5.08745	0.42172
C	0.10745	-2.85402	0.44009
C	1.47295	-2.66447	0.62963
C	2.01975	-1.40712	0.86879
C	3.38648	-1.20246	1.25247
H	4.12622	-1.98402	1.34362
C	3.52798	0.12325	1.49648
H	4.40908	0.65006	1.83077
C	2.26517	0.73660	1.19599
C	2.05424	2.11470	1.22364
C	0.87014	2.69004	0.76189
C	0.70470	4.10116	0.56449
H	1.44175	4.84975	0.81451
C	-0.51299	4.27842	-0.00696
H	-0.98567	5.20275	-0.30434
C	-1.10461	2.97944	-0.13362
C	-2.41123	2.77561	-0.57366
C	-4.49498	-2.82846	0.09726
C	-5.22114	-3.05594	-1.07773
H	-4.90008	-2.58493	-2.00243
C	-6.33748	-3.88768	-1.06979
H	-6.88788	-4.05787	-1.99029
C	-6.74273	-4.50421	0.11193
H	-7.61350	-5.15292	0.11755
C	-6.02481	-4.28676	1.28582
H	-6.33566	-4.76252	2.21122
C	-4.90783	-3.45596	1.27884
H	-4.35041	-3.28109	2.19444
C	2.36700	-3.85561	0.60648
C	2.66543	-4.47070	-0.61502
H	2.25467	-4.05246	-1.53020
C	3.49392	-5.58905	-0.65623
H	3.72152	-6.05576	-1.61014
C	4.03238	-6.10563	0.52045
H	4.67784	-6.97828	0.48749
C	3.74037	-5.49848	1.73982
H	4.15432	-5.89799	2.66091
C	2.91173	-4.38014	1.78347
H	2.67785	-3.91144	2.73526
C	3.14451	3.01618	1.68672
C	4.35107	3.11718	0.98268
H	4.49329	2.52780	0.08143
C	5.35890	3.97027	1.42297
H	6.28683	4.03937	0.86308
C	5.17600	4.73745	2.57132
H	5.96283	5.40272	2.91379
C	3.97786	4.64916	3.27625
H	3.82729	5.24292	4.17288
C	2.96945	3.79632	2.83665
H	2.03691	3.72736	3.38986
C	-3.17870	3.94730	-1.07965
C	-2.83588	4.53489	-2.30297
H	-2.01375	4.12080	-2.87981
C	-3.54303	5.63389	-2.78285
H	-3.26838	6.07593	-3.73595
C	-4.60015	6.16229	-2.04535
H	-5.15122	7.01968	-2.41975
C	-4.94584	5.58751	-0.82430
H	-5.76423	5.99806	-0.24046
C	-4.23976	4.48807	-0.34398
H	-4.50428	4.04630	0.61256
Co	-0.54377	0.06666	0.35388
O	-2.17577	-0.91796	3.10095
S	-1.19687	0.12860	2.65284
C	-1.88011	1.73857	3.05817
H	-1.12954	2.51037	2.88103
H	-2.74137	1.89945	2.40824
H	-2.18886	1.72166	4.10528
C	0.19385	0.09870	3.78872
H	0.72671	-0.84006	3.63179
H	0.85563	0.94098	3.58080
H	-0.20163	0.14938	4.80546

B. Co(TPP)(S-py-DTDA)(S-DMSO)

102
Energy: -3160726.0457902

S	0.01576	-1.74483	-2.79872
S	-0.14941	0.18848	-1.86433
N	1.68100	-1.66223	-2.90010
N	1.41988	0.56556	-2.16619
C	2.16070	-0.47680	-2.59026
C	3.61685	-0.25251	-2.74232
C	4.16580	1.02381	-2.60664
H	3.52701	1.87218	-2.38901
C	5.53829	1.18246	-2.76202
H	5.98169	2.17171	-2.66426
N	6.38051	0.18028	-3.03069
C	5.84316	-1.03761	-3.15763
H	6.53550	-1.84866	-3.37490
C	4.48607	-1.30644	-3.02857
H	4.10569	-2.31549	-3.13912
N	-2.44465	0.35440	-0.10426
C	-3.03648	1.53224	-0.49900
N	-0.84417	-1.86854	0.37495
C	-4.42989	1.32742	-0.76789
H	-5.11406	2.09296	-1.10242
N	1.34059	-0.21452	0.83947
C	-4.69477	0.02561	-0.49389
H	-5.64048	-0.49133	-0.56008
N	-0.24880	2.01294	0.34112
C	-3.45101	-0.58132	-0.11892
C	-3.29569	-1.94709	0.10535
C	-2.04341	-2.52880	0.28879
C	-1.83987	-3.94975	0.30906
H	-2.62834	-4.68561	0.25263
C	-0.50209	-4.15180	0.38632
H	0.03639	-5.08745	0.42172
C	0.10745	-2.85402	0.44009
C	1.47295	-2.66447	0.62963
C	2.01975	-1.40712	0.86879
C	3.38648	-1.20246	1.25247
H	4.12622	-1.98402	1.34362
C	3.52798	0.12325	1.49648
H	4.40908	0.65006	1.83077
C	2.26517	0.73660	1.19599
C	2.05424	2.11470	1.22364
C	0.87014	2.69004	0.76189
C	0.70470	4.10116	0.56449
H	1.44175	4.84975	0.81451
C	-0.51299	4.27842	-0.00696
H	-0.98567	5.20275	-0.30434
C	-1.10461	2.97944	-0.13362
C	-2.41123	2.77561	-0.57366

C	-4.49498	-2.82846	0.09726
C	-5.22114	-3.05594	-1.07773
H	-4.90008	-2.58493	-2.00243
C	-6.33748	-3.88768	-1.06979
H	-6.88788	-4.05787	-1.99029
C	-6.74273	-4.50421	0.11193
H	-7.61350	-5.15292	0.11755
C	-6.02481	-4.28676	1.28582
H	-6.33566	-4.76252	2.21122
C	-4.90783	-3.45596	1.27884
H	-4.35041	-3.28109	2.19444
C	2.36700	-3.85561	0.60648
C	2.66543	-4.47070	-0.61502
H	2.25467	-4.05246	-1.53020
C	3.49392	-5.58905	-0.65623
H	3.72152	-6.05576	-1.61014
C	4.03238	-6.10563	0.52045
H	4.67784	-6.97828	0.48749
C	3.74037	-5.49848	1.73982
H	4.15432	-5.89799	2.66091
C	2.91173	-4.38014	1.78347
H	2.67785	-3.91144	2.73526
C	3.14451	3.01618	1.68672
C	4.35107	3.11718	0.98268
H	4.49329	2.52780	0.08143
C	5.35890	3.97027	1.42297
H	6.28683	4.03937	0.86308
C	5.17600	4.73745	2.57132
H	5.96283	5.40272	2.91379
C	3.97786	4.64916	3.27625
H	3.82729	5.24292	4.17288
C	2.96945	3.79632	2.83665
H	2.03691	3.72736	3.38986
C	-3.17870	3.94730	-1.07965
C	-2.83588	4.53489	-2.30297
H	-2.01375	4.12080	-2.87981
C	-3.54303	5.63389	-2.78285
H	-3.26838	6.07593	-3.73595
C	-4.60015	6.16229	-2.04535
H	-5.15122	7.01968	-2.41975
C	-4.94584	5.58751	-0.82430
H	-5.76423	5.99806	-0.24046
C	-4.23976	4.48807	-0.34398
H	-4.50428	4.04630	0.61256
Co	-0.54377	0.06666	0.35388
O	-2.17577	-0.91796	3.10095
S	-1.19687	0.12860	2.65284
C	-1.88011	1.73857	3.05817
H	-1.12954	2.51037	2.88103
H	-2.74137	1.89945	2.40824
H	-2.18886	1.72166	4.10528
C	0.19385	0.09870	3.78872
H	0.72671	-0.84006	3.63179
H	0.85563	0.94098	3.58080
H	-0.20163	0.14938	4.80546

5.3.2. Co(TPP)(*N*-py-DTDA)(DMSO)

A. Co(TPP)(N-py-DTDA)(O-DMSO)

102
Energy: -3162792.1910105

N	-1.46191	-0.13307	-1.64567
C	-1.78557	-1.34278	-2.21476
N	-0.56361	2.02950	-0.11590
C	-3.04887	-1.24125	-2.90108
H	-3.51978	-2.04372	-3.44807
N	1.94079	0.83020	0.10744
C	-3.47358	0.04234	-2.76467
H	-4.36806	0.49118	-3.16785
N	1.04079	-1.33979	-1.40994
C	-2.50372	0.72138	-1.94154
C	-2.67572	2.00834	-1.41624
C	-1.78416	2.55669	-0.48294
C	-2.08606	3.70493	0.33224
H	-2.98686	4.29453	0.25755
C	-1.06003	3.85174	1.21242
H	-0.95517	4.59319	1.98929
C	-0.09197	2.83108	0.90601
C	1.18155	2.74857	1.47915
C	2.15035	1.85326	1.00664
C	3.55408	1.96149	1.30658
H	3.98839	2.69504	1.96858
C	4.19512	1.01601	0.56806
H	5.25471	0.81802	0.52026
C	3.18289	0.27952	-0.14473
C	3.41870	-0.89309	-0.87269
C	2.37440	-1.67880	-1.37913
C	2.54607	-3.03735	-1.83007
H	3.49211	-3.55375	-1.88643
C	1.30806	-3.52390	-2.10831
H	1.04573	-4.51278	-2.45120
C	0.37487	-2.44685	-1.89027
C	-0.97755	-2.48691	-2.24618
C	-3.90026	2.79188	-1.76969
C	-5.18137	2.33745	-1.41468
H	-5.28460	1.40319	-0.87167
C	-6.31661	3.08107	-1.73887
H	-7.29784	2.71554	-1.45126
C	-6.19187	4.29259	-2.42230
H	-7.07573	4.87038	-2.67502
C	-4.92378	4.75850	-2.77521
H	-4.81615	5.69920	-3.30680
C	-3.78820	4.01621	-2.44852
H	-2.80593	4.38625	-2.72614
C	1.56662	3.69425	2.57125
C	1.64987	5.07840	2.34829
H	1.43493	5.47437	1.36055
C	2.02070	5.94365	3.37847
H	2.08492	7.01059	3.18683
C	2.31469	5.43995	4.64749
H	2.60223	6.11401	5.44871
C	2.24004	4.06496	4.87979
H	2.46603	3.66475	5.86363
C	1.87227	3.19878	3.84946
H	1.81171	2.13050	4.03431
C	4.82193	-1.38144	-1.04830
C	5.59589	-1.79453	0.04837
H	5.16747	-1.76590	1.04545
C	6.90108	-2.25338	-0.13474
H	7.48329	-2.57330	0.72423
C	7.45339	-2.30756	-1.41632
H	8.46922	-2.66394	-1.55795
C	6.69125	-1.90513	-2.51504
H	7.11261	-1.94444	-3.51509
C	5.38500	-1.44887	-2.33311
H	4.79601	-1.13550	-3.18980
C	-1.56938	-3.75658	-2.76944
C	-1.13654	-4.32303	-3.97954
H	-0.35857	-3.82860	-4.55298
C	-1.70765	-5.50363	-4.45648
H	-1.36426	-5.92498	-5.39657
C	-2.72050	-6.13658	-3.73261
H	-3.16371	-7.05563	-4.10401
C	-3.16287	-5.57979	-2.53081
H	-3.94967	-6.06544	-1.96137
C	-2.59450	-4.39745	-2.05470
H	-2.93848	-3.96862	-1.11825
S	-3.34988	-3.14509	6.30865
S	-1.31467	-4.07293	6.52996
N	-2.90415	-2.33323	4.86094
N	-0.73197	-3.31488	5.10165
C	-1.64419	-2.55869	4.49491
C	-1.19886	-1.87641	3.24791
C	-2.06538	-1.05580	2.51570
H	-3.08370	-0.90627	2.85061
C	-1.61717	-0.43376	1.36127
H	-2.27535	0.20094	0.78597
N	-0.35871	-0.58138	0.89592
C	0.10369	-2.02596	2.75642
H	0.81424	-2.65052	3.28239
C	0.48292	-1.37242	1.59450
H	1.48503	-1.47699	1.20456
Co	0.22974	0.33149	-0.73994
O	0.78953	1.15301	-2.43147
S	1.43945	2.58739	-2.45640
C	3.00807	2.33460	-3.33147
H	3.45299	3.31342	-3.52243
H	3.65132	1.75333	-2.67060
H	2.82264	1.79715	-4.26301
C	0.50980	3.43281	-3.76269
H	0.51237	2.81872	-4.66479
H	-0.50627	3.56496	-3.39148
H	0.97438	4.40427	-3.94290

B. Co(TPP)(N-py-DTDA)(S-DMSO)

```
102
Energy: -3162699.1126753
N          1.05342        1.58690       -1.05736
C          0.54729        2.86975       -0.96950
N          1.73393       -1.11021       -0.73676
C          1.61576        3.82734       -1.07550
H          1.49238        4.89816       -1.02779
N         -0.97612       -1.80337       -0.76856
C          2.76241        3.12528       -1.27455
H          3.76107        3.50942       -1.41372
N         -1.65419        0.89182       -1.07548
C          2.41764        1.72983       -1.22445
C          3.35629        0.69468       -1.23425
C          3.00926       -0.62880       -0.95277
C          3.97420       -1.67191       -0.72507
H          5.04221       -1.55499       -0.82685
C          3.28308       -2.77760       -0.34354
H          3.67087       -3.75157       -0.08749
C          1.88638       -2.42942       -0.36494
C          0.85641       -3.34837       -0.14400
C         -0.48382       -3.03794       -0.38852
C         -1.54887       -4.00475       -0.36080
H         -1.43387       -5.04196       -0.08690
C         -2.67774       -3.36805       -0.76864
H         -3.66703       -3.78102       -0.88993
C         -2.32944       -1.98899       -0.98458
C         -3.25653       -0.98789       -1.29383
C         -2.91794        0.36965       -1.27798
C         -3.88534        1.43281       -1.34121
H         -4.94389        1.29302       -1.49758
C         -3.21269        2.59586       -1.13545
H         -3.60962        3.59896       -1.10786
C         -1.82264        2.25978       -0.98209
C         -0.80491        3.21218       -0.87701
C          4.79432        1.01245       -1.50393
C          5.58702        1.67876       -0.55706
H          5.15273        1.97042        0.39446
C          6.92777        1.95851       -0.82669
H          7.52982        2.47155       -0.08274
C          7.49379        1.57550       -2.04459
H          8.53692        1.79325       -2.25311
C          6.71310        0.91014       -2.99230
H          7.14571        0.61068       -3.94225
C          5.37260        0.62891       -2.72390
H          4.76350        0.11581       -3.46171
C          1.21847       -4.73047        0.30441
C          1.67977       -4.94728        1.61215
H          1.76113       -4.10739        2.29563
C          2.02613       -6.23013        2.03931
H          2.37687       -6.38171        3.05573
C          1.92010       -7.31348        1.16462
H          2.19042       -8.31123        1.49686
C          1.46687       -7.10760       -0.14023
H          1.38765       -7.94373       -0.82852
C          1.11880       -5.82550       -0.56801
H          0.77537       -5.66827       -1.58603
C         -4.68151       -1.36397       -1.56318
C         -5.51436       -1.83339       -0.53533
H         -5.12112       -1.92295        0.47277
C         -6.84174       -2.17528       -0.79800
H         -7.47355       -2.53419        0.00888
C         -7.35667       -2.05109       -2.09022
H         -8.38936       -2.31772       -2.29363
C         -6.53829       -1.57928       -3.11850
H         -6.93064       -1.47900       -4.12600
C         -5.21089       -1.23627       -2.85672
H         -4.57813       -0.87026       -3.65976
C         -1.18894        4.65224       -0.73187
C         -1.74091        5.11305        0.47353
H         -1.87580        4.41928        1.29796
C         -2.10851        6.45148        0.62027
H         -2.52974        6.79320        1.56096
C         -1.93314        7.34718       -0.43661
H         -2.21988        8.38819       -0.32260
C         -1.38945        6.89757       -1.64186
H         -1.25596        7.58627       -2.47070
C         -1.02035        5.55967       -1.78938
H         -0.60643        5.21259       -2.73128
S          0.80594        1.16041        7.63382
S         -1.36994        0.59470        7.61871
N          0.94336        0.97187        5.93119
N         -1.37526        0.36746        5.91525
C         -0.19401        0.60029        5.34754
C         -0.13801        0.42445        3.86987
C          1.04603        0.63637        3.15339
H          1.94896        0.93225        3.67145
C          1.06195        0.46851        1.77807
H          1.96925        0.63021        1.21518
N         -0.03306        0.10215        1.07835
C         -1.26699        0.04246        3.13502
H         -2.20860       -0.13529        3.63822
C         -1.17920       -0.10697        1.76015
H         -2.04387       -0.40049        1.18336
Co         0.03989       -0.10582       -0.87264
O          1.63261       -0.28435       -3.77318
S          0.22713       -0.30510       -3.23977
C         -0.70566        1.00105       -4.08442
H         -1.76533        0.92126       -3.84405
H         -0.30776        1.95579       -3.74129
H         -0.53130        0.87611       -5.15443
C         -0.58947       -1.78145       -3.90604
H         -0.10705       -2.64907       -3.45637
H         -1.65122       -1.76804       -3.66159
H         -0.43132       -1.77156       -4.98583
```

5.4. Dimeric {Co(TPP)(L)}$_2$ Complexes

5.4.1. CP Dimer, {Co(TPP)(*S*-py-DTDA)}$_2$

This structure was fully optimized at the B3LYP/SDD level of theory as an aid to assigning the experimental FTIR spectrum of CP **3** given in the paper, especially vibrational modes due to the bridging py-DTDA ligand.

```
184
Energy: -4078441.1965341 (B3LYP/SDD)
S         -3.88333       -1.59676       -2.94507
S         -4.48162        0.35696       -1.38861
N         -2.35624       -1.60510       -2.17975
N         -2.88131        0.26622       -0.78221
C         -1.99925       -0.63244       -1.33126
C         -0.58511       -0.57016       -0.87494
C         -0.16514        0.37467        0.08329
H         -0.88483        1.04663        0.53673
C          1.19206        0.44653        0.42245
H          1.54834        1.16962        1.14306
N          2.12929       -0.36314       -0.13775
C          1.72240       -1.29371       -1.04319
H          2.49110       -1.92644       -1.46398
C          0.38592       -1.42781       -1.43200
H          0.09656       -2.17031       -2.16669
Co        -5.92433       -0.01514        0.31661
N         -7.13798       -1.12758       -0.80500
C         -6.99353       -2.48938       -1.11021
N         -6.98753        1.60111       -0.16456
C         -7.94633       -2.88473       -2.12656
H         -8.01630       -3.87345       -2.55275
N         -4.91474        1.06796        1.63144
C         -8.70494       -1.78198       -2.41895
H         -9.51098       -1.69741       -3.13143
N         -5.08578       -1.66515        1.01355
C         -8.20653       -0.69214       -1.60493
C         -8.72189        0.60815       -1.66367
C         -8.13065        1.67360       -0.97391
C         -8.61059        3.03880       -1.04916
H         -9.50197        3.34955       -1.57187
C         -7.73284        3.81411       -0.33833
H         -7.77132        4.87895       -0.16680
C         -6.72462        2.92716        0.20483
C         -5.68003        3.36566        1.02865
C         -4.84501        2.46743        1.70211
C         -3.81660        2.87573        2.63767
H         -3.54890        3.89934        2.84968
C         -3.28414        1.73272        3.17273
```

H	-2.49845	1.64117	3.90703
C	-3.95686	0.61382	2.54390
C	-3.63336	-0.72155	2.81155
C	-4.17427	-1.77878	2.07203
C	-3.82552	-3.16852	2.29142
H	-3.17419	-3.52187	3.07567
C	-4.47724	-3.90231	1.33680
H	-4.46329	-4.97146	1.19140
C	-5.25655	-2.97339	0.54316
C	-6.10089	-3.37718	-0.49852
C	-9.92619	0.86953	-2.52126
C	-11.18848	0.34740	-2.15852
H	-11.28224	-0.23638	-1.24595
C	-12.32141	0.58835	-2.95780
H	-13.28668	0.18610	-2.65990
C	-12.20655	1.34726	-4.13897
H	-13.08071	1.53032	-4.75909
C	-10.95120	1.86628	-4.51194
H	-10.85108	2.44849	-5.42477
C	-9.82120	1.63206	-3.70658
H	-8.85294	2.02879	-4.00218
C	-5.49366	4.84121	1.23070
C	-5.03062	5.65126	0.16922
H	-4.79784	5.19287	-0.78887
C	-4.85675	7.03648	0.34668
H	-4.49123	7.64396	-0.47769
C	-5.15369	7.63410	1.58715
H	-5.02288	8.70477	1.72415
C	-5.62223	6.83548	2.64886
H	-5.86039	7.28887	3.60807
C	-5.78703	5.44913	2.47242
H	-6.15763	4.83829	3.29211
C	-2.66185	-1.02171	3.91488
C	-3.03294	-0.80967	5.26212
H	-4.02732	-0.43240	5.48909
C	-2.13501	-1.09848	6.30658
H	-2.43911	-0.93982	7.33847
C	-0.84831	-1.59266	6.01642
H	-0.15227	-1.81410	6.82174
C	-0.46668	-1.79757	4.67635
H	0.52671	-2.17004	4.44350
C	-1.36914	-1.51774	3.63391
H	-1.06852	-1.67131	2.60025
C	-6.08328	-4.81668	-0.92229
C	-4.95183	-5.35062	-1.58004
H	-4.10588	-4.70273	-1.79386
C	-4.92508	-6.70146	-1.97361
H	-4.05095	-7.09490	-2.48680
C	-6.02486	-7.54042	-1.70687
H	-6.00251	-8.58490	-2.00849
C	-7.15367	-7.01756	-1.04591
H	-8.00491	-7.65871	-0.82967
C	-7.18310	-5.66469	-0.65979
H	-8.05251	-5.26782	-0.14095
Co	4.12808	-0.10901	0.26822
S	8.27965	-1.48904	0.30722
S	6.38884	0.24147	0.82225
N	8.65790	-0.50185	-1.04632
N	7.04894	1.18187	-0.47346
C	8.16165	0.75066	-1.13300
C	8.74010	1.67052	-2.15289
C	8.24587	2.98361	-2.30728
H	7.42757	3.32726	-1.68390
C	8.83751	3.82421	-3.26598
H	8.48437	4.84343	-3.40411
N	9.86802	3.44096	-4.06603
C	10.33830	2.17468	-3.90721
H	11.16446	1.89145	-4.55474
C	9.81469	1.26475	-2.97264
H	10.22163	0.26438	-2.87308
N	4.39633	-2.08039	0.33020
C	4.96799	-2.88470	-0.65913
N	3.77508	-0.09399	2.23402
C	5.07112	-4.25195	-0.18666
H	5.51286	-5.06338	-0.74421
N	3.89720	1.85902	0.21919
C	4.52303	-4.28723	1.06984
H	4.43595	-5.13410	1.73343
N	4.52355	-0.12093	-1.67055
C	4.12433	-2.93017	1.40200
C	3.66840	-2.54803	2.67491
C	3.56638	-1.20029	3.05900
C	3.33329	-0.75926	4.42265
H	3.13255	-1.41144	5.25870
C	3.46134	0.60646	4.43514
H	3.38454	1.27235	5.28083
C	3.71172	1.02508	3.06919
C	3.81036	2.36551	2.66163
C	3.85425	2.73234	1.30620
C	3.72678	4.09931	0.83554
H	3.67288	4.96751	1.47480
C	3.66416	4.04934	-0.53385
H	3.57031	4.87215	-1.22618
C	3.79170	2.65478	-0.91858
C	3.90207	2.22217	-2.25111
C	4.30508	0.91751	-2.57460
C	4.65165	0.48264	-3.91715
H	4.54118	1.08046	-4.80835
C	5.14661	-0.79096	-3.81325
H	5.51570	-1.43062	-4.60041
C	5.05042	-1.17298	-2.41579
C	5.33535	-2.46605	-1.94689
C	3.39578	-3.62507	3.68500
C	2.28775	-4.48869	3.52666
H	1.62690	-4.35513	2.67317
C	2.03171	-5.51169	4.45920
H	1.17113	-6.16233	4.32299
C	2.88672	-5.69266	5.56370
H	2.69255	-6.48481	6.28289
C	3.99892	-4.84304	5.72645
H	4.67172	-4.98119	6.56953
C	4.24967	-3.81833	4.79552
H	5.11907	-3.17695	4.91686
C	3.82168	3.45253	3.69687
C	5.00526	4.19071	3.92679
H	5.89959	3.95236	3.35620
C	5.03692	5.21562	4.89063
H	5.95799	5.76865	5.05847
C	3.88190	5.52334	5.63608
H	3.90508	6.31664	6.37949
C	2.69606	4.79732	5.41006
H	1.79720	5.03149	5.97581
C	2.66816	3.76927	4.44916
H	1.74721	3.21867	4.27177
C	3.68710	3.22467	-3.34665
C	2.39961	3.76286	-3.57387
H	1.56694	3.43001	-2.95850
C	2.18428	4.70853	-4.59368
H	1.18506	5.10447	-4.75967
C	3.25766	5.13876	-5.39801
H	3.09337	5.87033	-6.18568
C	4.54608	4.61514	-5.17366
H	5.38373	4.94446	-5.78385
C	4.75842	3.66528	-4.15778
H	5.75739	3.27445	-3.98376
C	6.02632	-3.42452	-2.87078
C	7.38408	-3.20760	-3.20303
H	7.91182	-2.36149	-2.76845
C	8.05223	-4.09273	-4.06950
H	9.09852	-3.91932	-4.30972
C	7.37524	-5.19869	-4.62052
H	7.89383	-5.87944	-5.29175
C	6.02165	-5.41695	-4.29704
H	5.48823	-6.26426	-4.72185
C	5.35407	-4.53629	-3.42537
H	4.30602	-4.70281	-3.18596

6. References and Notes

(1) (a) Adler, A. D.; Longo, F. R., Kampas, F.; Kim, J. *J. Inorg. Nucl. Chem.* **1970**, *32*, 2443–2445.

(2) OriginPro 9.1.0, **2013**. OriginLab Corporation, One Roundhouse Plaza, Suite 303, Northampton, MA 01060, USA.

(3) Wojdyr, M. *J. Appl. Crystallogr.* **2010**, *43*, 1126–1128.

(4) (a) Rawson, J. M.; Banister, A. J.; Lavender, I. *Adv. Heterocycl. Chem.* **1995**, *62*, 140–248. (b) Wong, W. K.; Sun, C.; Wong, W. Y.; Kwong, D. W.; Wong, W. T. *Eur. J. Inorg. Chem.* **2000**, 1045–1054. (c) Robinson, S. W.; Haynes, D. A.; Rawson, J. M. *CrystEngComm*, **2013**, *15*, 10205–10211.

(5) Note: coordination polymer **3** dissociates into the monomer repeat unit in the LC-MS solvent (acetonitrile), accounting for the molecular ion peak corresponding to the formula $C_{50}H_{32}N_7S_2Co$.

(6) Bruker, *APEX II*, *SAINT* and *SADABS.* **2009**, Bruker AXS Inc., Madison, Wisconsin, USA.

(7) Sheldrick, G. M. *Acta Crystallogr., Sect. A.* **2008**, *64*, 112–122.

(8) Barbour, L. J. *J. Supramol. Chem.* **2001**, *1*, 189–191.

(9) Macrae, C. F.; Bruno, I. J.; Chisholm, J. A.; Edgington, P. R.; McCabe, P.; Pidcock, E.; Rodriguez-Monge, L.; Taylor, R.; van de Streek, J.; Wood, P. A. *J. Appl. Crystallogr.* **2008**, *41*, 466–470.

(10) Frisch, M. J. T.; Trucks, G. W.; Schlegel, H. B.; Scuseria, G. E.; Robb, M. A.; Cheeseman, J. R.; Scalmani, G.; Barone, V.; Mennucci, B.; Petersson, G. A.; Nakatsuji, H.; Caricato, M.; Li, X.; Hratchian, H. P.; Izmaylov, A. F.; Bloino, J.; Zheng, G.; Sonnenberg, J. L.; Hada, M.; Ehara, M.; Toyota, K.; Fukuda, R.; Hasegawa, J.; Ishida, M.; Nakajima, T.; Honda, Y.; Kitao, O.; Nakai, H.; Vreven, T.; Montgomery, J. A., Jr.; Peralta, J. E.; Ogliaro, F.; Bearpark, M.; Heyd, J. J.; Brothers, E.; Kudin, K. N.; Staroverov, V. N.; Kobayashi, R.; Normand, J.; Raghavachari, K.; Rendell, A.; Burant, J. C.; Iyengar, S. S.; Tomasi, J.; Cossi, M.; Rega, N.; Millam, J. M.; Klene, M.; Knox, J. E.; Cross, J. B.; Bakken, V.; Adamo, C.; Jaramillo, J.; Gomperts, R.; Stratmann, R. E.; Yazyev, O.; Austin, A. J.; Cammi, R.; Pomelli, C.; Ochterski, J. W.; Martin, R. L.; Morokuma, K.; Zakrzewski, V. G.; Voth, G. A.; Salvador, P.; Dannenberg, J. J.; Dapprich, S.; Daniels, A. D.; Farkas, Ö.; Foresman, J. B.; Ortiz, J. V.; Cioslowski, J.; Fox, D. J. Gaussian 09W; Gaussian Inc.: Wallingford, CT, **2009**.

(11) Heyd, J.; Scuseria, G. *J. Chem. Phys.* **2004**, *121*, 1187–1192.

(12) Ditchfield, R.; Hehre, W. J.; Pople, J. A. *J. Chem. Phys.* **1971**, *54*, 724–728.

(13) O'Boyle, N. M.; Tenderholt, A. L.; Langner, K. M. *J. Comput. Chem.* **2008**, *29*, 839–845.

(14) Tomasi, J.; Mennucci, B.; Cammi, R. *Chem. Rev.* **2005**, *105*, 2999–3093.

(15) Cheeseman, J. R.; Trucks, G. W.; Keith, T. A.; Frisch, M. J. *J. Chem. Phys.* **1996**, *104*, 5497–5509.

(16) Becke, A. D. *J. Chem. Phys.* **1993**, *98*, 5648–5652.

(17) Fuentealba, P.; Preuss, H.; Stoll, H.; Von Szentpály, L. *Chem. Phys. Lett.* **1982**, *89*, 418–422.

(18) Allen, F. H. *Acta Cryst.* **2002**, *B58*, 380–388.

(19) There are 117 structures containing neutral DTDAs when searching the CSD version 5.38 + 3 updates, with filters '3D coordinates determined' and 'only organics'. On analyzing the intramolecular S–S bond distances in these structures, two outliers were identified, both in one structure (refcode DIXMOO). These outliers were excluded from the analysis.

(20) Domagała, S.; Haynes, D. A. *CrystEngComm*, **2016**, *18*, 7116–7125.

(21) Kojima, T.; Sakamoto, T.; Matsuda, Y. *Inorg. Chem.* **2004**, *43*, 2243–2245.

(22) Boeré, R. T.; Moock, K. H.; Parvez, M. *Z. Anorg. Allg. Chem.* **1994**, *620*, 1589–1598.

(23) Walker, F. A.; Beroiz, D.; Kadish, K. M. *J. Am. Chem. Soc.* **1976**, *98*, 3484–3489.

(24) The reduction potential of 4-(2′-pyridyl)-1,2,3,5-dithiadiazolyl has been reported as –0.81 V in acetonitrile at 298 K (Hearns, N. G.; Preuss, K. E.; Richardson, J. F.; Bin-Salamon, S. *J. Am. Chem. Soc.* **2004**, *126*, 9942–9943). The

reduction potential of **2** is likely to be very similar as substituent effects are small due to the nodal plane of the SOMO on the C atom of the CNSSN ring.

(25) Shirazi, A.; Goff, H. M. *Inorg. Chem.* **1982**, *21*, 3420–3425.

(26) La Mar, G. N.; Walker, F. A. *J. Am. Chem. Soc.* **1973**, *95*, 1790–1796.

(27) Hanwell, M. D.; Curtis, D. E.; Lonie, D. C.; Vandermeersch, T.; Zurek, E.; Hutchison, G. R., *J. Cheminform.* **2012**, *4*, 17.